ERDC/CRREL TR-03-1

Cold Regions Research
and Engineering Laboratory

US Army Corps
of Engineers®
Engineer Research and
Development Center

Ice Storms in the St. Lawrence Valley Region

Kathleen F. Jones

January 2003

Abstract: The severe ice storm in January 1998 in Quebec, eastern Ontario, northern New York, and New England disrupted the lives of millions of people. The ice that accreted on trees and wires damaged electrical transmission and distribution lines, causing power outages that lasted many weeks in some areas. In this report, ice storms in the St. Lawrence Valley region of Quebec, eastern Ontario, and northern New York and Vermont are analyzed, focusing on the amount of ice on power lines. Although there are many photographs of ice-covered wires from this storm, only rough estimates of the equivalent radial thickness of ice on the wires can be obtained from these photos. The analysis in this report relies on historical weather data and ice accretion models to estimate the equivalent ice thickness on wires both in this storm and in past freezing-rain storms. The CRREL and Simple ice accretion models incorporate a physical model of the process of ice accretion with empirically determined parameters. Qualitative information from newspapers, *Storm Data,* and other reports on damaging storms supplement the model results to provide a better understanding of the climatology of ice storms in the region. Ultimately, all this information is used to calculate equivalent ice thicknesses from freezing rain for long return periods. For the St. Lawrence Valley region in the vicinity of Montreal, ice thicknesses on wires 10 m above ground and perpendicular to the wind for 50- and 200-year return periods are estimated to be 33 mm and 52 mm, respectively. Gust speeds concurrent with these ice thicknesses are about 20 m/s. Ice thickness estimates for the 1998 storm at the three weather stations in the Montreal area range from 48 to 55 mm.

COVER: Damage to power lines in the January 1998 ice storm.
Photos by Nathan Mulherin, Kathleen Jones, and Brian White.

How to get copies of ERDC technical publications:

Department of Defense personnel and contractors may order reports through the Defense Technical Information Center:

DTIC-BR SUITE 0944
8725 JOHN J KINGMAN RD
FT BELVOIR VA 22060-6218
Telephone (800) 225-3842
E-mail help@dtic.mil
msorders@dtic.mil
WWW http://www.dtic.mil/

All others may order reports through the National Technical Information Service:

NTIS
5285 PORT ROYAL RD
SPRINGFIELD VA 22161
Telephone (703) 487-4650
(703) 487-4639 (TDD for the hearing-impaired)
E-mail orders@ntis.fedworld.gov
WWW http://www.ntis.gov/index.html

For information on all aspects of the Engineer Research and Development Center, visit our World Wide Web site:

http://www.erdc.usace.army.mil

Technical Report
ERDC/CRREL TR-03-1

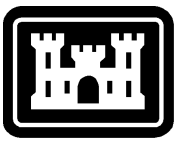

US Army Corps
of Engineers®
Engineer Research and
Development Center

Ice Storms in the St. Lawrence Valley Region

Kathleen F. Jones

January 2003

Prepared for
OFFICE OF THE CHIEF OF ENGINEERS

PREFACE

This report was prepared by Kathleen F. Jones, Research Physical Scientist, Snow and Ice Division, U.S. Army Engineer Research and Development Center (ERDC), Cold Regions Research and Engineering Laboratory (CRREL), Hanover, New Hampshire.

This work was supported through a Cooperative Research and Development Agreement with Vermont Electric Company and by the AT24 Basic Research Program at CRREL.

A number of people made invaluable contributions to this project. The author thanks Bob Davy at the Air Force Combat Climatology Center and Gary Beaney at Environment Canada for providing weather and precipitation data for the United States and Canada. Thanks also to Robert Morris at Environment Canada for providing the original data sheets for the 1998 ice storm for the stations in Canada. Keran Claffey at CRREL and Stephanie Poulin of Addesky Poulin both spent hours reading newspaper microfilms, finding and compiling articles about storm damage for the PDSs. Thanks to Gioia Cattabriga for her editorial assistance. Dr. Jon Peterka of Colorado State University and Dr. Edward Lozowski of the University of Alberta reviewed an earlier version of the report. Dr. Steven Daly and Dr. Edgar Andreas reviewed this version of the report. The quality and completeness of the report have been significantly improved by the incorporation of many of their recommendations.

CONTENTS

ILLUSTRATIONS

TABLES

Ice Storms in the St. Lawrence Valley Region

KATHLEEN F. JONES

1. SCOPE

1.1 Introduction

The severe ice storm in January 1998 in Quebec, eastern Ontario, northern New York, and New England disrupted the lives of millions of people. The ice that accreted on trees and wires damaged electrical transmission and distribution lines, causing power outages that lasted many weeks in some areas. In a report for the Federal Emergency Management Agency (FEMA), CRREL evaluated the severity of the storm in northern New England (Jones and Mulherin 1998). This report extends that analysis to the St. Lawrence Valley region of Quebec, eastern Ontario, and northern New York and Vermont, focusing on the amount of ice on power lines. Although there are many photographs of ice-covered wires from this storm, and the maximum thickness was reported for many of these ice samples, typically no information is provided on the shape of the accretion, whether the sample was intact, and how representative it was of the ice on the wires in that span. Thus, only rough estimates of the equivalent radial thickness of ice on the wires can be obtained from these samples. Documentation of past ice storms is even more sparse. Therefore, historical weather data are used to calculate ice thicknesses from freezing rain for long return periods in this region and to estimate the return period for a storm with the severity of the January 1998 storm.

1.2 Background

Both quantitative weather data and qualitative information on the severity of past freezing-rain storms are used to determine equivalent uniform radial ice thicknesses for long return periods on power lines, because of the dearth of definitive measurements of these ice thicknesses in these storms. The methodology used for this study to estimate ice thicknesses for freezing-rain storms

and calculate ice thicknesses for long return periods was developed to map ice thicknesses in the United States for ASCE Standard 7-1998 (ASCE 2000).

A number of terms are used frequently throughout this report. The term "freezing rain" is used to refer to both freezing rain and freezing drizzle, which consists of smaller drops and may occur with colder upper-air temperatures than freezing rain (Bocchieri 1980). The phrase "equivalent uniform radial ice thickness" refers to the thickness that the accreted ice would have, measured from the surface of the branch or wire to the surface of the ice, if it were spread uniformly thickly around the branch or wire. For brevity in this report this phrase is shortened to "equivalent ice thickness" in referring to a value determined from field measurements and sometimes "ice thickness" in referring to model results. The cross-sectional shape of actual ice accretions varies widely and the equivalent ice thickness must be calculated for an ice sample from a measure of the volume or the mass of the ice and the diameter and length of the branch or wire on which it accreted. Modeled ice thicknesses are typically reported as an equivalent uniform radial thickness.

Weather data are used as input to ice accretion models that determine the amount of accreted ice using empirical parameters in a physical model of the ice accretion process. Historical weather data in the United States and Canada are described in general in Section 2.1 and specifically for weather stations in the study region in Section 3.1. The archived weather data files include documentation of the precipitation type and measurements of the precipitation amount, wind speed, air temperature, dew point temperature, and air pressure. The accuracy of the ice thicknesses determined by an ice accretion model depends on both the quality of the weather data and the quality of the model, as well as on the decisions made by the user in applying the model to the data. Because weather instruments may not work well, or at all, in freezing rain, some of the data that are crucial in the calculation of the accreted ice thickness may be estimated by the weather observers, not measured at all, or measured incorrectly. Thus, using an ice accretion model to determine ice thicknesses on wires and conductors supplies only an estimate of the actual ice thickness even if the model is perfect. Furthermore, that estimate may apply only in the vicinity of the station where the data were collected. In freezing-rain storms the precipitation typically varies in time and location both in type (snow, rain, freezing rain, and ice pellets) and in amount. Thus the ice thickness on a structure a few kilometers from (or tens of meters higher than) the weather station may be significantly different from that at the station.

There are a number of ice accretion models that use weather data to estimate the amount of accreted ice. This study relies on the CRREL and Simple models,

which are summarized in Section 2.2. Because other models have been used to map extreme ice thicknesses in the United States and Canada, these models and model validation are also reviewed. In Section 2.3 decisions that are made in the data/model interface, but are independent of the model itself, are reviewed. The data/model interface significantly affects the model results, but is often ignored.

To balance the uncertainties inherent in modeling and to better understand the climatology of ice storms in the region, a compilation of information from newspaper accounts of freezing-rain storms, *Storm Data* (NOAA, 1959–1998), and other publications is included in the analysis. These sources do not supply quantitative information on equivalent ice thickness, but they do provide crucial information on the severity and extent of the storms. Ultimately, information from all these sources is used to determine ice thicknesses for long return periods and concurrent wind-on-ice speeds for power lines. The compilation of this qualitative data is described in Section 4.

In the extreme value analysis, superstations are formed to provide a longer period of record than single stations and thus reduce the error in estimating the ice thickness for long return periods. Stations are grouped into superstations based on similarities in the frequency of ice storms, the extent of damaging storms, and terrain as described in Section 5.1.

Because it is used to determine extreme wind speeds, the Gumbel distribution is often assumed to be appropriate for an extreme value analysis of ice thicknesses. I have found, however, that the generalized Pareto distribution provides a better fit. The extreme value analysis used in this study is discussed in Section 5. The fit of the generalized Pareto distribution to ice thickness extremes typically results in values that increase relatively rapidly with return period compared to a Gumbel distribution fit. In section 5.6 the method of moments fit of the Gumbel distribution to annual extremes is compared to a probability weighted moments fit of the generalized Pareto distribution to a partial duration series of ice thicknesses.

Both the absolute and relative severity of the 1998 ice storm has been a controversial issue. In Section 6 various aspects of the ice storm severity are discussed. The variation of ice thickness with orientation, height above ground, and during the course of the storm is presented in Sections 6.1 and 6.2. The geographical distribution of equivalent ice thicknesses in the Montreal area is discussed in Section 6.3. Finally, Section 6.4 deals with the variation in estimated extreme ice thicknesses from 1973 to the present in the Upper St. Lawrence Valley.

2. WEATHER DATA AND ICE ACCRETION MODELS

2.1 Weather data

United States. In the United States historical weather data are archived at the National Climate Data Center (NCDC) and the Air Force Combat Climatology Center (AFCCC). Weather data are collected by the National Weather Service (NWS), the Navy, Army, and Air Force, the Federal Aviation Administration (FAA), and other state and federal agencies. At weather stations in the United States, temperatures are measured to the nearest 1°F, wind speeds to the nearest knot, and precipitation amounts to hundredths or tenths of an inch, varying over time and from station to station. Temperature is archived in tenths of a degree Celsius, wind speeds in tenths of a meter per second, and precipitation amounts in millimeters (AFCCC) or hundredths of an inch (NCDC). In the last few years, with the change to Metar archive standards, temperatures are archived to the nearest whole degree Celsius.

Before the weather data are archived, they are checked using quality control software to correct any data errors that can be automatically corrected and to flag apparent problems that require a manual check of the data. NCDC does a further manual quality control of NWS and Navy weather records to check and correct data that were flagged and to fill in missing data elements and records. AFCCC provides the same level of manual quality control for the Army and Air Force data. Weather data from the FAA and other agencies do not go through this higher level of quality control. Thus AFCCC archives high-quality-controlled Army and Air Force weather data, and lower-quality-controlled NWS, Navy, and FAA data. NCDC archives high-quality-controlled NWS and Navy weather data and lower-quality-controlled FAA data. AFCCC archives weather data from stations outside the United States as well, with no additional quality control.

The weather data archived at AFCCC include only 6- and 24-hourly accumulations of precipitation. The period of record of the data archived electronically typically begins in 1973, except for stations that were commissioned more recently. For NCDC-archived weather data, precipitation data are archived either hourly or daily. The period of record for the computer-archived NCDC data begins in the 1940s at many of the NWS and Navy weather stations. However, for a number of years, typically 1965 through 1972, but sometimes extending into the 1980s, weather records were archived only every three hours, even though hourly measurements were made. The daily precipitation data are available in a set of *Cooperative Summary of the Day* compact discs.

The data for this study at Massena through 1993, Watertown through 1992, and Burlington through August 1993 was acquired a few years ago from the NCDC archives, and thus have gone through manual quality control. The more recent data for those stations, however, are from the AFCCC archives and have had only automatic quality control.

Canada. Eight of the 14 weather stations in the St. Lawrence Valley region are in Canada. Since weather data for the entire period of record for these stations was not available from AFCCC, additional hourly weather data, as well as daily precipitation data for the entire period of record, were obtained from Environment Canada (EC). For the 1998 ice storm, hourly data from the Observations Météorologiques en Surface forms provided by Environment Canada* were used to correct and fill gaps in the electronically archived data from AFCCC. Environment Canada archives temperature in tenths of a degree Celsius, wind speeds in tenths of a kilometer per hour, and precipitation amounts in millimeters.

Measurements. The most important parameters in determining ice thicknesses from freezing rain are the precipitation rate and wind speed during the freezing-rain storm. The dependence of the ice thickness on these parameters from the Simple model (Jones 1996a) is shown in Figure 1. Ice thicknesses in the Simple model are independent of air temperature, but even in models in which air temperature is a factor in determining the load, for example the CRREL (Jones 1996b), Makkonen (Makkonen 1985, 1996), MRI (MRI 1977), and Châiné (Châiné and Castonguay 1974) models, it has little effect as long as the temperature is below freezing. Both anemometers and precipitation gauges may be adversely affected by accreted ice, and freezing-rain storms sometimes cause power outages at weather stations. Thus, the expertise and dedication of the weather observers may have a significant effect on the quality of the recorded wind speed and precipitation data. The variation in the quality of weather measurements over time and from station to station in the St. Lawrence Valley region is not known.

2.2 Ice accretion models

2.2.1 Freezing rain

Equivalent ice thickness. There are many models that use weather data to determine the ice thickness on a wire from freezing rain. The CRREL model and

* Personal communication, Robert Morris, Manager, Information Services Division, National Archives and Data Management Branch, Meteorological Services of Canada, 2000.

the sometimes more conservative Simple model, similar to the Goodwin model (Goodwin et al. 1983), were both used in this project. These models, like many others, express the amount of ice in terms of the equivalent radial ice thickness R_{eq}. (A list of symbols is in Appendix A.) R_{eq} is the ice thickness that would be measured if the actual ice accretion on a wire was distributed uniformly thickly around the wire**.** For a given R_{eq} the weight of ice (kg/m) increases with wire diameter. In field measurements the equivalent thickness of ice on a wire with diameter D can be calculated from the mass m of ice accreted on a length L of the wire:

$$R_{eq} = -\frac{D}{2} + \left(\frac{D^2}{4} + \frac{m}{\pi \rho_i L} \right)^{1/2} \tag{1}$$

where $\pi \approx 3.14$ and ρ_i is the density of glaze ice ($\approx$0.9 g/cm^3).

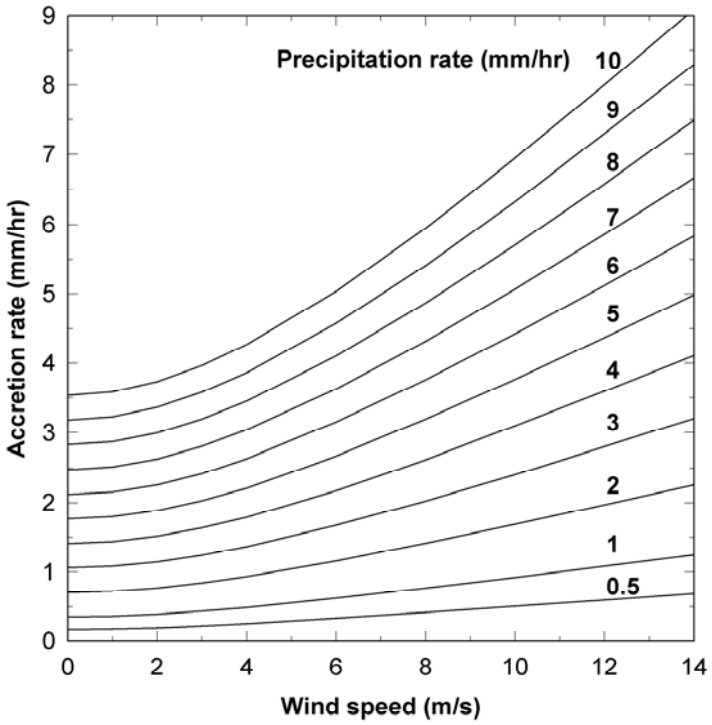

Figure 1. Dependence of ice thickness on precipitation rate and wind speed from the Simple model.

R_{eq} is smaller than the maximum thickness of typical rough, eccentric, or icicled accretions (Fig. 2a–d). Figures 2a and b show the eccentric and uniform

ice accretions that are typical when the impinging precipitation freezes relatively quickly. In Figure 2c the ice has frozen more slowly on an electric fence with icicles forming as the unfrozen precipitation began to drip off. The ice in Figure 2d accreted in a knobby shape on the wire in this span, which was sagging to less than 2 m above ground because of the slack induced by a broken pole a few spans away. It is likely that this knobby accretion was generated by the pole breaking earlier in the storm, with significant ice on the wire. The wire then rotated as it sagged, so that the icicles that had been below the wire became nearly horizontal. Freezing rain then continued to fall on this larger area, forming new icicles below the wire. This knobby accretion was directly above the electric fence shown in Figure 2c. This variety of ice shapes indicates how misleading a measurement of the maximum ice diameter or thickness is as a proxy for the equivalent ice thickness.

Simple and CRREL ice accretion models. The Simple model determines the equivalent ice thickness from the amount of freezing rain and the wind speed in hours with freezing rain:

$$R_{eq} = \sum_{j=1}^{N} \frac{1}{\rho_i \pi} \left[(P_j \rho_o)^2 + (3.6 U_j W_j)^2 \right]^{1/2} \qquad (2)$$

where

R_{eq} is in mm

P_j = precipitation amount (mm) in the jth hour

ρ_o = density of water (1 g/cm^3)

U_j = wind speed (m/s) in the jth hour

W_j = liquid water content (g/m^3) of the rain-filled air in the jth hour
= $0.067 P_j^{0.846}$ (Best 1950a)

N = duration of freezing-rain storm (hr).

R_{eq} does not depend on the air temperature because it is assumed that all the available precipitation freezes. Then, because the ice is uniformly thick around the wire, R_{eq} does not depend on the wire diameter. The CRREL model uses a heat-balance calculation to determine how much of the impinging precipitation freezes directly to the wire and how much of the runoff water freezes as icicles. If it is cold enough and windy enough, the ice thicknesses determined by the CRREL and Simple models are the same. However, if the air temperature is near freezing and wind speeds are low, the CRREL model calculates smaller ice thicknesses than the Simple model. In those conditions much of the impinging

precipitation may freeze as icicles and some may drip off without freezing. The CRREL model requires the user to specify the diameter of the wire on which the accretion of ice is to be modeled. However, this model, like the MRI and Makkonen models, shows very little dependence of R_{eq} on wire diameter.

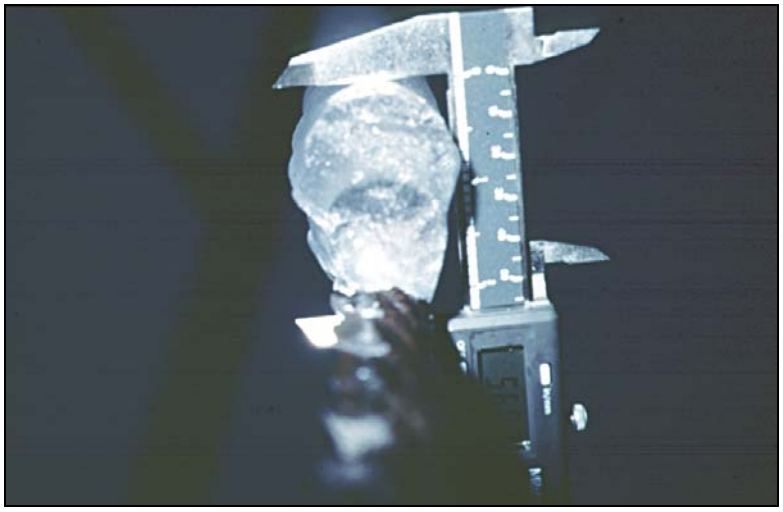

a. Accreted glaze ice on a guy in Louisville.

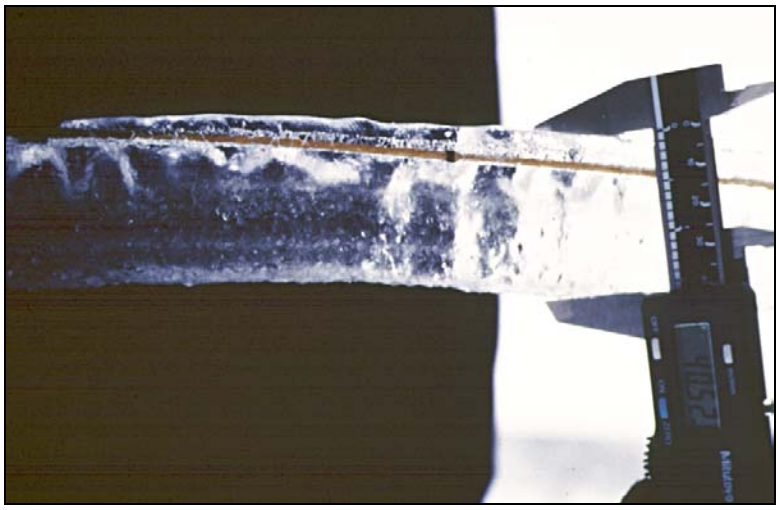

b. Accreted glaze ice on a blade of grass in Ogdensburg.

Figure 2. Examples of shapes of accreted glaze ice in the 1998 ice storm in New York. Calipers show measured ice dimension in mm. (Photographs by Nathan D. Mulherin.)

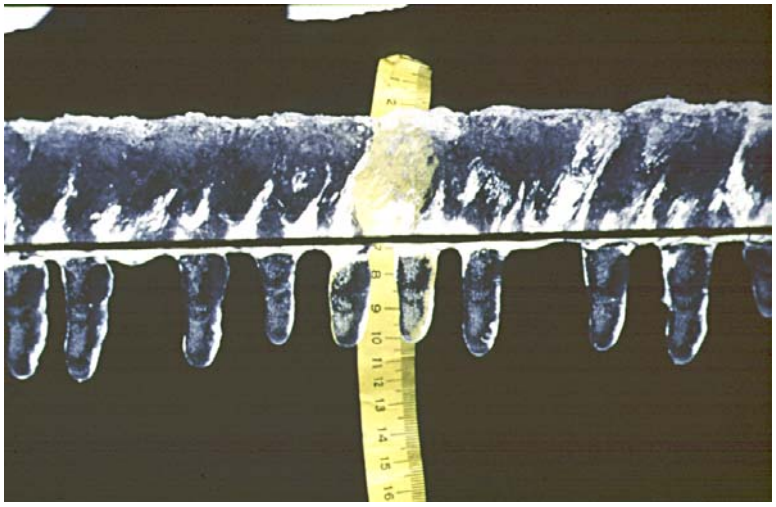

c. Accreted glaze ice on an electric fence in Hamilton.

d. Accreted glaze ice on Triplex wire above fence (shown in Fig. 2c, above) in Hamilton.

Figure 2 (cont'd).

While the CRREL model calculations are more detailed than the Simple model calculations, it does not necessarily provide a more accurate ice thickness. The parameters used in the heat-balance calculation are from wind-tunnel studies of rough cylinders, which may not well represent the heat-balance for the variety of shapes of ice-covered wires (Fig. 2). Even if the heat-balance calculation is

perfect, vertical and horizontal variations in air temperature and dew point temperature from the archived temperature could cause significant variations in the ice thickness determined by the CRREL model. The Simple model is more robust, determining the ice thickness only from the reported precipitation type, amount of precipitation, and wind speed.

Other ice accretion models. The MRI, Makkonen, and Chaîné models as well as the CRREL and Simple models are discussed and compared in Jones (1996a).

The MRI model tends to determine smaller ice thicknesses than the CRREL model, because water that does not freeze immediately is ignored, rather than being allowed to freeze to form icicles. However, in using that model, or the Goodwin model, the user is required to specify the fall speed of the raindrops, and the model results depend significantly on the speed that is chosen. If a low fall speed is assumed, the modeled ice thickness is larger than it is if a higher fall speed is assumed for the same precipitation rate. This occurs because if the drops are falling slowly the water content of the air must be higher to produce the same rate of accumulation of water on the ground as when the drops are falling faster. The fall speed assumption determines how much water is available to be blown on the wire and potentially freeze. In the Simple, CRREL, MRI, and Chaîné models, the liquid water content W is expressed in terms of the precipitation rate P, implicitly incorporating a fall speed for the raindrops. The relationship used in equation 2 results in a fall speed $U_T(\text{m/s}) = 4.15P^{0.154}$. This is obtained from equating the vertical flux of the rain water based on the precipitation rate with that based on the liquid water content $\rho_o P = WU_T$. Terminal velocities of raindrops are typically given in terms of the drop diameter. Using the power law relationship for drop velocity in Atlas and Ulbrich (1977) with the drop size distribution in Best (1950a) results in a liquid water content averaged terminal velocity $4.05P^{0.155}$ (Appendix C). For precipitation rates between 0.5 and 3 mm/h, this formula gives a terminal velocity between 1 and 3% smaller than is obtained from the Best liquid water content.

The Makkonen model tends to be almost as conservative as the Simple model, primarily because it assumes that a significant portion of the water that does not freeze immediately is incorporated in the accretion. Because of this, there is less water available to freeze as icicles than in the CRREL model.

The Chaîné model is based on wind tunnel tests that were done by Stallabrass and Hearty (1967) to investigate sea-spray icing. A number of unjustified assumptions and extrapolations were made in Chaîné and Castonguay (1974) to mold this data into a formulation for freezing rain (Appendix B) and the results indicate a significant variation of ice thickness with wire diameter. For small

cylinders the ice thickness from the Chaîné model is much larger than that from the Simple model, and for large-diameter cylinders it is much smaller.

Variation of R_{eq} with wire diameter. While the Chaîné model is not credible, the variation of equivalent ice thickness with diameter is appealing to many users. A paper by Lanctot et al. (1960) showed an increase in equivalent ice thickness with decreasing cylinder diameter in laboratory experiments. However, the relatively small effect indicated is probably due to the lack of wind in those experiments that was required to maintain a uniform precipitation pattern. Although ice accreted on small-diameter twigs and wires looks more impressive than ice on a large-diameter branch or conductor, there is little evidence to indicate that the equivalent ice thickness increases as diameter decreases. Measurements made by CRREL's ice storm team of natural ice accretions from freezing rain on trees, wires, and fence rails indicate that the equivalent ice thickness does not vary in a consistent way with the diameter of the substrate (Fig. 3).

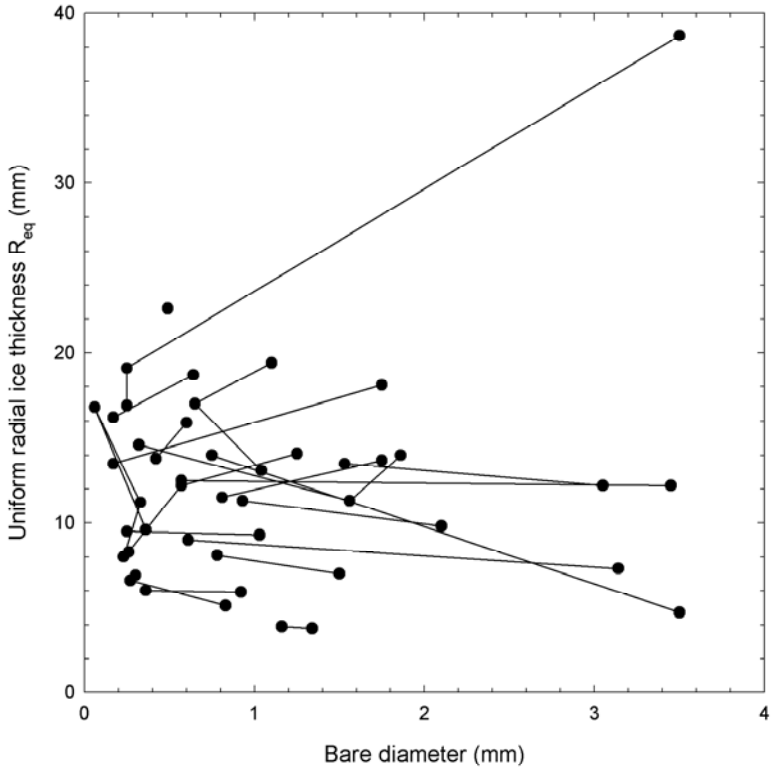

Figure 3. Variation of equivalent uniform radial ice thickness with diameter, from field measurements. Lines are drawn between values for samples collected at the same site.

The variation in R_{eq} shown in this figure may be due to the material and color of the substrate, its exposure and orientation to the wind, and changes in orientation during the storm as branches sagged under the weight of the ice. Heat generated by the current in conductors of power lines also affects the amount and shape of the ice that accretes. Although additional measurements of equivalent ice thickness from severe freezing-rain storms should be collected to resolve this issue, it is reasonable to assume—based on the concepts in the Simple model, results from detailed heat-balance models, and measurements in freezing-rain storms—that the equivalent ice thickness on a wire is independent of the diameter of the wire.

Model validation. There have been some attempts at model validation. Felin (1988) compared data from Hydro Quebec's Passive Ice Meters (PIM), using the measurement of the maximum ice thickness on the 25-mm-diameter cylinder, with MRI model simulations assuming a drop fall speed of 4.1 m/s. The correlation between the simulations and the measurements was low, which she attributed to the simplifying assumptions in the MRI model and possibly to wind turbulence and the orientation of the PIM cylinder. However, it is likely that treating the PIM measurement as the equivalent uniform radial ice thickness was a significant component in the lack of correlation.

Yip and Mitten (1991) compared 61 PIM measurements with Chaîné, Makkonen, MRI, and Goodwin model results using weather data at nearby weather stations. The ice measurements and weather data were assembled by Meteorological and Environmental Planning Limited (MEP) in 1984 and Environmental Applications Group in 1987. No information on how the models used the weather data or how the PIM ice measurements were interpreted is provided in the 1991 paper. The results show that the ice thicknesses from the Chaîné model tend to be larger than the ice measurements, and the ice thicknesses from the other three models tend to be smaller. The mean observed PIM ice measurement was 7 mm, while the mean model R_{eq} ranged from 2 to 8 mm. The root-mean-square difference between the modeled R_{eq}s and the PIM measurements was 7 mm for all four models.

Yip (1993) provided an indirect comparison of Chaîné model R_{eq}s and measured ice thicknesses. She used annual maximum ice thickness data on the 25-mm cylinder from 20 PIM sites, with between 13 and 16 years of data at most sites. She estimated equivalent ice thicknesses from the PIM measurements by multiplying the measured values by 0.5. The 30-year return period ice thickness was determined by fitting a Gumbel distribution to these data. She compared these results to 30-year ice thicknesses calculated from a Gumbel analysis of between typically 25 and 38 years of annual maximum values from Chaîné

model results at the same stations. The difference between the PIM and Chaîné extremes ranged from –7 mm to 10 mm. These results are difficult to interpret because they are affected by the differences in the periods of record of the PIM and Chaîné annual maxima.

Jones (1996b) compared the measured equivalent ice thickness on a horizontal cylinder in a single freezing-rain storm with Chaîné, MRI, Makkonen, Simple, and CRREL model ice thicknesses using collocated weather data. The 2-mm measured ice thickness was matched by all models except Chaîné, which was 2 mm too high.

Newfoundland and Labrador Hydro et al. (1998) reported on the results of a 4-year Canadian Electricity Association (CEA) study comparing ice weights on three test spans in 22 freezing-rain storms with ice weights determined by the Chaîné, MRI, and Makkonen models using weather data measured at the test span sites. The ice weight was calculated from measurements of the tension in the conductor or the vertical load in an insulator string of a suspension tower. The best-fit line between the modeled and measured ice weights was determined. Omitting two anomalous cases provided the best correlation over the whole range of ice weights up to 31 N/m (equivalent to a 20-mm equivalent ice thickness). These results showed that the Chaîné model was high by about 60% and the Makkonen model by up to 20%, while the MRI model was about 25% low.

In all these comparisons, not only the ice accretion models, but also the user interface between the weather data and the model and the assumptions made in determining the equivalent ice thickness from the measurements that were made are being tested. However, the contribution of errors from these latter two sources is typically not discussed and the lack of agreement between modeled and measured ice thicknesses is attributed to shortcomings of the models.

2.2.2 Supercooled fog

In some freezing-rain storms fog (visibility less than 800 m) or mist (visibility greater than 800 m) is also observed at air temperatures below 0^{o}F. The supercooled droplets in the fog or mist may also form ice on trees and wires. The mass of ice that accretes on a wire depends on the diameter of the droplets, liquid water content of the fog, wind speed, temperature, and diameter of the wire. For an assumed droplet diameter, the liquid water content of the fog or mist can be estimated from the measured visibility

$$W = \frac{1.3\ \rho_o d_s}{V} \tag{3}$$

where

d_s is the Sauter mean diameter of the fog droplets (μm)

V is the visibility (m)

W is the liquid water content of the fog or mist (g/m^3).

This formula comes from the dependence of the extinction coefficient on liquid water content in fog and the relationship between visibility and extinction coefficient for a threshold contrast of 5% (Kumai 1973). The Sauter mean diameter is the ratio of the total volume of the droplets to their total cross-sectional area. An assumed droplet diameter and the liquid water content calculated from the measured visibility using equation 3 can then be used with the measured wind speed to estimate the mass of ice that accretes in each hour that fog or mist is observed. The collision efficiency of the fog droplets with the wire is calculated using formulas in Finstad et al. (1988), based on the diameter of the ice-covered wire in each hour. It is assumed that the rate of cooling is sufficient to freeze all the impinging cloud droplets, and that the ice accretes as glaze uniformly thickly around the wire.

The mode of the distribution of median volume droplet diameters from 20 years of measurements in supercooled fogs at Mt. Washington Observatory is between 10 and 15 μm (Jones 1990). Measurements of droplet distributions in supercooled fogs at Mt. Washington indicate that the Sauter mean diameter is essentially the same as the median volume diameter (Jones and Koh 1995). A fog and mist droplet diameter of 15 μm was assumed when these conditions were observed in the archived data from the St. Lawrence Valley region. This resulted in a negligible contribution to the accreted ice thickness from fog and mist in freezing-rain storms. However, this result depends strongly on the assumed droplet diameter, both because liquid water content depends linearly on droplet diameter in equation 3 and because the collision efficiency increases significantly with droplet diameter. The dependence of the modeled equivalent ice thickness on droplet diameter for a 2-cm-diameter wire and a wind speed typical of freezing-rain storms (5 m/s) is shown in Figure 4 for visibilities from 50 to 1000 m. For fog droplet diameters between 10 and 25 μm, the equivalent ice thickness ranges over two orders of magnitude. Thus, at least in these low-wind conditions, we cannot rely on visibility measurements to provide a good estimate for the contribution of in-cloud icing to the accreted ice thickness, without simultaneous measurements of the typical fog droplet diameter.

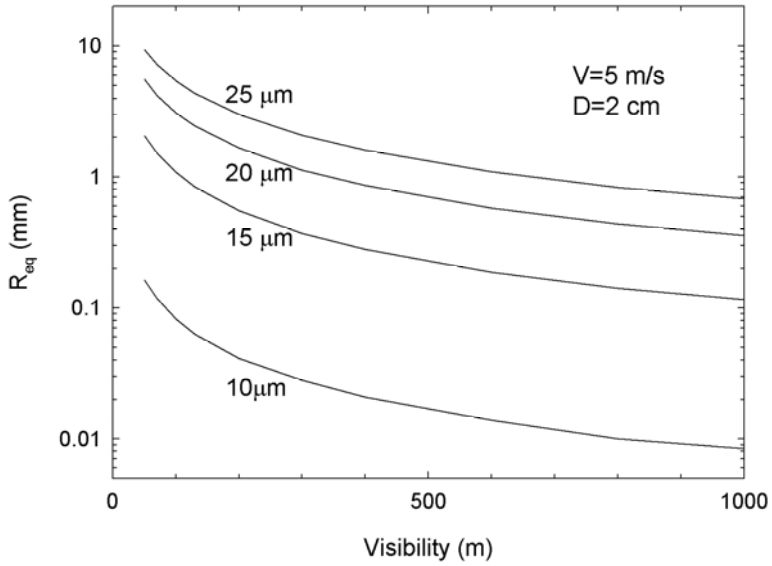

Figure 4. Dependence of ice thickness on droplet diameter in freezing fog for a 2-cm-diameter wire in a wind speed of 5 m/s for a one-hour duration.

2.3 Data/model interface

When weather data are used to determine ice thicknesses on wires, a number of decisions must be made about the data that are separate from the model, but can significantly affect the results. These include 1) prorating 6-hourly and 24-hourly precipitation amounts to each hour, 2) deciding how much of the precipitation accretes as ice when there are other types of precipitation, such as rain, snow, or ice pellets, mixed with freezing rain, 3) correcting the measured wind speed from the height above ground of the anemometer to the height of the wire, 4) dealing with wire orientation to the wind and variability in wind direction, 5) at NWS stations, interpolating the weather data when it was archived only every third hour, 6) deciding when a freezing-rain storm ends. Each of these aspects of determining the ice thicknesses from weather data is discussed in this section.

2.3.1 Prorating accumulated precipitation

The weighting factors used to prorate 6- and 24-hourly precipitation amounts to each hour are shown in Table 1. These weights were originally intended to be the typical precipitation rate in mm/hr for each type and intensity of precipitation. The weight assigned to each hour in the weather record is determined by the present weather codes for the hour, with the weight set to zero if there is no precipitation. For example, if the only type of precipitation reported in an hour is

light freezing rain, the weighting factor for that hour is 1.8. In the next hour with moderate freezing drizzle and light snow, the weighting factor is (0.3+0.6)/2 = 0.45. The fraction of the accumulated precipitation attributed to each hour is the weighting factor for the hour divided by the sum of weighting factors for the six or 24 hours in which precipitation accumulated. This fraction is then multiplied by the accumulated amount to obtain the estimated hourly precipitation amount. If these two hours are the only hours with precipitation in a 6-hr period in which 2 mm of precipitation fell, 80% (= 1.8/2.25) or 1.6 mm would be assigned to the hour with light freezing rain and 20% (= 0.45/2.25), or 0.4 mm would be assigned to the next hour.

Table 1. Weighting factors used to prorate 6- and 24-hourly precipitation amounts to each hour.

Precipitation intensity/type	Rain	Rain showers	Drizzle	Freezing rain	Freezing drizzle	Snow	Snow grains	Ice pellets	Snow showers	Snow pellets	Hail
Light	1.8	1.8	0.1	1.8	0.1	0.6	0	1.8	0.6	0.6	1.8
Moderate	5.1	5.1	0.3	5.1	0.3	1.3			1.3	1.3	5.1
Heavy	13.0		0.8			2.5					

Table 1 is based on a table provided by Tsoi Yip of the Atmospheric Environment Service (AES), which she used to prorate 24-hourly precipitation amounts for an ice thickness map of Canada. This Canadian table was originally provided in an unpublished report by Meteorological and Environmental Planning, Ltd. (MEP) for Environment Canada in August 1984[*]. Quoting from the MEP report,

"The methodology follows an 'intensity weighting factor' method developed at Ontario Hydro. A table was derived of average hourly intensities (water equivalent) for all precipitation types reported in the Digital Archive. Rainfall and drizzle intensities were taken from MANOBs while snowfall intensities were derived from Richards' (1954) relationships between visibility and snowfall intensity at Malton Airport, Toronto. The value of moderate freezing rain was decreased to 4.0 mm/hr based on information presented in Stallabrass (1983) on maximum precipitation intensities during glaze storms. Freezing rain or drizzle should not be associated with heavy intensities because of the characteristics of the meteorology governing the generation of falling supercooled droplets. The rest of the precipitation intensities were derived mainly on the basis of experience, as very little information exists for the selection of quantitative values. The assumptions made in completing the table were

[*] Personal communication, Philip Jarrett, Head, Engineering Climatology Section, Environment Canada, 1999.

1) Showery-type precipitation has the same hourly intensity as its corresponding continuous precipitation counterpart.

2) Ice crystals have a negligible water equivalent.

3) Frozen droplet precipitation types (e.g., ice pellets and hail) have the same water equivalent intensity as rain."

The main difference between Table 1 and the Canadian version is the larger weighting factor for moderate freezing rain, equal to that for moderate rain in Table 1. The information in Stallabrass (1983) does not justify the decrease in the weighting factor of the moderate rain rate from 5.1 to 4.0. In that paper, Stallabrass presents information from a 10-year study by Bell Canada at Toronto International Airport, in which all freezing-rain storms with total precipitation amounts greater than 2.5 mm were identified. The maximum precipitation rate in those 23 storms was 4.8 mm/hr. There is no mention of whether the precipitation type was drizzle or rain, or whether the precipitation intensity was light or moderate.

Prorating precipitation to each hour becomes less accurate as the accumulation time increases. Thus 6-hourly accumulations should be prorated more accurately than 24-hourly accumulations, particularly if the type of precipitation changes during the period over which it is accumulated. On the other hand, for precipitation measurements to be accurate enough for this application, the precipitation amount must be reported for the period in which it fell. This may not occur when the precipitation freezes in the gauge and is measured only when the temperature warms to above freezing. The primary precipitation data sets for this study are the 6-hourly data at military stations in the United States and daily precipitation data in Canada and at National Weather Service and FAA stations in the United States.

2.3.2 Mixed precipitation types

In freezing-rain storms the type of precipitation varies from hour to hour, and in any hour there will often be two or even three types of precipitation reported. A further subdivision of the prorated hourly precipitation amounts is not attempted. Instead all the precipitation in an hour in which freezing rain falls is assumed to accrete to the wire as if it were freezing rain. The models are also allowed to accrete precipitation that was described as rain or drizzle if the air temperature was freezing or below. These assumptions are conservative. They allow the modeled ice thicknesses to represent the possibly more severe conditions in the vicinity of the weather station, where perhaps all the precipitation is freezing rain rather than the mixture of precipitation types observed at the weather station.

2.3.3 Ice pellets

In both the CRREL and Simple models, ice thicknesses may be determined for two cases: 1) allowing ice to accrete only in hours in which the precipitation type is reported as freezing rain or a combination of freezing rain and other types of precipitation, and 2) allowing ice to accrete also in hours in which the precipitation type is ice pellets. Freezing rain and ice pellets occur in the precipitation-type transition region of winter storms (Stewart 1992), which typically is bounded by snow on one side and rain on the other. Freezing rain and ice pellets develop in the same meteorological conditions, namely a layer of warm air over a layer of cold air. Snowflakes, formed in clouds above the layer of warm air, melt as they fall through the warm air. These water drops then cool while falling through the layer of cold air below. For the right combinations of cold and warm layer thicknesses and temperatures, the raindrops may supercool in the cold air layer, but remain liquid and ultimately freeze on impact with a structure. However, there are two scenarios in which the precipitation falls as ice pellets rather than freezing rain: 1) if the cold air layer is thick enough and cold enough, the rain drops freeze partially or entirely, forming ice pellets, and 2) if the warm air layer aloft is relatively thin or cold, the snowflakes may not melt completely before falling into the cold air layer. In the first case structures at higher elevations or high enough above ground may be in freezing rain while ice pellets are observed at weather stations. The inclusion of ice pellets in modeling ice thicknesses at weather stations is intended to estimate ice thicknesses that *may* have occurred on structures near to, but perhaps higher than, the weather station. The CRREL ice storm team observed this in a storm in February 1996 in Tennessee where freezing rain damaged trees and power lines on Lookout Mountain, a suburb of Chattanooga, while ice pellets were falling at the Chattanooga airport.

2.3.4 Anemometer and wire heights above ground

Ice thicknesses on wires are often calculated at 10 m above ground, but may be calculated at any height. Because wind speed increases with height above ground through the earth's boundary layer, the ice thickness also increases with height, as shown by equation 2. Thus, it is important to know how far above ground the wind speed is measured. The anemometer height varies from station to station and has typically varied over time at any weather station. The rate of increase of wind speed with height depends on the roughness of the terrain and the exposure of the site. In this study the wind speed was assumed to be proportional to the 1/7 power of the height, following ASCE Standard 7-93 (1993) for exposure C, which is appropriate at these airport weather stations. Thus

$$U_W = U_A \left(\frac{h_W}{h_A} \right)^{1/7} \quad (4)$$

where U_W and U_A are the wind speeds at the height above ground of the wire h_W and the height above ground of the anemometer h_A, respectively. In strong winds meteorologists prefer the semi-logarithmic law wind profile, which depends on the roughness length (Simiu and Scanlan 1996) rather than the power law profile used by engineers. For low grass the minimum roughness length is 0.01 m and for tall grass the maximum roughness length is 0.1 m. Semi-logarithmic profiles for these two cases are shown in Figure 5 along with the power law profile for a measured wind speed of 7.5 m/s at 10 m above ground. This figure shows that equation 4 is very close to the semi-logarithmic profile with a roughness length of 0.01 m; however, it obtains higher winds below the anemometer height and lower winds above that height when compared to the semi-logarithmic profile with a 0.1-m roughness length.

If the air is stably or unstably stratified, rather than neutrally stratified, the actual wind profile deviates from the semi-logarithmic law wind profile. The deviations may be significant (10 to 20%) for low wind speeds (Simiu and Scanlan 1996). Thus equation 4 provides only an estimate of the actual wind profile at weather stations. Average wind profiles over forested terrain are even more complex (Oliver 1971), with low wind speeds in the tree canopy and a steep gradient above the average canopy height. Therefore, wind speeds adjusted to the wire height at weather stations provide only an estimate of the actual wind speed at any location along a right-of-way for a power line.

2.3.5 Wire orientation and wind direction

Both the CRREL model and the Simple model compute the ice thickness on a wire whose orientation changes as necessary so that it is always perpendicular to the wind to give the largest effect of wind-blown rain. This assumption is conservative for power lines, particularly for line routes that are nearly parallel to the prevailing wind direction in freezing-rain storms. However, for line routes that are perpendicular to a consistent prevailing wind direction in freezing-rain storms the assumption is only slightly conservative. The effect of the varying wind direction on the modeled ice thickness is determined by calculating ice thicknesses in the Simple model on wires that are always parallel to the wind and on wires with fixed orientations from north ranging from 0^o to 150^o in 30^o increments:

$$R_{\mathrm{eq}}(\theta,\phi) = \sum_{j=1}^{N} \frac{1}{\rho_{\mathrm{i}}\pi}\left\{\left(P_{\mathrm{j}}\rho_{\mathrm{o}}\right)^2 + \left(3.6V_{\mathrm{j}}W_{\mathrm{j}}\sin\left[\theta-\phi\right]\right)^2\right\}^{1/2} \tag{5}$$

where θ *is* the wire direction and ϕ is the wind direction. Unless otherwise stated, the modeled ice thicknesses presented in this report are for a wire that is always perpendicular to the wind direction.

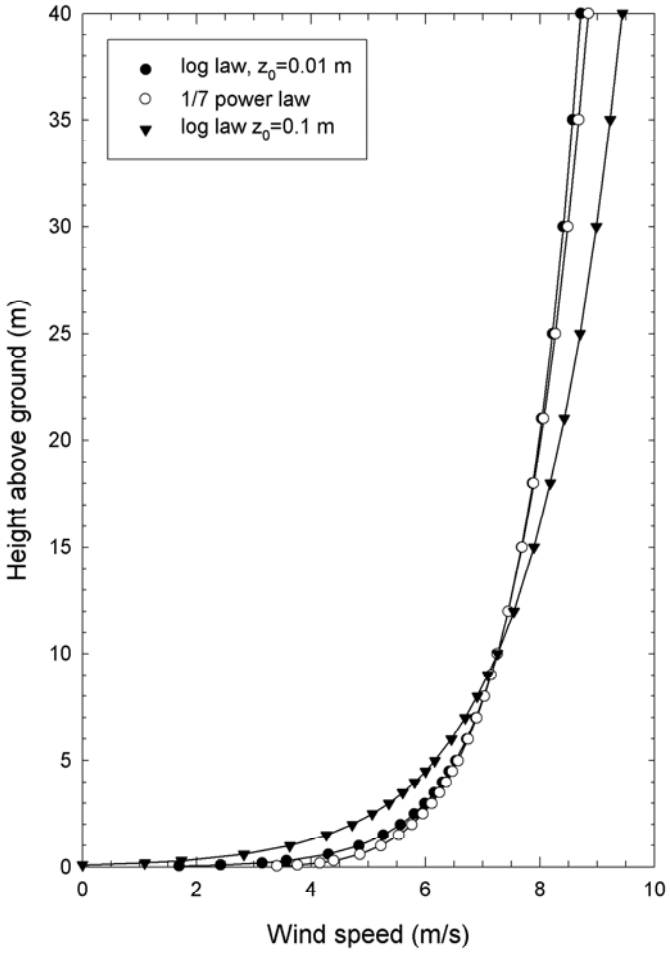

Figure 5. Semi-logarithmic wind speed profiles compared to the 1/7 power law profile for a measured wind speed of 7.5 m/s at 10 m above ground.

2.3.6 Interpolating three-hourly data

At NWS stations, from about 1965 to about 1972 or as late as 1981 at some stations, weather data were archived electronically only every three hours, at

0000, 0300, 0600, 0900, 1200, 1500, 1800, and 2100 Universal Time (UTC), even though measurements were made every hour. These gaps in the data are handled by assuming that the weather was the same as the archived hour in the two hours immediately after. The sensitivity of the modeled ice thicknesses to this interpolation was investigated by comparing the ice thickness obtained using interpolated weather data and the original hourly data for one severe freezing-rain storm at Springfield, Illinois, in 1978. The hourly and interpolated three-hourly values differed by only 1 mm, or 2% of R_{eq}. The original handwritten hourly data are available at NCDC and are expected to be archived electronically in the next few years*. In the St. Lawrence Valley region, the stations affected by this archiving anomaly are Burlington and Massena.

2.3.7 Storm end

An important aspect of preprocessing the weather data before running ice accretion models is deciding when a freezing-rain storm ends. That choice affects both the maximum wind-on-ice load and the maximum equivalent ice thickness for the storm. The maximum wind-on-ice load may occur following the ice storm, if a cold front accompanied by higher winds moves into the storm area.

For the Canadian map of 50-yr ice thicknesses, EC defined the end of a freezing-rain storm as the first hour after freezing rain ends in which the air temperature goes above 1°C, or 24 hours after freezing rain ends, whichever occurs first. For this study, as for the U.S. ice thickness map, storms are ended only at the first hour after freezing rain ends when the air temperature goes above 1°C. This choice is more conservative than the Canadian and sometimes results in ice accreting on top of previously accreted ice that is many days or weeks old. Ideally, the sublimation and melting of accreted ice and the shedding of partially melted ice would be modeled. However, both melting and shedding are more dependent on local factors than is the accretion of ice because melting by direct or reflected solar radiation and the effect of accreted ice shape on shedding are significant. The effect of solar radiation depends on the terrain, orientation of the wire from north, color of the wire, ground cover, and the albedo of the possibly snow-covered ground. The shape of the ice accretion on a particular wire depends on the diameter and torsional stiffness of the wire, any Joule heating in the wire during the storm, and the local wind speed and temperature. The rate of melting or of shedding after partial melting also depends on the Joule heating in the wire after the storm.

* Personal communication, J. Neal Lott, Research Physical Scientist, Data Access Branch, National Climatic Data Center, 2002.

3. ST. LAWRENCE VALLEY REGION

3.1 Weather data

Data from 22 weather stations in and near the St. Lawrence Valley region were requested from AFCCC for this study. In the course of preprocessing the weather data, seven of the stations in Canada (Frelighsburg, Grenadier, La Tuque, l'Acadie, Pointe des Monts, Trois Rivieres, and Villeroy) were found to not be usable because present weather, which indicates what kind of precipitation is occurring in each hour, was not archived for the station. At another station, Riviere du Loup, present weather was archived for only 3.5 years, not long enough to provide a useful sample of freezing-rain storms. The remaining 14 stations are mapped in Figure 6 and listed with their location, elevation, periods of record (POR), and sources of the archived weather and precipitation data in Table 2.

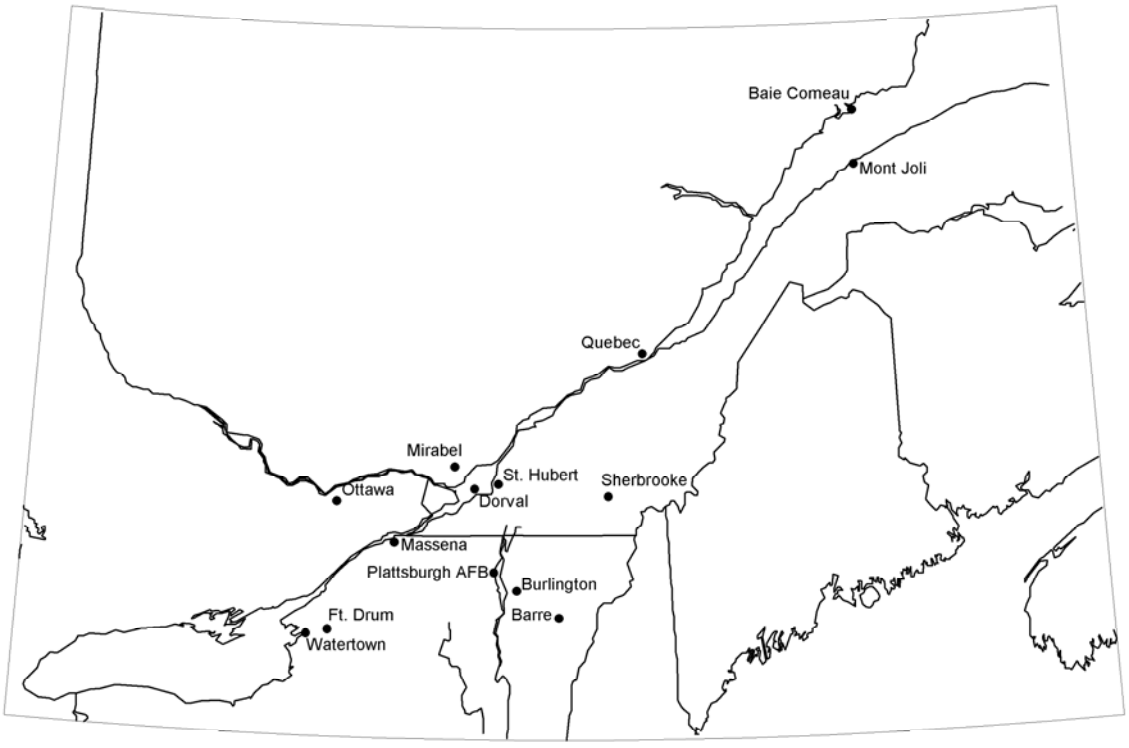

Figure 6. Weather stations in the St. Lawrence Valley region.

Table 2. Weather stations in the St. Lawrence Valley region.

Weather station		Call letters	Elev. (*m*)	Source of data	Hourly weather data POR	Daily precip data POR	Overall POR
Ottawa	ON	YOW	114	AFCCC EC	1/73–3/98 1/54–12/73	1/54–12/98	1/54–3/98
Baie Comeau	QC	YBC	22	AFCCC	7/77–3/98	—	7/77–3/98
Mont Joli	QC	YYY	52	AFCCC	1/73–3/98	—	1/73–3/98
Montreal Dorval	QC	YUL	36	AFCCC EC	1/73–3/98 1/54–12/73	1/54–12/98	1/54–3/98
Montreal Mirabel	QC	YMX	82	AFCCC EC	11/75–3/98	10/75–12/98	11/75–3/98
Montreal St. Hubert	QC	YHU	27	AFCCC EC	1/73–3/98 1/54–12/73	1/54–12/98	1/54–3/98
Quebec City	QC	YQB	73	AFCCC EC	7/73–3/98 1/54–12/73	1/54–12/98	1/54–3/98
Sherbrooke	QC	YSC	241	AFCCC EC	1/73–6/77, 1/82–3/98 1/62–12/81	5/62–12/98	5/62–3/98
Fort Drum	NY	GTB	207	AFCCC	11/88–3/98	—	11/88–3/98
Massena	NY	MSS	65	AFCCC	1/49–3/98	8/48–12/98	1/49–3/98
Plattsburgh	NY	PBG	72	AFCCC	1/73–12/92	2/81–12/93	1/73–12/92
Watertown	NY	ART	99	AFCCC	5/49–12/64, 1/73–3/98	5/49–1/98	5/49–12/64, 1/73–3/98
Barre/Montpelier	VT	MPV	355	AFCCC	1/73–3/98	1/73–6/96	1/73–3/98
Burlington	VT	BTV	104	AFCCC	1/48–3/98	1/40–1/98	1/48–3/98

3.2 Model results

The accretion of ice on a 25.4-mm-diameter wire 10 m above the ground was modeled for all the freezing-rain storms at each of the 14 weather stations using the CRREL and Simple ice accretion models. Time series of the weather and modeled ice and wind loads are shown in Figure 7a and b for two severe storms in the St. Lawrence Valley region: the February 1961 storm at Montreal–Dorval and the December 1973 storm at Quebec City. Both CRREL and Simple model results are shown, accreting only freezing rain (see Section 2.3.3). Present weather is shown in the top panel. Freezing rain is indicated by Z, ice pellets by I, snow by S, and fog or mist by F. Wind-on-ice loads are calculated using a drag coefficient $C_D = 1$ in both models; however, the computation of the load is done differently for the two models. The Simple model wind-on-ice load is based on the compact wire plus ice diameter, equal to $D + 2R_{eq}$. The CRREL model wind-on-ice load is based on the average cross-sectional dimension of the ice-covered

wire, taking into account the spacing (45 icicles/meter), length L_i, and diameter of the icicles. The cross-sectional area of icicles is $45 D_i L_i$ in each meter so the cross-sectional width used in the wind load calculation is $D + 2t + 0.45 D_i L_i$, where t is the uniform radial thickness of the ice that freezes immediately to the wire. This is discussed further in Section 5.4.

The storms at Montreal–Dorval and Quebec City illustrate some of the variety in weather conditions that are associated with freezing rain. In the 1961 storm at Dorval freezing rain was accompanied by high winds. The maximum wind-on-ice load occurred just after freezing rain ended. At Quebec City in December 1973 there were two episodes of freezing rain with moderate winds, separated by two days of very cold temperatures. The maximum wind-on-ice load occurred just after the first freezing rain episode.

In addition to detailed results for each hour of each storm, one-line summaries of each storm are generated for an overview of the storms at each station and for input into the extreme value analysis. The summary of each storm includes the start and end dates of the storm, the maximum equivalent ice thicknesses with the concurrent maximum wind speed, and the maximum wind-on-ice loads with the concurrent maximum equivalent ice thickness, for both the CRREL and Simple models. These values are provided for the case in which ice accretes only in hours with freezing rain and also for the case in which ice also accretes in hours in which the reported precipitation type is ice pellets. Thus there may be four different modeled ice thicknesses for each storm at each station. This summary information for each storm at each station is used in comparing modeled equivalent ice thicknesses with qualitative storm damage information and in the extreme value analysis.

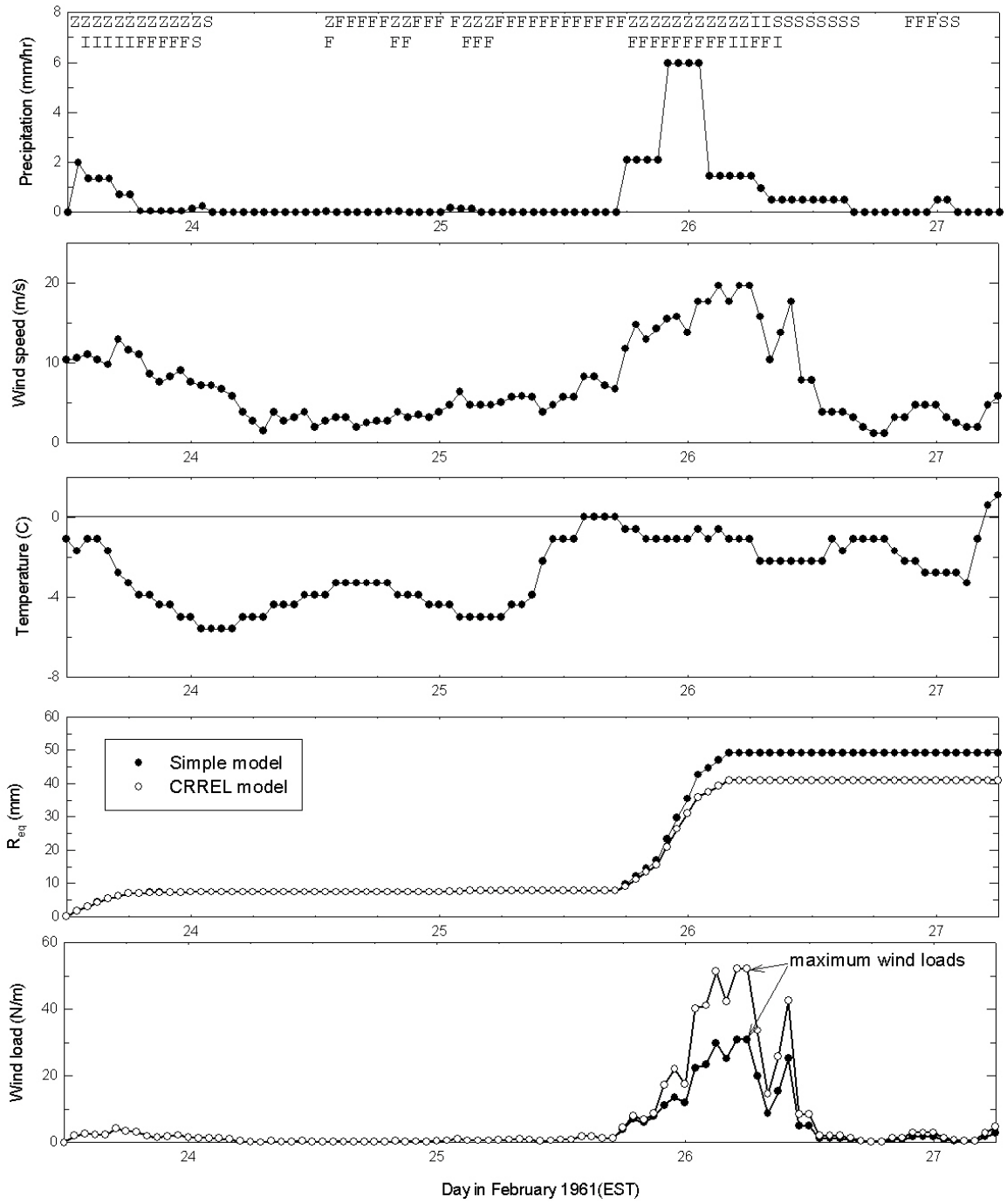

a. February 1961 storm at Montreal–Dorval.

Figure 7. Time series of the weather and modeled ice and wind loads.

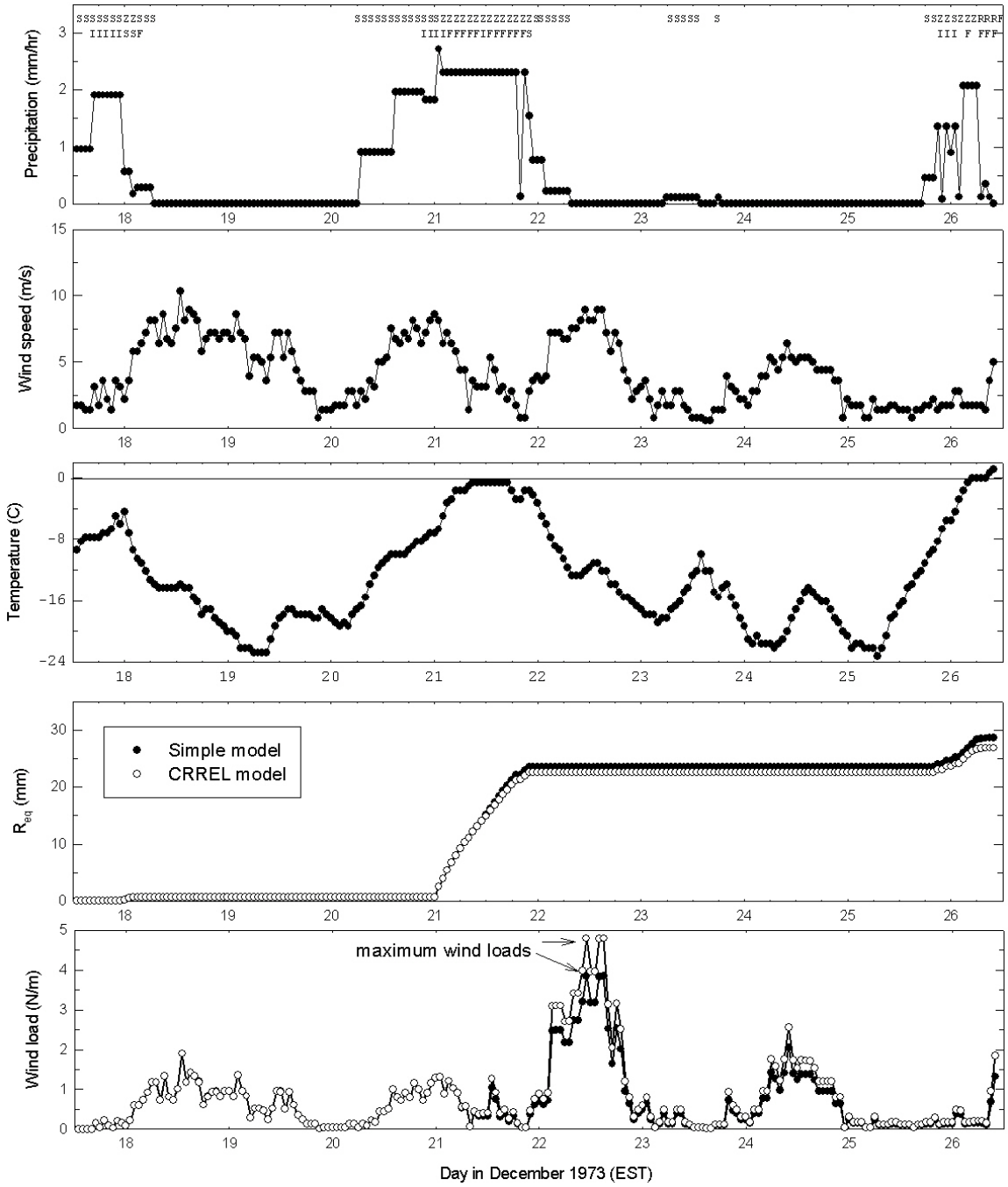

b. December 1973 storm at Quebec City.

Figure 7 (cont'd). Time series of the weather and modeled ice and wind loads.

4. POTENTIALLY DAMAGING STORMS

4.1 Definition

To check the model results, Potentially Damaging Storms (PDSs) in the St. Lawrence Valley region were chosen and qualitative information was obtained for these storms. Three criteria were used for choosing PDSs: 1) the accretion of 13 mm or more of ice from freezing rain only by the CRREL model at one or more stations, or 2) the accretion of 13 mm of ice from freezing rain only by the Simple model at one or more stations, that is also at least 6 mm more ice than the CRREL model result, or 3) the accretion of 13 mm of ice from freezing rain and ice pellets by either the CRREL or Simple model, at one or more stations, that is also at least 6 mm more than the CRREL model result for freezing rain only. A criterion is checked only if the prior criteria are not satisfied. The second criterion is used to investigate the justification for using results from the sometimes more conservative Simple model, rather than the CRREL model, in the extreme value analysis. Similarly, the third criterion is used to investigate the justification for including ice pellets in the ice thickness in the extreme value analysis. Thirteen mm (0.5 in.) was chosen as the PDS threshold both because that amount of ice is likely to damage trees and power lines and because it provides a reasonable number of storms for the in-depth investigation. Because tree damage may occur with small amounts of ice, storms with equivalent radial ice thicknesses less than 13 mm may also cause power outages.

A PDS continues as long as freezing-rain events at stations in the region continue, with freezing rain beginning at one station before the event at another station has ended. Recalling that, by definition, storms end only when the air temperature warms to above 1°C (Section 2.3), PDSs may be weeks or occasionally even months long in this region where cold winters are typical.

PDSs are test storms that *may* be damaging ice storms. Reports of downed trees and outages in the power distribution system, and perhaps in the power transmission system, are expected if the actual equivalent ice thicknesses are as high as the modeled ice thicknesses. In the 1940s and 1950s damage to telegraph lines and phone lines got more notice than damage to power lines, with lists of isolated cities and towns included in storm reports. In recent years cable television outages have been noted as well. Quantitative equivalent ice thicknesses cannot be determined from these qualitative damage reports because of the many factors contributing to ice storm damage, including, but not limited to, the design ice load and overload factors, construction errors, age, accumulated prior dam-

age, defects in components, maintenance history, dynamic loads, impact loads, high winds, cold temperatures, and progressive failure.

4.2 PDSs in the St. Lawrence Valley region

Sixty-one storms were identified in which the equivalent ice thicknesses determined by the models satisfied at least one of the three criteria at one or more stations. In 30 of the PDSs the first criterion (Z_{CRREL}) was satisfied. In ten additional storms the first criterion was not satisfied at any stations but the second criterion (Z_{Simple}) was. Twenty-one additional PDSs did not satisfy the first and second criteria at any station, but met the third criterion ($Z+IP_{CRREL}$ or $Z+IP_{Simple}$). For each PDS the start and end dates of the storm were determined and R_{eq}, from freezing rain only and from freezing rain and ice pellets, was mapped for both the CRREL model and the Simple model (Appendix D). Information was obtained primarily from newspapers, but also from *Storm Data* and other reports, on the severity of each PDS to check the modeled equivalent ice thicknesses and determine the extent of the storm.

4.2.1 Newspapers

Newspaper microfilms were obtained from local, university, state, and national libraries during and following each PDS for cities with weather stations where the modeled values were about 7 mm or more. The newspaper coverage often mentioned the location, extent, duration, and cause of any power outages and sometimes compared the storm to past ice storms. Sometimes the only effect of the precipitation that was mentioned was slippery roads, with traffic accidents and school closures being the only problems of note.

4.2.2 Storm Data

Storm Data is a National Oceanographic and Atmospheric Administration (NOAA) publication that summarizes destructive weather-related occurrences including freezing-rain storms, hurricanes, lightning strikes, tornadoes, and blizzards. It has been published since 1959 and each monthly publication is ordered alphabetically by state. The information in *Storm Data* is compiled by state using information from police reports, newspaper articles, and weather spotters. Qualitative information on the type of storm (freezing-rain storm, tornado, etc.), locations (states, forecast zones, counties, cities, or highways) where the storm was particularly destructive, and severity (number of deaths, dollar amount of damage, number of days without power, highways closed) are often included in the storm description along with the dates of the storm. Prior to 1959 the same kind of information was included in *Climatological Data,*

National Summary (NOAA 1950–1959*)*. No distinction is made in *Storm Data* between failures in the power distribution system and failures of transmission lines. *Storm Data* is a prime source for storm damage information in the United States, but it does not cover Canada.

4.2.3 Other reports

Papers describing two of the storms were published in peer-reviewed journals (Mahaffey 1961, Chaîné 1973).

4.3 Storm footprints

Using these sources along with the modeled ice thicknesses previously mapped, the footprint of the severe portion of each of the PDSs was determined. This determination was based on the available information, which was sometimes incomplete, vague, or conflicting. The storm footprint delineates the region with ice storm damage to overhead lines, trees, and communication towers. The ice thickness may vary significantly within the footprint of any PDS and among different PDSs. The storm footprints are compiled in Appendix D and short descriptions of the PDSs are in Table 3. This table lists the criterion (case and model) that was used to choose this storm to investigate, the start and end dates of the storm, and a summary of the severity and damage information. The case is either freezing rain only (Z) or freezing rain and ice pellets (Z+IP), as discussed in Section 2.3.3. The best model and case results are also indicated for each storm in the last column. Z_{CRREL} and Z_{Simple} refer to the CRREL and Simple models, respectively, accreting ice only in hours with freezing rain. ZIP_{CRREL} and ZIP_{Simple} refer to the CRREL and Simple models accreting ice both in hours with freezing rain and in hours with ice pellets. "$Z(IP)_{CRREL}$ best" indicates that the CRREL model accreting ice either from freezing rain only or from freezing rain and ice pellets provided the best equivalent ice thickness. For example, storm number 44 from 1 March to 7 March 1987 was chosen as a PDS based on results from the CRREL model, accreting ice only in hours with freezing rain. For that storm, the ice thicknesses determined by both the CRREL model and the Simple model, accreting ice only in hours with freezing rain, are consistent with the damage that was reported.

Newspaper reports often quote utility spokesmen on the cause of outages. Tree damage to distribution lines is the primary cause of outages in many ice storms because even a relatively small equivalent ice thickness generates a large weight of ice on the many twigs and branches of a tree (Jones 1999). The equivalent ice thickness necessary to cause severe tree damage depends on many factors, including the tree species, growth habit, age of the tree, previous disease

or damage, whether the tree has leaves or needles when the ice storm occurs, how wet or frozen the ground is, and the effectiveness of the local utility's tree-trimming program. The vast majority of damage to power lines in Maine in the January 1998 storm was from trees and branches falling on distribution lines and lower voltage transmission lines in narrow right-of-ways. In addition to tree damage to overhead lines and heavy ice loads on conductors and wires of transmission and distribution lines, outages in the PDSs were attributed to pole fires, transformers exploding, galloping wires causing short circuits or structural damage, sleet jumping (tree branches springing up into the wires of distribution lines when melting ice sheds), flashovers sometimes associated with fog, frozen switches, insulator problems, broken shield wires, frozen condensation inside transformers, wet snow either alone or accompanying freezing rain, drivers losing control on slippery roads and crashing into poles, the unexplained collapse of a bus bar at a substation, and technical problems. The duration of outages often depended on the extent of the storm and the population density. In rural areas where long distribution lines supply power to relatively few people and access roads are blocked by fallen trees and branches, it is more labor-intensive to completely restore power than in a more compact, heavily populated area. Only some of the PDSs were damaging storms. A number of the storms that were chosen based on the third criterion were actually snowstorms that were severe enough to make driving difficult and close schools, but did not affect overhead lines.

The information from the PDSs was used to help choose the model (CRREL or Simple) and case (accreting freezing rain only or freezing rain plus ice pellets) for the extreme value analysis. As shown in Table 4, two of the 61 storms were chosen based on apparently erroneous precipitation data. Not enough qualitative information was obtained for seven of the remaining 59 storms to determine the icing severity and storm footprint. Most of these storms were identified based on high modeled ice thicknesses at Baie Comeau or Mont Joli. Newspaper coverage was not obtained for many of those storms because there are only weekly newspapers in the small towns in that region. In eight of the PDSs the equivalent ice thicknesses from all the models was too high. Equivalent ice thicknesses determined by allowing the accretion of ice pellets was a good choice in only 12 of the remaining 44 PDSs. However, in 37 and 36 PDSs, respectively, results from the CRREL and Simple models, accreting ice only in hours with freezing rain, were consistent with the severity of damage, or the lack of damage. Results from these two simulations are used in the extreme value analysis.

Table 3. Descriptions of PDSs.

#	Case	Model	Start	End	Description and Comments
1	Z+IP	Simple	12/30/48	12/31/48	Ice 2" in diameter in New York; ice on wires as thick as a man's wrist in Vermont; miles of wires and poles broken; $Z(IP)_{Simple}$ best.
2	Z+IP	Simple	2/14/50	2/15/50	More than 1/2" ice on wires in Central Square and Lacona, New York; communications disrupted; ZIP_{Simple} best.
3	Z	CRREL	11/7/51	11/7/51	Ice and wind storm in Massena area; 1/2" of ice on runway; power out for several hours in downtown and longer in rural area; 1942 ice storm recalled; windy in Cornwall, Canada; no data in Canada; Z_{CRREL} or Z_{Simple} best.
4	Z	CRREL	3/21/55	3/22/55	In Ontario this was a rain, wet snow, and wind storm that caused flooding; blizzard in Montreal; Z_{CRREL} loads are too high.
5	Z	Simple	11/27/59	12/3/59	Power and phone line damage from weight of ice and ice-covered trees in Burlington area and Franklin and Grande Isle counties; lines were recently refurbished so damage was not as bad as it might have been; ice at highest elevations in southeast Vermont but little damage; floods in northeast Vermont; radio tower in Boonville, (south of Watertown) toppled by ice and snow; $Z(IP)_{Simple}$ best.
6	Z	Simple	3/30/60	4/2/60	No information from Quebec City.
7	Z	CRREL	2/23/61	3/3/61	Severe ice storm followed by heavy wet snow and brief period of high winds in the St. Lawrence valley; compared to storm of '42–'43 when power was out for a week in Montreal; power and phone lines and trees snapped; 460-ft tower in Potsdam toppled; greater Montreal area, Franklin, and St. Lawrence counties in NY hit hard; mostly snow east of Quebec City; severe outages in Victoriaville region; in Ontario worst ice storm since February 1950; flooding in western Vermont; Hydro Quebec reported outages in its 44kV to 230 kV systems with worst damage to wires exposed to the wind; $Z(IP)_{CRREL}$ or Z_{Simple} best.
8	Z	CRREL	1/25/64	2/5/64	Ice storm in Quebec City region caused heavy damage to power lines in communities on the north side of the river; $Z(IP)_{CRREL}$ or $Z(IP)_{Simple}$ best.
9	Z+IP	CRREL	2/21/65	3/2/65	Snow and wind in Quebec City with power outages from gusts and falling branches (data show mostly snow and ice pellets at weather station); Z_{CRREL} or Z_{Simple} best.
10	Z	CRREL	11/16/65	11/25/65	Ice-laden trees and power and phone poles snapped in Ottawa area; 1 to 1.25" ice in Nepean; winds gusting to 50 mph in some rural areas; neighboring communities harder hit than Ottawa; power outages in Montreal, but storm described as primarily snow in Montreal and Quebec City; Z_{CRREL} or Z_{Simple} best.

Table 3 (cont'd). Description of PDSs.					
#	**Case**	**Model**	**Start**	**End**	**Description and Comments**
11	Z	CRREL	12/12/65	12/31/65	Slippery roads, accidents, cancelled air flights, closed schools, and sparkling trees; all model results are too high.
12	Z	Simple	3/4/66	3/14/66	No information from Quebec City.
13	Z+IP	CRREL	1/27/67	2/5/67	Bad snowstorm; Z_{CRREL} or Z_{Simple} best.
14	Z	CRREL	12/8/67	12/12/67	Slippery roads in Montreal and short outages; worst storm in Mauricie region since 1954; wires broke from weight of ice; 2" of ice covering 1/4" wires; in some towns trees caused spotty failures; area with outages stretched from Louiseville to Batiscan; 1085-ft tower on Mt. Carmel in Trois Rivieres toppled under weight of 1" of ice; phones out in Beauce and Dorchester; $Z(IP)_{CRREL}$ or $Z(IP)_{Simple}$ best.
15	Z	Simple	3/22/68	3/23/68	Worst ice storm of the season in Quebec City area; considerable damage from freezing rain and wind; $Z(IP)_{Simple}$ best.
16	Z+IP	Simple	11/28/68	12/5/68	No information from Ottawa.
17	Z+IP	CRREL	12/28/68	1/18/69	Heavy snowstorm with some freezing rain; Z_{CRREL} or Z_{Simple} best.
18	Z	CRREL	1/25/69	1/31/69	Ice and wind in Ottawa region and western Quebec caused massive power outages; Hull, Aylmer, and Gloucester hardest hit; some phones out; slippery roads and closed schools in Massena (recalled 1942 storm); slippery roads and accidents in Montreal; not much in Quebec; Z_{CRREL} or Z_{Simple} best.
19	Z+IP	Simple	12/27/69	1/29/70	Severe snowstorm in Montreal area and Vermont; Z_{CRREL} or Z_{Simple} best.
20	Z	CRREL	1/25/71	2/26/71	Snow in Ottawa 2/9 and 2/24; icy roads in Massena 2/23; trees and wires bent under ice and snow in Ogdensburg; Montreal (1-hr outage) had snow and 60-mph winds; Sherbrooke and Quebec had snow; all model results are too high.
21	Z+IP	CRREL	12/15/71	12/16/71	Quebec area had snow with some freezing rain; freezing rain fell from there to Sudbury–North Bay area, but no outages were mentioned; photo of ice-covered tree in Ottawa; Z_{CRREL} or Z_{Simple} best.
22	Z+IP	CRREL	2/22/72	3/8/72	Power knocked out at dam near Quebec City, causing outages from there to Montreal; first reports mentioned high-voltage wires near Laval touching to cause outage as well, but discounted later; failure at dam occurred when bus bar collapsed in 735-kV system; cause unknown, mentioned Hydro Quebec report 1275; freezing rain caused local outages in the Hull and Papineauville areas; Z_{CRREL} or Z_{Simple} best.

Table 3 (cont'd).

#	Case	Model	Start	End	Description and Comments
23	Z+IP	CRREL	3/22/72	3/28/72	Severe snowstorm in Quebec City; freezing rain in the Laurentides most severe in the rural 300-sq.-mi. area defined by LaChute–Berthieville–Ste. Adele–Laval north of Montreal; distribution lines hard hit; 1–2" of ice on wires with 40–50 mph winds; ice only within 50 ft of the ground; outages lasted more than three days up to a week; described as the most damaging storm ever in the rural areas north of Montreal; Z_{Simple} best.
24	Z+IP	CRREL	12/13/72	1/1/73	Storm with snow, rain, ice pellets, and wind in Quebec City; snow followed by freezing rain and rain in Montreal; Z_{CRREL} or Z_{Simple} best.
25	Z	CRREL	1/28/73	2/3/73	Freezing rain in greater Quebec City and east caused heavy damage to the power and phone lines on the north shore of the river; 2" thick ice in some regions; 1" ice on phone poles; outages caused by ice-covered trees falling on wires; some outages lasted longer than a day; $Z(IP)_{CRREL}$ or $Z(IP)_{Simple}$ best.
26	Z	CRREL	12/14/73	12/28/73	Flooding threatened in Vermont; slippery roads in New York and scattered outages from ice-covered branches falling on wires and frozen switches; thick ice on trees and wires in Massena; outages in Quebec City and east to Mont Joli and Gaspé; severe outages in Mont Joli region, many without power east of Quebec for up to six days; water filtration system out in Ste. Foy; mostly snow with some freezing rain in Sherbrooke and Montreal; circuit breakers tripped by ice in Montreal; some relatively minor outages in southwest Montreal (pole knocked down by truck, circuit breakers tripped) and short outage in Ottawa; worst ice storm since 1961; worst ice storm of the century in the lower St. Lawrence region; gusty winds after storm; Z_{CRREL} or Z_{Simple} best.
27	Z	CRREL	12/9/75	12/15/75	Snowstorm and icy roads in Montreal; nothing interesting in Quebec; slush in Ottawa; all model results are too high.
28	Z	Simple	12/26/75	1/26/76	Outages in Quebec City area; not windy; Z_{CRREL} best.
29	Z	CRREL	2/28/76	3/6/76	Severe ice storm in southwestern Ontario; Ottawa escaped brunt of storm, but heavy rain followed freezing rain and flooding was a problem; all model results are too high.
30	Z	CRREL	12/20/76	2/27/77	Outages throughout eastern Ontario and Ottawa valley from ice and winds gusting to 60 km/hr; 3/4 of city without power in Aylmer; outages in Sept Isle caused by winds of 100 to 130 km/hr in snow, rain and wind storm; snow in Montreal and Quebec City; Z_{CRREL} or Z_{Simple} best.
31	Z	CRREL	12/22/77	2/25/78	Freezing rain caused outages in Quebec City area; flooding in Beaupre, east of Quebec City; technical problem in Churchill caused outage in large parts of Montreal, Quebec City, and the Eastern Townships; Z_{CRREL} best.

Table 3 (cont'd). Description of PDSs.

#	Case	Model	Start	End	Description and Comments
32	Z	CRREL	3/21/78	4/6/78	Snow and rain in Montreal; snow and slush in Quebec City; Z_{CRREL} or Z_{Simple} best.
33	Z+IP	CRREL	1/1/79	1/26/79	Snow, ice pellets, freezing rain, and rain in Vermont caused icy sidewalks and closed roads; snow followed by freezing rain in Ottawa caused icy roads and cancelled flights; outages affected many in Montreal; ice on wires and transformers with winds up to 30 mph; outages in the Sherbrooke area caused by ice and wind; snow, ice pellets, and freezing rain in Montreal, many outages caused by ice on wires and transformers; hardly any freezing rain in Quebec City; Z_{CRREL} or Z_{Simple} best.
34	Z+IP	CRREL	11/25/80	12/3/80	Freezing rain caused transformer wires to snap in West Island communities of Montreal; Z_{CRREL} or Z_{Simple} best.
35	Z+IP	CRREL	1/23/82	2/15/82	Snow followed by freezing rain in Vermont; snow and freezing rain in Montreal closed schools and highways; snow in Eastern Townships; snow in Quebec City; Z_{CRREL} or Z_{Simple} best.
36	Z+IP	Simple	12/15/82	12/25/82	Outages in the Quebec City metro area; warmed up quickly in Montreal area; Z_{CRREL} or Z_{Simple} best.
37	Z	Simple	1/10/83	1/11/83	No information from Baie Comeau.
38	Z+IP	CRREL	11/5/83	11/6/83	Wind, ice, and wet snow on trees in Montreal and Joliette region caused outages; worst disaster for trees in Montreal, especially on Mont-Royal, in 20 years; Z_{Simple} best.
39	Z	CRREL	11/28/83	2/4/84	Outages in Gatineau from freezing rain in late November. In early December outages caused by wet snow in Montreal; in mid-December flooding in Vermont and Sherbrooke area; widespread outages in Lewis and St. Lawrence counties (NY) from freezing rain; severe outages in Quebec City and Montreal, worst since early 70s in Quebec City (2 cm of ice), worst in 25 years in Montreal; in Belleville (west of Kingston) ice-laden trees broke power lines, also outages in Cornwall, but worse in Montreal area; Z_{CRREL} or Z_{Simple} best.
40	Z	Simple	11/12/84	11/12/84	No information from Mont Joli.
41	Z+IP	CRREL	1/1/85	2/23/85	Flooding in northern New York at the end of December following brief slippery roads from freezing rain; fog and freezing rain and ice pellets in eastern Ontario and western Quebec caused slippery roads, flight cancellations; outages in Montreal from freezing rain; flooding from Huntingdon south; Hydro Quebec reported no significant problems in transmission or distribution system because ice did not last long; no mention of storm in Baie Comeau weekly newspaper; Z_{CRREL} or Z_{Simple} best.

Table 3 (cont'd).					
#	**Case**	**Model**	**Start**	**End**	**Description and Comments**
42	Z	CRREL	1/19/86	3/18/86	Rain, sleet, and snow in Vermont caused scattered outages in CVPS, GMP, and Washington Electric service areas and downed CVPS transmission line; ice and wind in the Quebec City region caused outages from Quebec City north to Riviere du Loup; outages lasted many days, similar to storm in 1983; in Rimouski worst since December 1973; freezing rain hit Gaspé area also causing outages; 230-kV line failed; 2" of ice on wires; no outages on the north coast of the river; in March snow, rain, and freezing rain; slippery roads; no outages; $Z(IP)_{CRREL}$ or $Z(IP)_{Simple}$ best.
43	Z	CRREL	12/2/86	2/28/87	Freezing rain coated trees with 1/2" of ice in Ottawa area; numerous outages in Ottawa–Carlton region left 25% of city without power; comparable to 1973 storm; worst storm in memory of Ottawa operations manager; half of city's trees damaged or destroyed—most widespread damage in 25 years; Z_{CRREL} or Z_{Simple} best.
44	Z	CRREL	3/1/87	3/6/87	In New York the ice storm caused outages from Hammond to Potsdam and Massena; not too bad in Massena because of good tree trimming but trouble with circuit that feeds Canada; compared to 1942 storm; rain instead in most of Jefferson and Lewis counties; main Hydro Quebec line down in Ottawa in storm with freezing rain and 40–60 km/hr winds; main transmission line down in Cornwall; Brockville hardest hit; Hydro Quebec spokesman blamed galloping; outages on the south shore in Montreal; Ontario Hydro reported pole fires, sleet jumping; Z_{CRREL} or Z_{Simple} best.
45	Z	Simple	11/25/87	11/30/87	Scattered outages throughout Ottawa and Nepean; warmed quickly with freezing rain changing to rain; Z_{CRREL} best.
46	Z	Simple	11/13/89	11/15/89	No ice storm; $Z(IP)_{CRREL}$ best.
47	Z	CRREL	11/21/89	1/26/90	Freezing rain in Ottawa, but no mention of outages; snow in Montreal; all model results are too high.
48	Z	CRREL	12/4/90	12/30/90	Record snow and wind and some freezing rain in Ottawa and Montreal but no outages mentioned; freezing rain and rain in Quebec City and Gaspé peninsula causing slippery roads; outages south of Quebec City from transformer exploding; Z_{CRREL} best.

Table 3 (cont'd). Description of PDS.					
#	Case	Model	Start	End	Description and Comments
49	Z	CRREL	3/1/91	3/17/91	Major ice storm in New York's Champlain and St. Lawrence Valleys and west; ice storm caused outages across Vermont; mixed precip in Ottawa; freezing rain and ice pellets in Montreal region, many outages; flooding in Eastern Townships but heavy damage to sugarbushes north of Sherbrooke with worse damage south of there at higher elevations; outages in Estrie to thousands because of trees broken by the wind; outages in Quebec City because of high winds; Z_{CRREL} or Z_{Simple} best.
50	Z+IP	CRREL	12/3/91	12/9/91	Major snowstorm; all model results are too high.
51	Z	CRREL	1/4/92	1/24/92	Cold, freezing rain, rain, and snow in Montreal area; ice and wind in Baie Trinite with 4–5" of ice on trees and wires; long outages on south shore between Pocatiere and Matane; compared to December 1973 storm; still ice on wires on 1/14 when a snowstorm hit the area; $Z(IP)_{CRREL}$ or $Z(IP)_{Simple}$ best.
52	Z+IP	CRREL	3/10/92	3/19/92	Ice and snowstorm in New York closed schools; flooding in Montpelier; in south shore towns near Montreal outages caused by glaze and wind, and flooding; more ice on north shore than south shore; Z_{CRREL} or Z_{Simple} best.
53	Z	CRREL	4/22/92	4/25/92	No information from Mont Joli.
54	Z+IP	Simple	11/28/94	11/29/94	Snow and rain in Montreal area; Z_{CRREL} best.
55	Z	CRREL	1/6/95	1/15/95	Outages in distribution lines and main lines in Montreal in fog and freezing rain; wet in Ottawa with freezing rain causing slippery roads; slippery roads in Quebec City; Z_{CRREL} best.
56	Z+IP	CRREL	1/20/95	3/12/95	No information from Baie Comeau.
57	Z	Simple	2/23/96	3/12/96	Storm not mentioned in Baie Comeau weekly; probable error in Baie Comeau precip data (delete storm).
58	Z	CRREL	12/28/96	1/22/97	Severe ice storm north of Montreal; especially in Laurentides and Lanaudiere regions; hydro pylon tumbled in Louiseville; power out in Mt. Tremblant ski area; 10,000 km of Hydro Quebec lines and 200,000 poles affected; nobody has seen so much ice before, worst in Hydro Quebec history; 51 cows electrocuted; sugar bushes severely damaged; ice as thick as 2" in spots; $Z(IP)_{CRREL}$ or $Z(IP)_{Simple}$ best.
59	Z	Simple	1/23/97	1/25/97	Snowstorm; probable error in Fort Drum precip data (delete storm).
60	Z	CRREL	2/21/97	2/27/97	Many outages in five-day period in Montreal from ice and violent winds to 100 km/hr; galloping cables mentioned; severe snowstorm in Quebec City; Z_{Simple} best.
61	Z	CRREL	12/23/97	1/10/98	Severe widespread ice storm affecting the St. Lawrence valley and vicinity from Watertown to Massena, Ottawa, Burlington and Sherbrooke; Z_{CRREL} or Z_{Simple} best.

Table 4. Distribution of PDSs by best model/icing type.				
	Z_{CRREL}	Z_{Simple}	*Z+IP*	Total
PDS	30	10	21	61
Error in data	0	2	0	2
Insufficient information	1	4	2	7
All model results too high	7	0	1	8
Good model and case	37	36	12	44

The compiled footprints from the 44 damaging ice storms are shown in Figure 8. This compilation of footprints is shown quantitatively in Figure 9, which indicates the number of times each weather station was in a damaging ice storm and the number of times pairs of neighboring stations were in the same damaging storm. The areas of these 44 storm footprints are compiled in Figure 10.

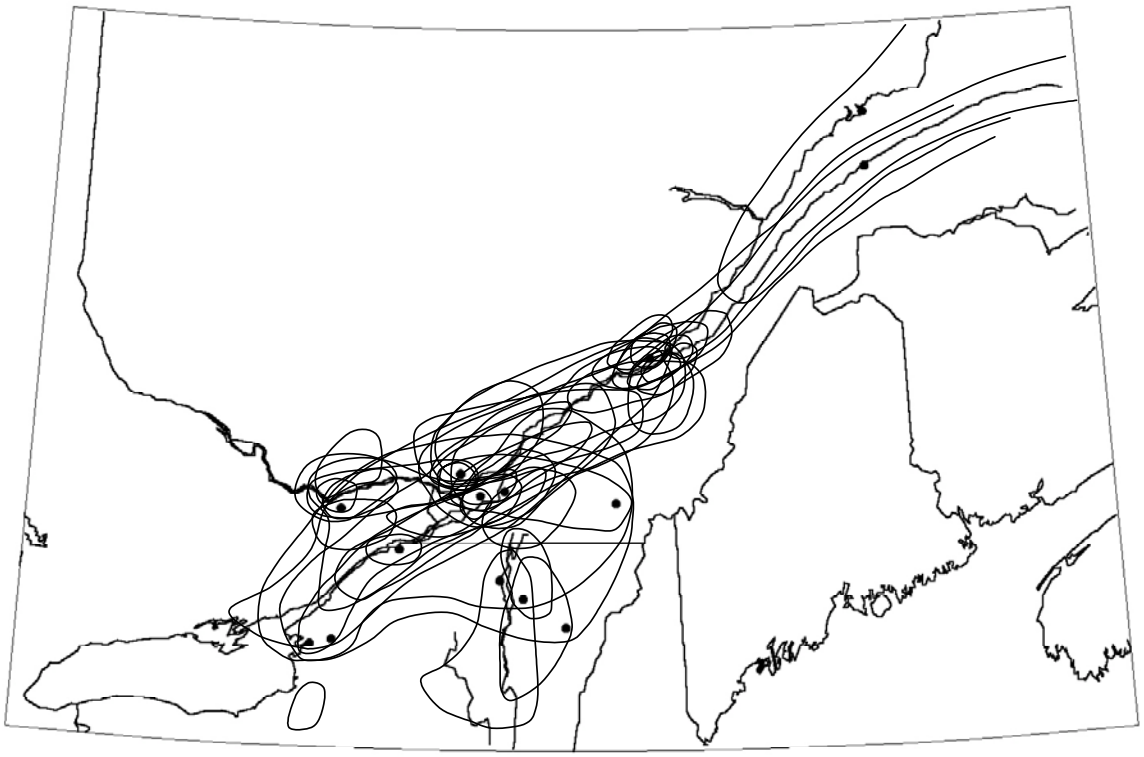

Figure 8. Compilation of damaging storm footprints for the 44 damaging storms in Table 4.

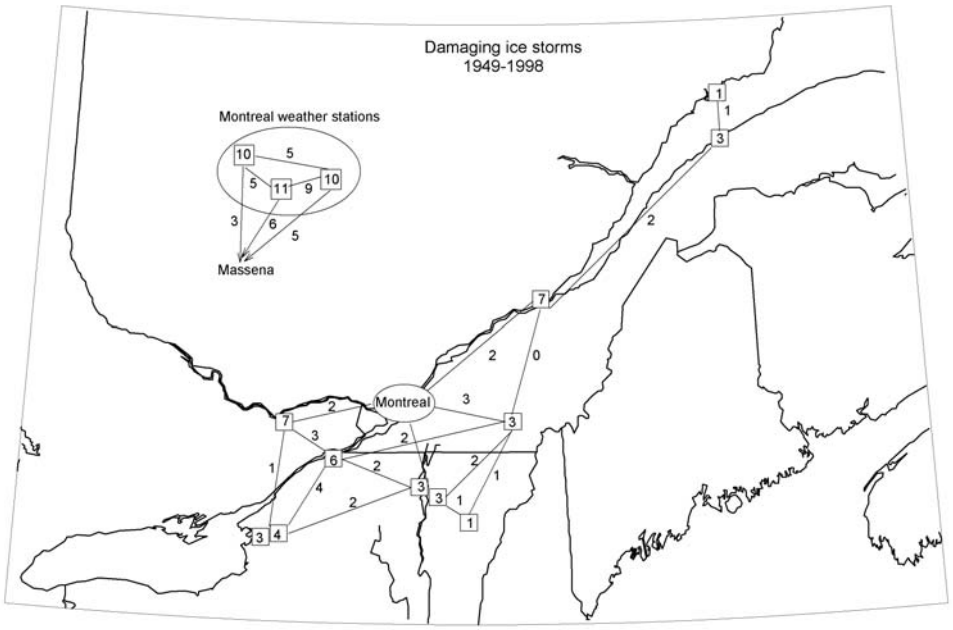

Figure 9. Occurrence of damaging ice storms for each station and station pairs. The value in the box at each station is the number of damaging ice storms at that location. The number on the line connecting two stations is the number of times those stations were in the same damaging ice storm, e.g., there were seven damaging ice storms at Quebec City and three at Sherbrooke. None of the storms that were damaging at Sherbrooke were also damaging at Quebec.

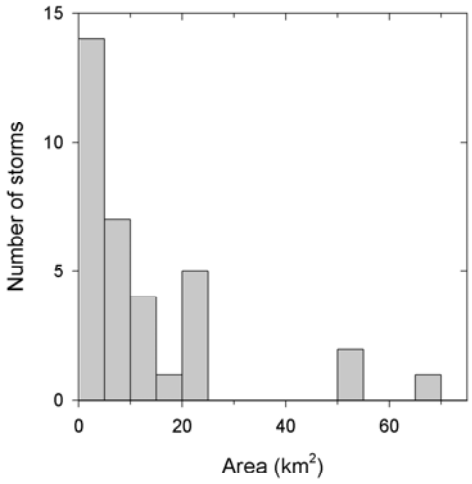

Figure 10. Distribution of footprint areas of the 44 damaging ice storms in the St. Lawrence Valley region.

4.4 Storms prior to the period of record

A number of the newspaper accounts of damaging ice storms in Canada and the United States compared those storms to the ice storm of December 1942–January 1943. Contemporaneous information on that storm was supplied by *Local Climatological Data* (NOAA 1942) and the *Massena Observer*. In northern New York the storm covered an area from Malone to Gouverneur and was called the "worst ice storm in the North Country's history." Cold weather following the freezing rain kept accreted ice from melting until 15 January. Later articles in the *Massena Observer* compared the 1942 storm to one on 26–27 March 1913 that covered an area from Malone to Cape Vincent destroying hundreds of miles of telegraph and telephone lines. More than two months later, on 2 June, not all the lines had been repaired. An editorial in the *Canton Plain-dealer*, reprinted in the *Massena Observer*, described the 1942 storm as less severe than the 1913 storm, but with more serious consequences because of the increased reliance on electric power for milking machines, heat, stoves, refrigerators, and illumination. That concern continues to be expressed, most recently in an editorial in the Russellville, Arkansas, *Courier* (Okert 2000) after two damaging ice storms in December 2000: "In the twentieth century we came to depend on electricity for many of our basic needs, such as heat and light, as well as a myriad of modern conveniences, including televisions, computers, refrigerators, washing and drying machines, telephones and scores of kitchen and household appliances. In fact, we no longer think of those things as conveniences but rather as necessities."

Equivalent ice thicknesses for these two early storms were estimated using the available weather data. There was no weather station in Massena in either 1913 or 1942. In Canada in 1913, there is daily temperature and rain and snow data for Ottawa, Montreal at McGill University, and Quebec City, and wind data at Montreal. At all three stations the maximum daily temperature was freezing or below for 26–27 March. Wind speed estimates from the measured speeds at 8 a.m. and 8 p.m. are 10 mph on the 26th and 22 mph on the 27th. Assuming that the measured precipitation on those days is freezing rain, a 30-mm equivalent ice thickness is estimated from the Montreal data, at the unknown anemometer height. The temperature warmed to above freezing on the 29th, so ice remained on trees and wires for two days after freezing rain ended. At both Ottawa and Quebec City the precipitation fell primarily as snow rather than freezing rain.

For the 1942 storm there is hourly data at Ottawa Airport and Rockcliffe (northeast of the airport), and daily data for those two stations, along with Quebec City, Dorval, and Montreal at McGill University. The hourly data indicate that the Ottawa area saw freezing rain and ice pellets on the afternoon of the

27th, which changed to snow, then freezing rain most of the day on the 29th and the morning of the 30th, again followed by snow. The hourly wind data at Rockcliffe shows very low wind speeds for a day beginning the evening of the 29th, while wind speeds remained high at Ottawa a few miles away. The low measured winds may be because the anemometer at Rockcliffe was frozen during that time, so an average wind speed of 19 mph, obtained from the Ottawa data, was used for all four stations. From the temperature data and precipitation totals, it appears that the ice storm lasted longer in the Montreal area than in the Ottawa area, with a significant amount of freezing rain falling on the 30th at the Montreal stations. Equivalent ice thickness estimates based on this information and assumptions range from 24 mm at Ottawa to 42 mm at Dorval, at the unknown anemometer height. The ice probably remained on trees and wires for weeks as temperatures stayed below freezing until mid-January.

5. EXTREME ICE THICKNESSES AND CONCURRENT WIND-ON-ICE SPEEDS

The modeled ice thicknesses at the 14 weather stations in the St. Lawrence Valley region were used to determine 50-yr return-period ice thicknesses by the peaks-over-threshold method (Simiu and Heckert 1995, Hosking and Wallis 1987, Walshaw 1994, Wang 1991, Gross et al. 1994, and Abild et al. 1992) and grouping the stations into superstations (Peterka 1992).

5.1 Superstations

The superstation concept is presented in Peterka (1992) for extreme wind speeds. The 50-yr return-period wind map in ASCE 7 (ASCE 1993) shows small regions in the Midwest with high winds. Peterka argued that these small-scale spatial variations in the estimated 50-yr wind speed were not real but were due to sampling errors from determining the parameters of the extreme value probability distribution from relatively short data records. He suggested that the records of extreme winds from different weather stations with the same wind climate be appended to each other to form a superstation with a much longer period of record. The long period of record of a superstation supplies many more extremes to use in the extreme value analysis and thus produces better estimates of the parameters of the extreme value distribution. For example, Peterka created a wind superstation that included 29 stations in 11 states and had a 924-yr period of record. The limitation on forming the superstation was the requirement that the maximum annual winds from the different stations in the superstation should be uncorrelated. If extreme winds at two stations are highly correlated, then including the second station supplies no new information on the extreme wind climate.

Sampling errors in the estimation of extreme loads can be significant for the electronic data records of weather stations in the St. Lawrence Valley region, which have periods of record ranging from about 10 to 50 years. At any weather station the probability that the 50-yr return-period ice thickness has occurred increases as the period of record increases. However, large ice thicknesses with long return periods may have occurred at a station with a short period of record, and conversely, only short return-period ice thicknesses may have occurred at a station with a longer period of record. Thus, 50-yr return-period ice thicknesses, which are calculated from the extremes in the available sample, may change significantly as each season of ice storms is added to the historical record at a single station.

In forming the superstations in the St. Lawrence Valley region, the number of damaging storms (those compiled in Figure 8) at each station and the number of times adjacent stations were in the same damaging storm (shown in Figure 9), the frequency of ice storms causing at least 1 mm of ice (Simple model, freezing rain only) at each station (Fig. 11), station elevation (Fig. 12), along with latitude, proximity to water and relief (all shown in Figure 13), were all taken into account. (The wind roses shown in the latter figure are discussed in section 6.1.) A balance was sought between grouping only stations likely to have the same severe icing climatology against the desire to generate as long a period of record as possible to reduce sampling error.

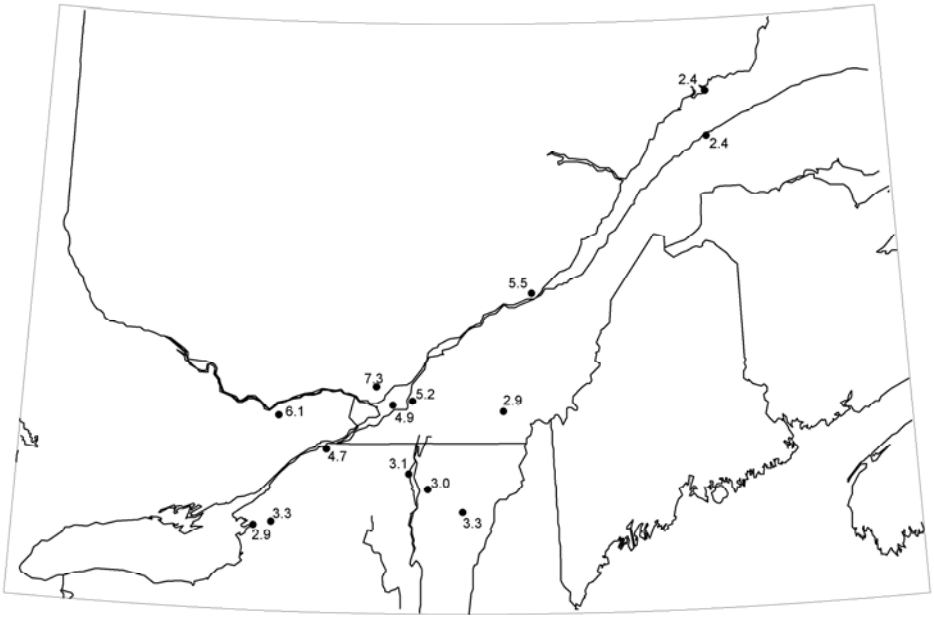

Figure 11. Frequency (number per year) of ice storms causing at least 1 mm of ice.

Ultimately, three superstations were defined in this region, leaving Barre separate. Figure 14 shows the superstation groupings as well as the periods of record for the stations and superstations. Consideration was given to grouping the three Montreal stations in their own superstation based on the greater frequency of damaging storms at those stations. However, that difference may not be real, but rather a result of having a relatively dense network of stations there. Furthermore, the storm frequency and the surrounding terrain are similar to the other stations in the upper St. Lawrence Valley. The number of stations in each of the superstations ranges from two in the Lower Valley, to five in the Southern, to six

in the Upper Valley. The length of the period of record ranges from 46 years to 249 years. Shorter periods were actually used for the Southern and Upper Valley superstations in the extreme value analysis because of the correlation between station pairs. This is discussed in section 5.3.

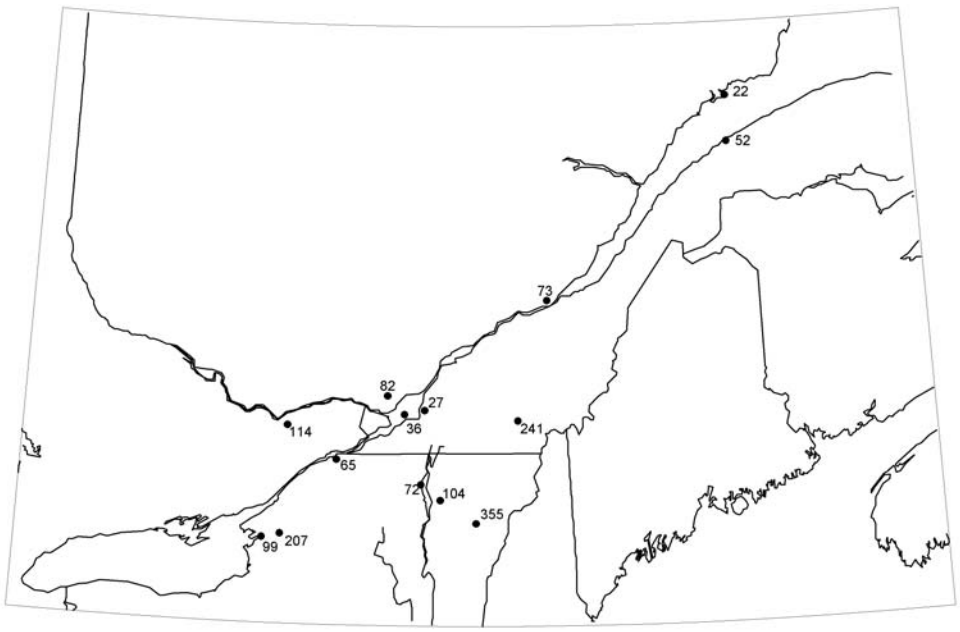

Figure 12. Elevation (m) of stations in the St. Lawrence valley region.

5.2 Peaks-over-threshold method

The epochal method is often used to provide a sample of extremes for determining the parameters of an extreme value distribution. The epoch considered is typically one year, the maximum value is found for each year in the period of record, and these annual maxima then determine the parameters of a type I (Gumbel), II (Frechet), or III (reverse Weibull) extreme value probability distribution. Gringorten (1963b) suggests the use of multi-year epochs.

The peaks-over-threshold (POT) approach is better than the epochal method for dealing with ice thicknesses for the following reasons:

- The derivation of the double exponential Gumbel distribution assumes a large number of events per year (Nash 1966). While this is a reasonable assumption for wind events, the frequency of freezing-rain storms is relatively small, even in this region where winters are cold.

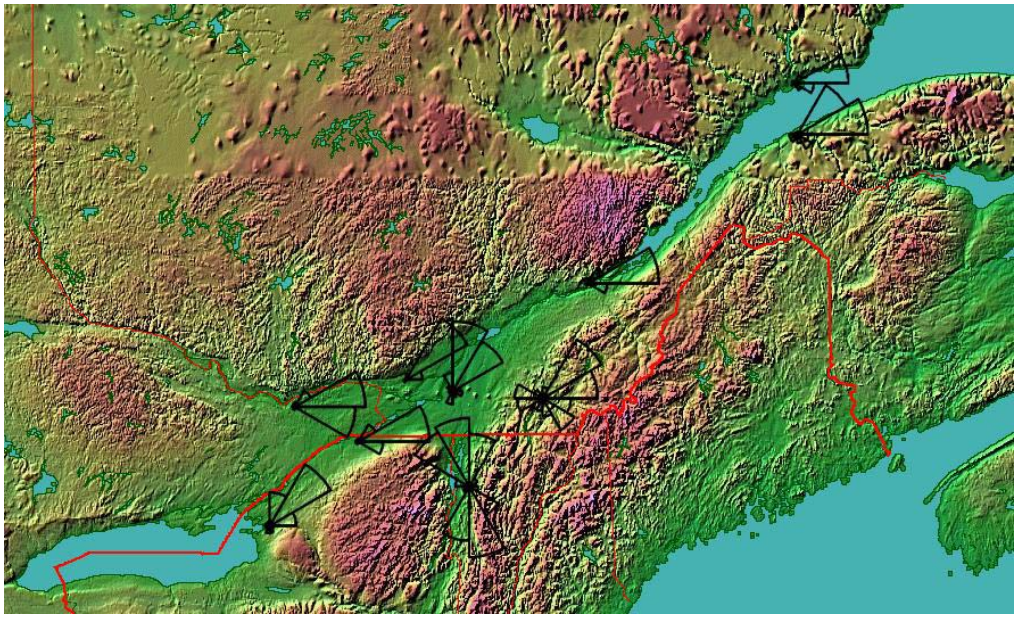

Figure 13. St. Lawrence valley region relief map with wind roses for hours with freezing rain. (After http://fermi.jhuapl.edu/states/us/big_us_color.gif.)

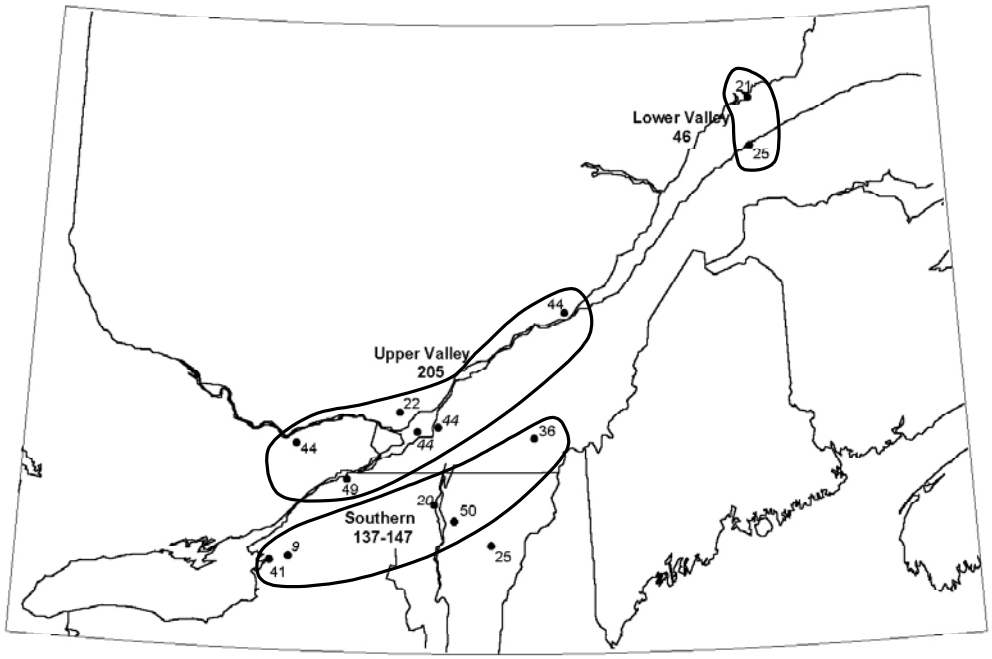

Figure 14. Superstation groupings with period of record in years for the stations and superstations.

- Some winters have no measurable freezing rain. In those years the maximum ice thickness is zero, which would have to be considered part of the extreme population in the epochal method.
- Some years will have more than one severe ice storm, each of which may cause larger ice thicknesses than the most severe storms in milder years. The epochal method would not include these severe-but-not-worst-that-year storms in the estimation of the parameters of the extreme value distribution.
- Because the calendar year ends in the middle of the winter, one could argue that it makes more sense to choose maximum ice thicknesses for the season rather than for the calendar year. In one study the parameters of the extreme value distribution depended on whether the calendar or seasonal year was used (Laflamme 1993).

These problems are avoided using the POT method because 1) the assumption of a large number of events per year is not made and 2) values are chosen as members of the extreme population if they exceed a specified threshold. The excess of the value over this threshold is used to determine the two parameters of the generalized Pareto distribution (GPD):

$$\begin{aligned} F(x) &= 1-\left[1-\frac{k(x-u)}{\alpha}\right]^{1/k} \qquad k \neq 0 \\ &= 1-\exp\left[\frac{-(x-u)}{\alpha}\right] \qquad k = 0. \end{aligned} \tag{6}$$

The threshold value is u, the shape parameter is k, and α is the scale parameter. The cases $k = 0$, $k < 0$, and $k > 0$ correspond to the extreme value distribution types I (shortest infinite tail), II (longer infinite tail), and III (finite tail length, $x < \alpha/k$) shown in Figure 15. Typically k ranges between –0.5 and 0.5. If the data are correctly described by a GPD, then k is not dependent on the load chosen as the threshold, as long as the threshold is chosen high enough. ElFashny et al. (1998) found that the GPD was one of the most suitable distributions to characterize extreme ice thicknesses.

The parameters k and α of the distribution were determined using probability weighted moments (Abild et al. 1992, Wang 1991, Hosking and Wallis 1987; L-moments in Hosking and Wallis 1997). This method is unbiased and particularly efficient for distributions with $k < 0$, which seems to be generally true of the extreme ice thickness data. Estimates of the GPD parameters are provided by

$$k = \frac{4b_1 - 3b_0 + u}{b_0 - 2b_1}$$
$$\alpha = (b_0 - u)(1 + k)$$

where (7)

$$b_0 = \frac{1}{l}\sum_{i=1}^{l} x_{(i)}$$
$$b_1 = \frac{1}{l}\sum_{i=1}^{l} \frac{i-1}{l-1} x_{(i)}$$

(Wang 1991), where the $x_{(i)}$ are the ordered sample $x_{(1)} \leq x_{(2)} \leq ... \leq x_{(l)}$ of values greater than the threshold u.

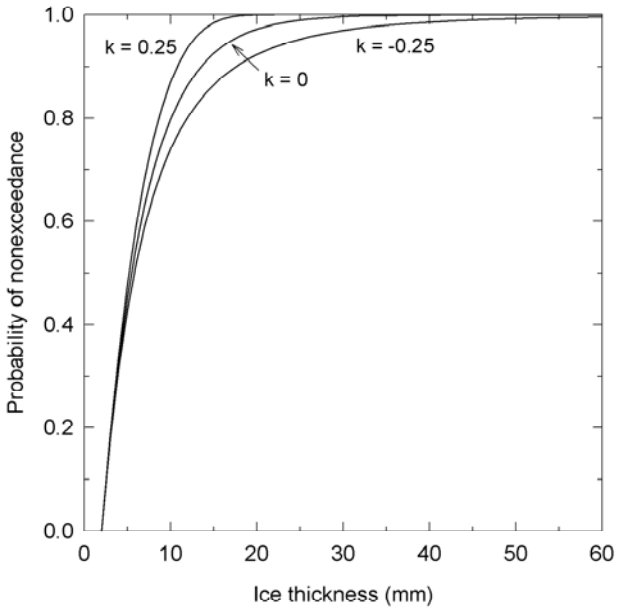

Figure 15. Generalized Pareto cumulative probability distribution.

A variety of methods can be used to define the threshold u. It should be high enough that only true extremes are used to estimate the parameters of the GPD, but low enough that there are sufficient data so sampling error is not a problem. Some authors specified the threshold as a percentile of the number of cases. For example, Walshaw (1994) used a threshold at about the 95th percentile of his 10 years of hourly maximum wind gusts. Sometimes the threshold is determined on

a physical basis (Abild et al. 1992). In this study the threshold for each superstation was chosen so that the average occurrence rate of the sample of extremes was about one/year.

Once the parameters of the distribution have been determined, the load x_T corresponding to a specified return-period T is calculated from

$$x_T = u + \frac{\alpha}{k}\left[1 - (\lambda T)^{-k}\right] \tag{8}$$

where λ is the occurrence rate (number per year) of values exceeding the threshold.

5.3 Correlations

If the ice thicknesses at pairs of stations in the superstation are correlated, then the concatenation of data from a number of stations in a superstation does not supply new information and the apparently long period of record for the superstation is not real. However, if the correlation between stations is low the stations are essentially independent.

Although the superstations are chosen with the help of the compilation of footprints of damaging storms (Section 5.1), it does not follow that extreme storms within a superstation are necessarily correlated. Ice thicknesses within the storm footprint may vary significantly from station to station. Furthermore, the damaging storms that were identified are only a fraction of storms that make up the sample of extreme ice thicknesses, i.e., those higher than the threshold.

The correlation between each pair of stations in each superstation was determined. For each pair of stations, storms that overlapped in time, i.e., an ice storm began at one station before one ended at the other station, were paired. If the ice thickness for either or both of these storms exceeded the threshold for the superstation, that pair of thicknesses was included in determining the correlation for the station pair. The extreme ice thicknesses in the sample are bounded from below by the threshold, so they are not normally distributed. Therefore, the non-parametric Spearman rank-order correlation coefficient r_s (Press et al. 1987) was used, rather than the commonly used Pearson correlation coefficient, which requires that the two variables be near normally distributed. The strength of the association between stations is given by the square of r_s. Simultaneous ice thicknesses are plotted for Dorval/St. Hubert ($r_s = 0.30$) and Massena/Quebec City ($r_s = -0.21$) in Figure 16.

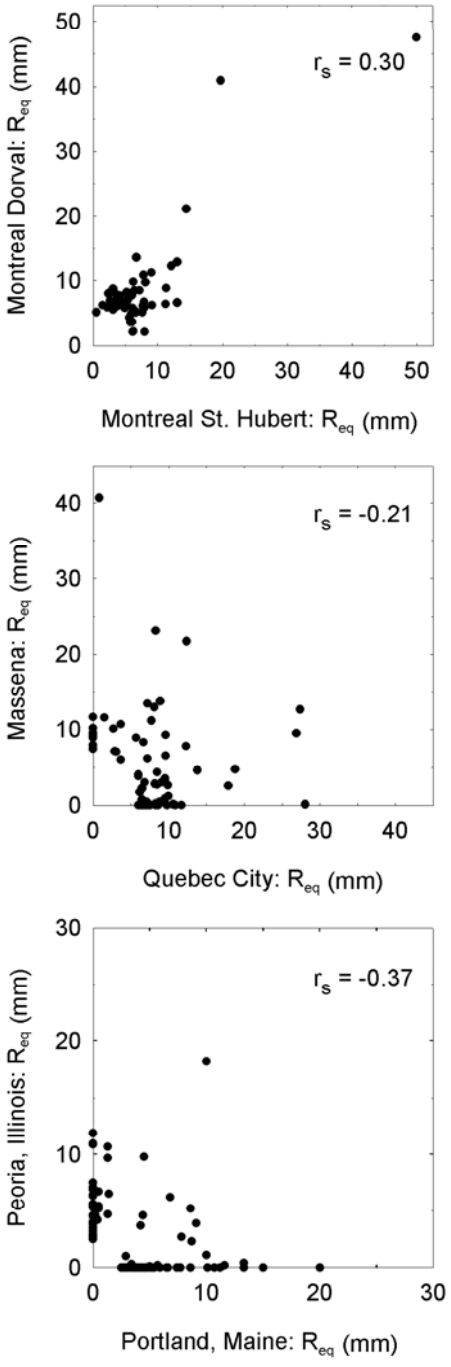

Figure 16. Simultaneous extreme ice thicknesses for Dorval/St. Hubert (top) (r_s = 0.30), Massena/Quebec City (middle) (r_s = –0.21), and Peoria/Portland (bottom) (r_s = –0.37).

The correlation coefficient r_s is presented in Table 5 for each station pair in each superstation. For comparison, the correlation between ice storms in Portland, Maine, and Peoria, Illinois, was also calculated. These stations were chosen because the period of record for both stations is long (1949–1995), both are in zones with high 50-yr return period ice thicknesses (1.25" and 1", respectively, ASCE 2000), and the stations are far enough apart (1600 km) that they are not expected to be hit by the same ice storms. For this pair $r_s = –0.37$, and, as shown in Figure 16 (bottom), significant ice thicknesses typically occur at one station with no ice at the other station. Thus, in this context, negative correlation coefficients indicate a lack of correlation.

Table 5. Correlation of station pairs.

Station pairs		r_s
Mirabel	St. Hubert	0.09
	Dorval	0.17
	Ottawa	0.01
	Quebec City	–0.06
	Massena	–0.14
St. Hubert	Dorval	0.29
	Ottawa	–0.12
	Quebec City	–0.28
	Massena	0.02
Dorval	Ottawa	–0.07
	Quebec City	–0.24
	Massena	0.14
Ottawa	Quebec City	–0.16
	Massena	–0.11
Quebec City	Massena	–0.29
Fort Drum	Watertown	0.02
	Plattsburgh	0.40
	Burlington	0.25
	Sherbrooke	–0.03
Watertown	Plattsburgh	–0.09
	Burlington	–0.07
	Sherbrooke	0.04
Plattsburgh	Burlington	–0.11
	Sherbrooke	–0.26
Burlington	Sherbrooke	–0.29
Mont Joli	Baie Comeau	0.17

In some cases the correlation between a pair of stations was high enough that the stations were not included in the same superstation. In the Southern superstation r_s ranged from –0.16 for Plattsburgh/Sherbrooke to 0.40 for Fort Drum/Plattsburgh. Because of the relatively high correlation between Fort Drum and Plattsburgh, the Southern superstation is analyzed twice in the extreme value analysis, once including Plattsburgh but not Fort Drum, and once including Fort Drum but not Plattsburgh. In the Upper Valley superstation r_s ranged from –0.28 for Quebec City/St. Hubert to 0.29 for St. Hubert/Dorval. Because of the relatively high correlation between St. Hubert and Dorval, the Upper Valley superstation is also analyzed twice in the extreme value analysis, once including Dorval but not St. Hubert, and once including St. Hubert but not Dorval.

5.4 Wind-on-ice speeds

The amount of ice that accretes on a wire is affected by the speed of the wind that accompanies the freezing rain. Wind speeds during freezing rain are typically moderate, ranging between about 2 and 7 m/s. However, the ice that accretes on a wire may last for days or weeks after the freezing rain ends, as long as the weather remains cold. Thus the ice-laden wires may be exposed to high winds that occur after the storm. The wind speeds to use in combination with extreme ice thicknesses are determined from the modeled wind-on-ice loads at the weather stations in this region.

As described in Section 3.2, the summary information for each freezing-rain storm includes the calculated maximum wind-on-ice load at the maximum ice thickness (a conditional maximum) as well as the maximum wind-on-ice load that occurred at any time during the storm (the absolute maximum). The peaks-over-threshold method was used to calculate the parameters of the distribution of extreme wind-on-ice loads for individual weather stations and the three superstations. By assuming that the maximum wind-on-ice load in each storm occurs with the maximum ice thickness, which is somewhat conservative (Fig. 17), one can back-calculate the wind-on-ice speed U_c from the 50-yr return-period wind-on-ice load F_{50} and the 50-yr return-period ice thickness R_{eq50}:

$$U_c = \sqrt{\frac{2F_{50}}{\rho_a C_D (D + 2R_{eq50})}} \,. \tag{9}$$

ρ_a is the density of air, D is the diameter of the bare wire, and $C_D = 1$ is the drag coefficient. As can be seen by its formulation, U_c is the wind speed that when used in combination with the 50-yr return-period ice thickness gives the 50-yr return-period wind-on-ice load. It is not an extreme wind. Essentially the same

value is obtained if the 100-yr or 200-yr ice thicknesses and wind-on-ice loads are used to calculate U_c.

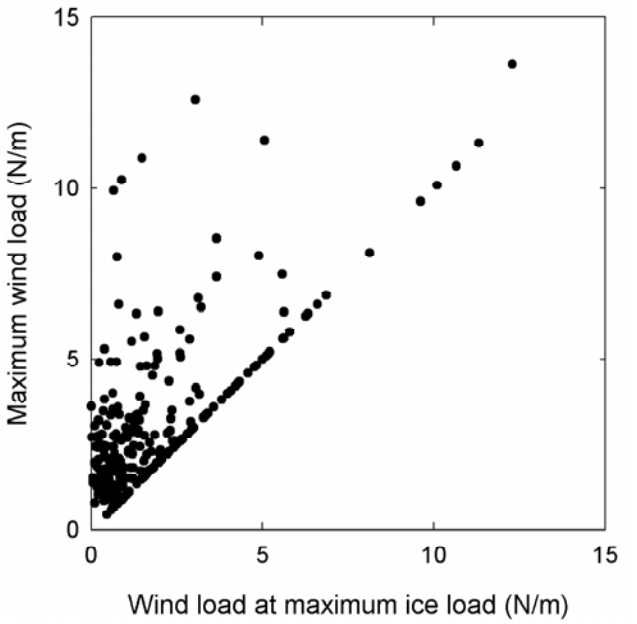

Figure 17. Comparison of the maximum wind-on-ice load with the maximum wind-on-ice load at the maximum ice thickness.

When U_c is calculated from the Simple model results, the wind-on-ice load is determined for the compact ice cross section $D + 2R_{eq}$. However, when it is calculated using the CRREL model results, U_c accounts, albeit crudely, for the increase in wind drag on the iced wire because of icicles, while retaining an ice thickness expressed in terms of the equivalent uniform radial ice thickness. Recall (Section 3.2) that, in the CRREL model, the wind-on-ice load is calculated using the average maximum ice plus wire cross-section width $D + 2t + 0.45D_iL_i$, which is larger than $D + 2R_{eq}$ when there are icicles. Thus the concurrent wind speed determined from the CRREL model is typically greater than that determined from the Simple model.

The wind-on-ice loads calculated for each storm are based on the 1- or 2-minute average wind speeds that are reported at each regular hourly observation at the weather stations. Therefore U_c is an hourly wind speed, rather than a 3-s gust speed or a fastest-mile wind speed. Gust speeds are recorded at military weather stations in the United States whenever there is a rapid change in wind speed with at least a 10-knot difference between the high and low speeds. The gust speed is recorded as part of the regular hourly observations if it occurs

within ten minutes of the observation. Otherwise it is recorded in a special weather observation. In a previous study (Jones 1997), I used gust speeds at a number of Army and Air Force weather stations to calculate the gust-on-ice speed $G_{c,}$ and then determined the ratio between G_c and U_c:

$$f_{gust} = G_c / U_c = 1.34. \tag{10}$$

This value is larger than the ratio of a 3-s gust speed to the speed for that gust averaged over one or two minutes (1.21 to 1.29) calculated from the Durst curve (ASCE 2000), because the archived hourly wind speeds are measured at a fixed time rather than at the time of the gust.

G_c was estimated from U_c for each station and superstation in the region using f_{gust}.

5.5 Extreme ice thicknesses and concurrent wind speeds

A threshold ice thickness was chosen for each superstation to give an occurrence rate of about one/year for the sample of extremes. This resulted in threshold ice thicknesses varying from 2.2 to 6.9 mm and occurrence rates λ for extreme ice thicknesses varying between 0.96 and 1.05 per year in the superstation record. In Figure 18, fitted GPDs with parameters determined by equation 7 are compared to the sample of extreme ice thicknesses from the Simple model for the three superstations. The plotting position of the ith value is

$$p_i = \frac{i - 0.4}{n + 0.2} \tag{11}$$

where n is the number of years of record and $i = 1,\ldots,n$ is the rank of the ice thicknesses from largest to smallest. This is a compromise plotting position that is nearly unbiased for all distributions (Cunanne 1978). In this figure the vertical scale is chosen so that the fitted curve is a straight line if the shape parameter $k = 0$. For $k < 0$ the curve is concave down, indicating a smaller increase in return period with increasing ice thickness than for $k = 0$, as is shown for the three superstations. For Barre, $k > 0$, the return period increases rapidly with increasing ice thickness and the maximum ice thickness is $\alpha/k = 23$ mm.

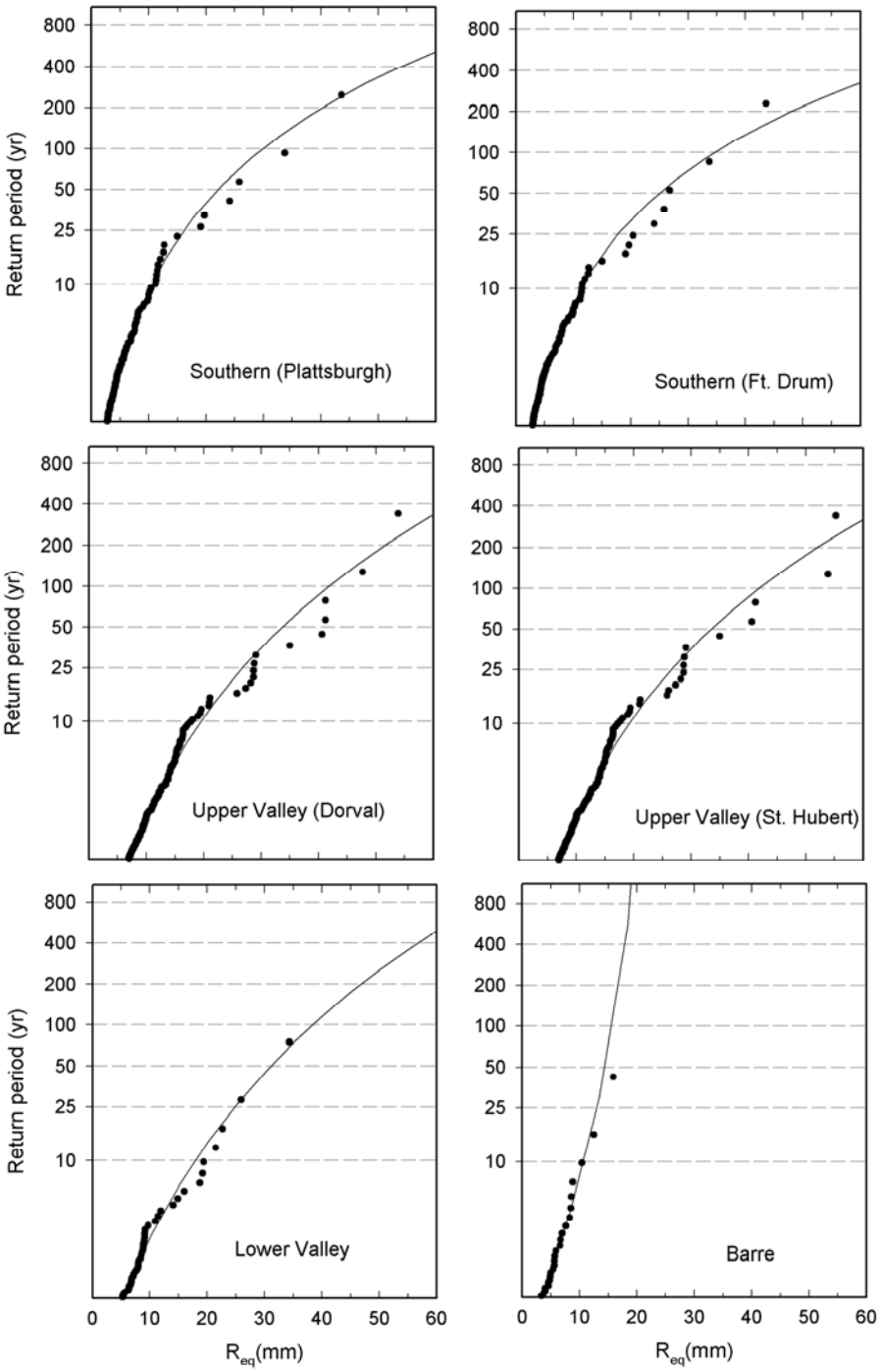

Figure 18. Fitted GPDs and the samples of extreme ice thicknesses from the Simple model for the three superstations and Barre.

Table 6. Results of extreme value analysis.

	N years	Simple model				CRREL model			
		R_{eq50} (mm)	R_{eq100} (mm)	R_{eq200} (mm)	U_c (m/s)	R_{eq50} (mm)	R_{eq100} (mm)	R_{eq200} (mm)	U_c (m/s)
Barre/Montpelier	25	14	16	17	13	12	14	16	14
Southern–Plattsburgh	**147**	**22**	**30**	**40**	**13**	**14**	**19**	**24**	**16**
Southern–Fort Drum	**137**	**25**	**35**	**48**	**12**	**17**	**23**	**30**	**15**
Burlington	50	17	24	34	11	11	13	16	13
Watertown	41	31	42	58	13	20	26	34	18
Plattsburgh	20	10	12	15	13	9	11	14	14
Sherbrooke	36	23	32	43	11	15	20	26	14
Fort Drum	9	37	59	95	10	30	49	80	11
Upper Valley–Dorval	**205**	**34**	**42**	**52**	**14**	**30**	**38**	**49**	**17**
Upper Valley–St. Hubert	**205**	**33**	**42**	**52**	**14**	**30**	**38**	**49**	**17**
Massena	49	27	36	49	15	24	32	43	18
Montreal Dorval	44	34	47	66	15	30	40	54	18
Montreal Mirabel	22	52	70	94	12	46	66	97	14
Montreal St. Hubert	44	31	44	63	15	28	39	55	19
Ottawa	44	27	30	33	15	26	31	36	16
Quebec	44	31	37	44	13	29	36	45	15
Lower Valley	**46**	**31**	**38**	**46**	**15**	**24**	**30**	**38**	**16**
Baie Comeau	21	21	24	27	17	11	11	11	21
Mont Joli	25	40	55	76	14	32	45	62	15
REGION	**477**	**30**	**38**	**47**	**14**	**25**	**31**	**39**	**17**

The extreme value analysis for ice thicknesses for the stations and superstations is summarized in Table 6 for the CRREL and Simple models, accreting only freezing rain. The table lists the number of years in the period of record and the results of the extreme value analysis for 50-, 100-, and 200-yr return periods for each station and superstation. For the Upper Valley superstations, which include the Montreal area, the 50-year ice thickness based on the Simple model is 33 or 34 mm, increasing to 42 mm for a 100-year return period, and 52 mm for a 200-year return period. Note that the extreme ice thicknesses for individual stations with one or more high values in the period of record tend to be higher than those for the corresponding superstation. For example, the 100-yr ice thicknessess at Dorval and Mirabel are 47 and 70 mm, respectively, compared to 42 mm for both Upper Valley superstations. This occurs because the highest thicknesses at the individual stations are assigned to a higher probability of occurrence than they are in the superstation, which has a much longer period of record. This

phenomenon is especially pronounced at Mirabel and Fort Drum, with 22-year and nine-year records, respectively. On the other hand, relatively few significant ice storms occurred at Plattsburgh in the 20 years of record from 1973 through 1992.

The extreme ice thicknesses for the Southern superstation are smaller than for the Upper Valley superstation. The extreme ice thicknesses for the Lower St. Lawrence Valley are only slightly smaller than those for the Upper St. Lawrence Valley. However, the periods of record for the data archived by AFCCC for both Baie Comeau and Mont Joli are relatively short. Additional hourly weather data and high-quality daily precipitation data for these stations were not obtained from Environment Canada because the stations were expected to be of only peripheral importance in understanding the severe icing climatology in the Montreal area. Furthermore, the lack of a daily newspaper in the region around Baie Comeau and Mont Joli made it difficult to establish the true severity of the PDSs that occurred in that region. To better determine extreme ice thicknesses for the Lower St. Lawrence Valley, it should be reanalyzed in conjunction with the surrounding region including the Gaspé Peninsula, New Brunswick, and northern Maine.

Utilities sometimes use a design case of an extreme ice thickness with no wind. However, as freezing-rain storms are accompanied by at least some wind, there is not a no-wind ice thickness larger than those in Table 6. The concurrent wind speed U_c is shown in Table 6 for both the Simple and CRREL models. U_c is essentially independent of return period, so the speeds shown in Table 6 are the averages of the 50-, 100-, and 200-yr calculated values. As expected, the concurrent speeds from the CRREL model are higher than those from the Simple model, by a few meters per second. The gust-on-ice speed G_c is 34% higher than U_c (equation 10). Using the CRREL gust speed along with the Simple model ice thickness would result in a 50% increase in the design gust-on-ice load for the Upper Valley superstation compared to using the Simple model gust speed, which is calculated with no compensation for the likely less-compact shape of an actual ice accretion.

The 50-yr return period ice thicknesses and concurrent gust speeds from the Simple model are mapped in Figure 19. The superstation boundaries on the northern and southern sides of the St. Lawrence, shown by dashed lines, are based on the change in terrain (Fig. 13). The location of the boundary between the Upper and Lower Valley superstations, downriver from Quebec City, is based on the compiled damaging storm footprints in Figure 8. A 50-year ice thickness south of the Southern superstation is not shown, because of the imprudence of generalizing from the 25 years of record at Barre. For the map of 50-year return period ice thicknesses in the United States for the 1998 revision of ASCE 7

(ASCE 2000), Barre was ultimately included in an amorphous group of stations in the Northeastern states that did not belong in any homogeneous superstation. Ice thicknesses are not mapped for the Lower Valley because of concerns about the data quality from AFCCC at Mont Joli and Baie Comeau.

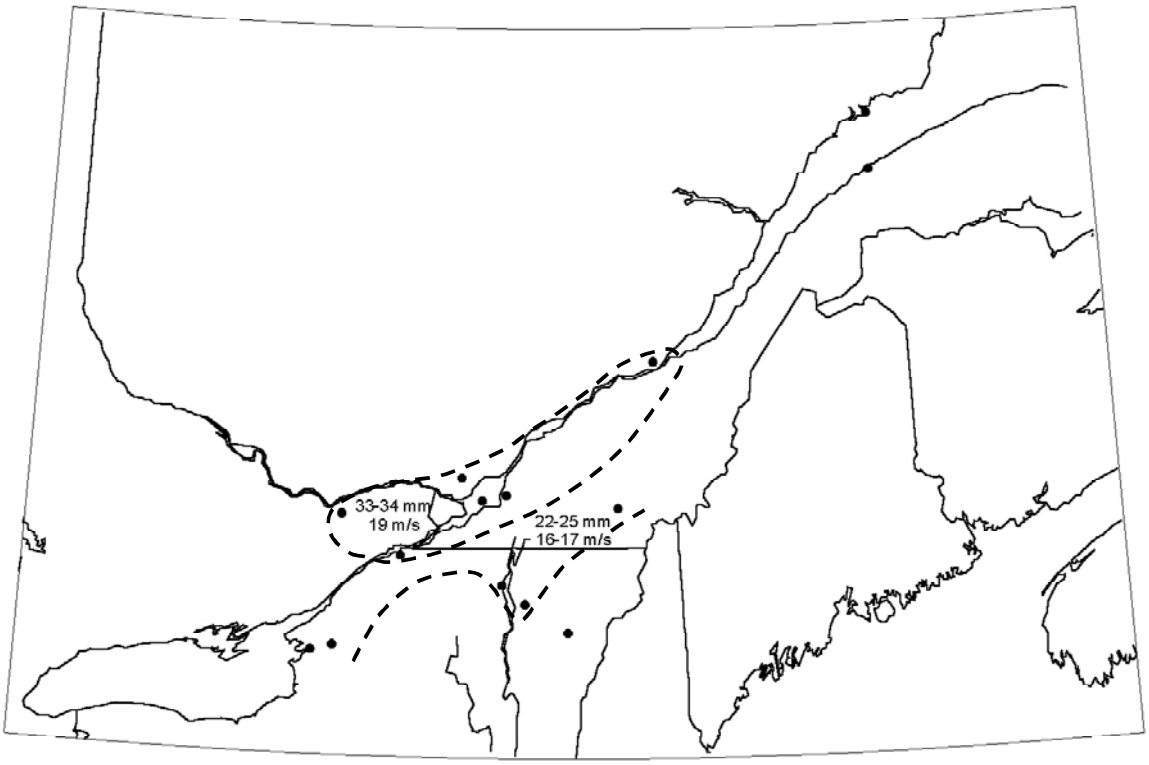

Figure 19. Map of 50-yr return-period ice thicknesses and concurrent gust speeds from the Simple model.

5.6 Gumbel extreme value analysis

Since the Gumbel distribution

$$P(x) = \exp\left(-\exp\left[-\alpha\left(x-u\right)\right]\right) \tag{12}$$

is often used by utilities for extreme value analyses (ASCE 1991), the results of a Gumbel analysis are compared to the peaks-over-threshold analysis used in this study. The assumption of a large number of events per year that leads to the double-exponential Gumbel distribution is not satisfied for ice storms (Section

5.2). Therefore, the Gumbel distribution can be considered the appropriate distribution for estimating extreme ice thicknesses only if the distribution provides a good fit to the data.

The method of moments recommended in ASCE Manual 74 (ASCE 1991) is used to determine the parameters α and u of the Gumbel distribution from the data for the Upper Valley–St. Hubert superstation. For the 209 annual maxima, the mean is 9.9 mm and the standard deviation is 8.1 mm, so $\alpha = 0.158$/mm and $u = 6.2$ mm. The best-fit Gumbel line and the sample of extremes are shown on the left in Figure 20. Ice thicknesses are plotted at the unbiased Gringorten plotting positions $p_i = (i–0.44)/209.12$ (Gringorten 1963), where i is the rank of each ordered value from smallest to largest. This is used instead of the widely used Weibull plotting position $p_i = i/(n+1)$, which is unbiased only if the underlying distribution is uniform (Cunanne 1978). If the extreme ice thicknesses were consistent with a Gumbel distribution, they would plot in a straight line, contrary to what is shown in this figure. The Gumbel fit is constrained by the requirement that the tail shape parameter k is zero, while in the generalized Pareto distribution k is determined by the data. As a result of this constraint, the Gumbel analysis shows a relatively narrow range in ice thicknesses from 20 to 40 mm for return periods varying from 10 to 200 years, while the thicknesses from the peaks-over-threshold analysis, plotted to the right of the Gumbel plot at approximately the same scale, vary from 19 to 52 mm for the same range in return periods. The poor fit of the Gumbel curve to the data results in an estimate of a 2200-year return period for the 1998 ice storm, compared to 250 years for the GPD analysis.

5.7 Spatial loads

The concept of spatial loads applies to both design wind speeds and design ice thicknesses for transmission lines. The wind and ice maps in ASCE 7 are used in the design of both communication towers and power lines. They show 50-yr return period values at a point. However, the large horizontal extent of power lines compared to point structures, such as communication towers, results in an increased risk of exceeding the 50-yr return period point thickness somewhere along the line. For example, in Montreal there is a 64% probability that the ice thickness will exceed the 50-yr return-period value at least once in any 50-yr period (Table 7). However, ice storms that occur anywhere between Montreal and Ottawa affect transmission lines extending between the two cities. Thus, designing a single microwave tower and a transmission line that extends tens or hundreds of miles for the same ice thickness results in a greater risk of failure for the transmission line than for the tower. The risk of exceeding the 50-yr return period point ice thicknesses in Figure 19 anywhere along a transmission line route increases with the length of the line. Similarly, the risk of exceeding the

50-yr return period point ice thickness anywhere in a utility's service area increases with the extent of the service area. Spatial effects are discussed in Gringorten (1973) for general weather systems, in Golikova et al. (1983) for ice storms, for tornadoes in Twisdale (1982), and for hurricanes in Vickery and Twisdale (1995), among others.

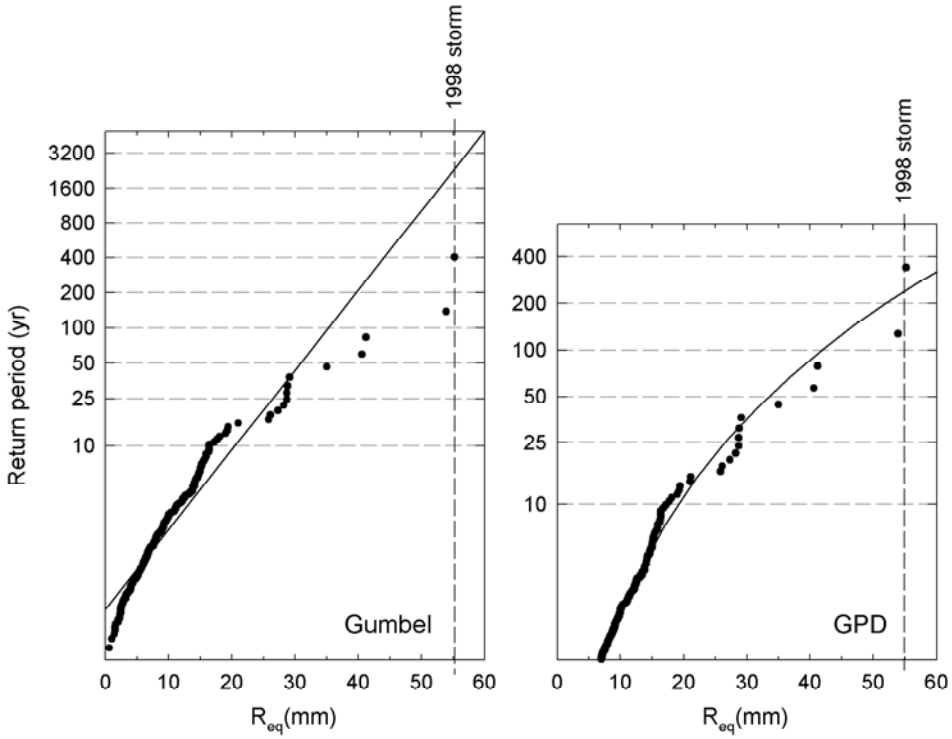

Figure 20. Best-fit Gumbel distribution compared to the best-fit GPD for the Upper Valley (St. Hubert) superstation.

This spatial load concept is different from the superstation concept. Extreme spatial ice thicknesses can be estimated for the Upper Valley by using the largest ice thickness for each storm in the Upper Valley in the extreme value analysis. Taking all storms with at least a 13-mm ice thickness from the Simple model at one of the six weather stations in the Upper Valley gives a sample of 45 extremes in 50 years ($\lambda = 0.90$) with a threshold value $u = 12$ mm. Fitting the generalized Pareto distribution to this sample of spatial extremes using probability weighted moments results in ice thicknesses of 35, 42, and 50 mm for 25-, 50-, and 100-yr return periods, respectively. This means, for example, that there is a 2% probability in any year for an ice storm with ice thicknesses of at least 42 mm to occur somewhere in the Upper Valley. The extreme value analysis of point ice

thicknesses for the Upper Valley superstation (Table 6) shows that a 42-mm ice thickness has only a 1% annual probability of exceedance at a given location in the Upper St. Lawrence Valley.

Table 7. Probability of exceeding the return-period value at least once at a point.
$p_N = 1 - (1 - p_1)^N$

N	Return period (years) for load				
(years)	50	100	250	500	1000
1	0.02	0.01	0.004	0.002	0.001
10	0.18	0.10	0.04	0.02	0.01
20	0.33	0.18	0.08	0.04	0.02
30	0.45	0.26	0.11	0.06	0.03
40	0.55	0.33	0.15	0.08	0.04
50	0.64	0.39	0.18	0.10	0.05
100	0.87	0.63	0.33	0.18	0.10
250	0.99	0.92	0.63	0.39	0.22
500	1.00	0.99	0.87	0.63	0.39
1000	1.00	1.00	0.98	0.86	0.63

6. JANUARY 1998 ICE STORM

The ice storm in January 1998 affected a region extending from northern New York to the coast of New Brunswick. It was particularly severe in the St. Lawrence Valley and Champlain Valley region of southwestern Quebec, northern New York, northwestern Vermont, and eastern Ontario. Modeled ice thicknesses at the end of the storm on a wire always perpendicular to the wind at 10 m above ground in the Upper St. Lawrence Valley ranged from 35 mm for Ottawa to 55 mm for St. Hubert. Time series of the weather conditions and the modeled accumulation of ice are shown in Figure 21 a–c for Ottawa, Massena, and St. Hubert. Note that from late on the 6th to early on the 7th a constant wind speed of 3 m/s is shown at St. Hubert in Figure 21c. The St. Hubert weather data showed no wind for those hours. When that occurs, the processing software continues to use the last non-zero wind speed until another non-zero wind speed occurs. This is done to compensate for possibility that the anemometer is frozen. This correction had almost no effect on the modeled ice thickness because there was little precipitation during that period. At each of these stations, the CRREL model and the Simple model obtain essentially the same ice thicknesses.

6.1 Variation with orientation and height above ground

The ice thicknesses presented and discussed in this report are on wires that remain perpendicular to the wind direction throughout the freezing-rain storms. On a real wire with a fixed orientation to north the ice may not be as thick, and the reduction in thickness depends on both the orientation of the wire and the variability in wind direction during the freezing-rain storms. Wind roses for hours with freezing rain during the period of record are shown in Figure 13 for a sample of the weather stations in the study region. The wind veers from the north–northeast at St. Hubert, toward the northeast at Mirabel, toward the east–northeast at Massena and the east at Ottawa and then back to the northeast at Watertown. This shows the strong influence of the St. Lawrence Valley and the orientation of higher terrain along the edge of the valley.

During the 1998 storm the wind direction was consistent with these historical averages. Wires of power lines oriented with the wind would have accumulated less ice than is shown in Figure 21 and on the map in Appendix D, because they were not affected by wind-blown rain. On the other hand, wires oriented perpendicular to the prevailing wind direction but higher above ground would have accumulated more ice than Figure 21 shows.

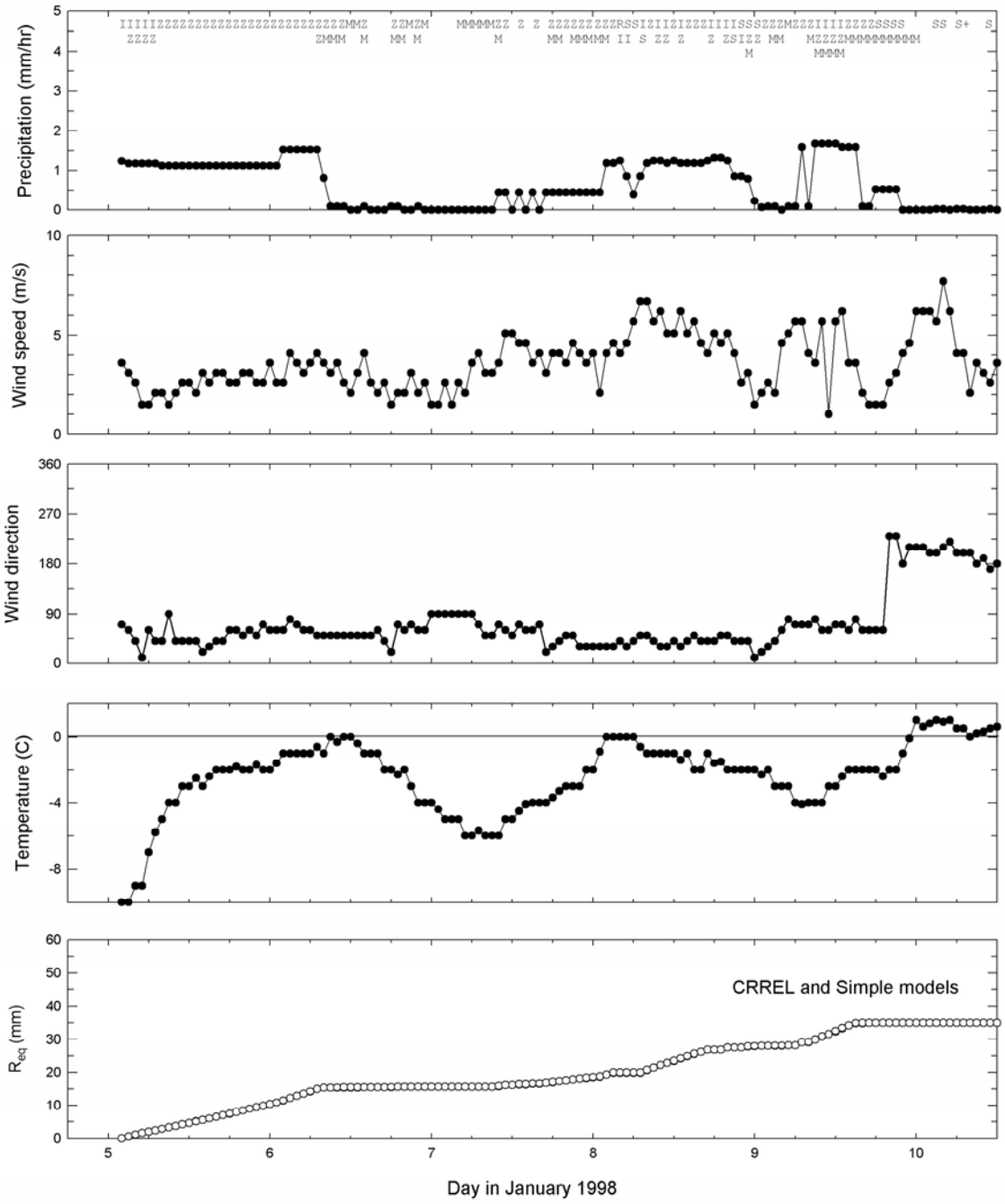

a. Ottawa.

Figure 21. Time series of the weather conditions and modeled accumulation of ice for the 1998 ice storm.

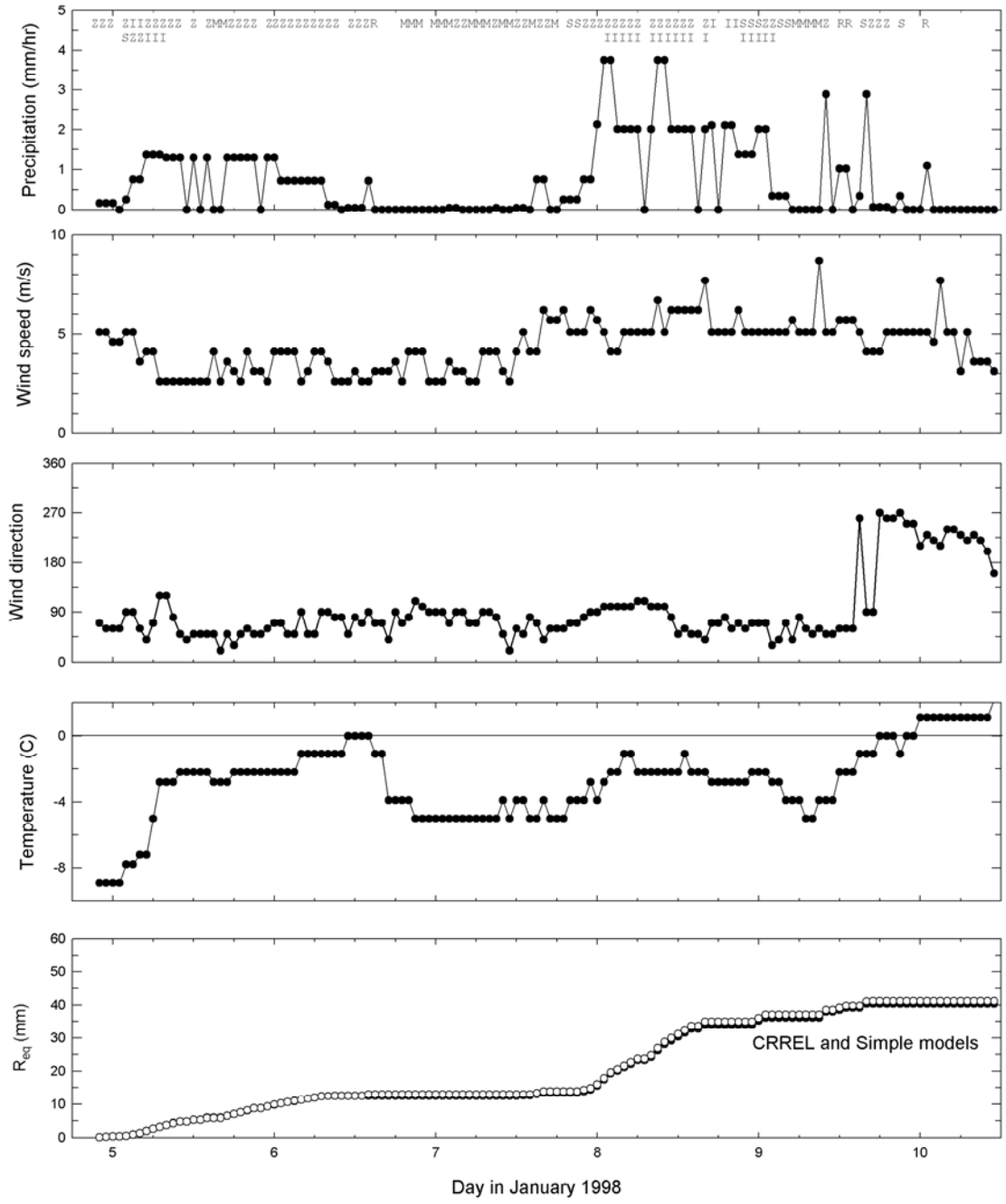

b. Massena.

Figure 21 (cont'd). Time series of the weather conditions and modeled accumulation of ice for the 1998 ice storm.

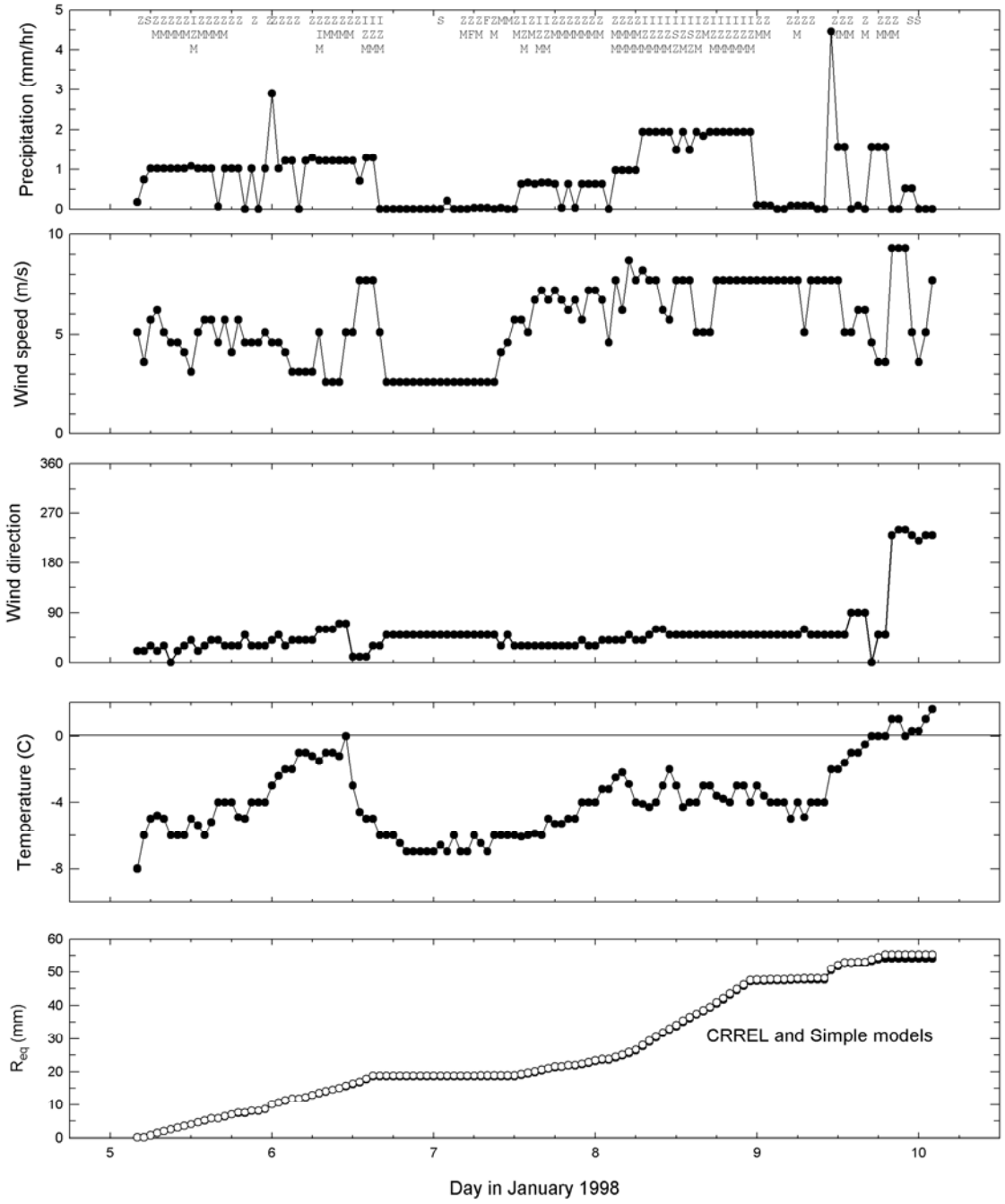

c. St. Hubert.

Figure 21 (cont'd).

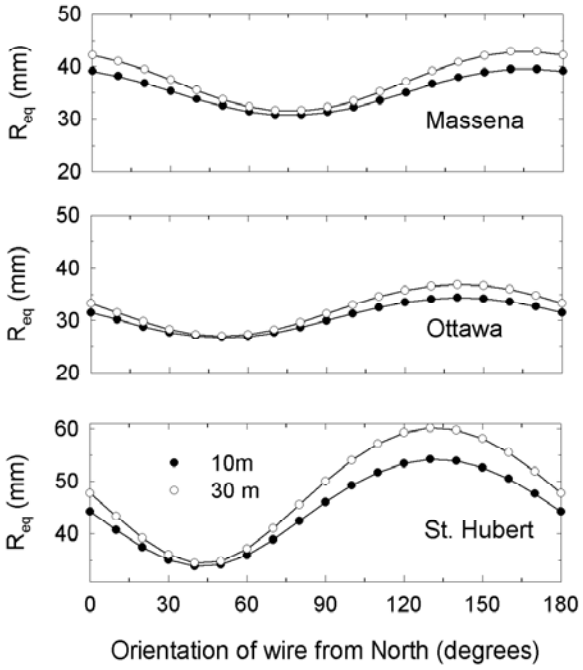

Figure 22. Variation of ice thickness with wire orientation for 10 and 30 m above ground in the 1998 ice storm for St. Hubert, Ottawa, and Massena.

The variation of ice thickness with orientation of the wire at two heights above ground is shown in Figure 22 for Massena, Ottawa, and St. Hubert using the Simple model ice thicknesses. The variation of ice thickness with orientation and height increases with increasing wind speed and decreasing variability in the wind direction while freezing rain is falling. The more pronounced effect of wire orientation at St. Hubert than at Ottawa and Massena is due primarily to the higher average wind speed reported at St. Hubert. This higher wind also leads to an even more pronounced effect at higher elevations above ground.

6.2 Variation with orientation and time

The variation in time of the ice thickness for different line orientations as the ice storm progressed can be shown in terms of the return period. Table 8 shows the time period in which the ice thickness attained the 5-, 10-, 25-, 50-, 100-, 150-, and 200-year level during the storm using the Simple model ice thicknesses determined from the data at St. Hubert. Table 8 shows, for example, that on hypothetical wires that remained parallel to the wind direction throughout the storm, the ice accreted to the 5-year return period thickness on Wednesday night, 25 years on Thursday night, and had almost reached a 50-yr thickness at the end of the storm. However, wires that remained perpendicular to the wind direction

during the storm were more severely affected. Ice accreting on these wires exceeded the 10-year return period value on Tuesday afternoon, 50 years by noon on Thursday, 150 years late Thursday night, 200 years by noon on Friday, and ultimately reached an almost 250-year return period value. The time-dependent return period of ice thicknesses on real wires and conductors with fixed orientations would fall between the values for the hypothetical wires in this table.

Table 8. Severity of icing during the 1998 ice storm in terms of return period (St. Hubert).

Day	Time	Orientation of span relative to wind direction	
		Perpendicular	Parallel
Tuesday 6 January	1–6 am		
	7 am–noon	5	
	1–6 pm	10	
	7 pm–midnight		
Wednesday 7 January	1–6 am		
	7 am–noon		
	1–6pm		
	7 pm–midnight		5
Thursday 8 January	1–6 am	25	
	7 am–noon	50	10
	1–6 pm		
	7 pm–midnight	100/150	25
Friday 9 January	1–6 am		
	7 am–noon	200	
	1–6 pm		
	End of storm	245	45

6.3 Geographical distribution

A map of accumulated freezing rain over the St. Lawrence Valley region is included as Figure 6.3 in a report on the ice storm by Milton and Bourque (1999). That map was not used in this report for estimating the geographical distribution of the ice thickness across the storm footprint because of a number of concerns about the derivation of the values of total freezing rain (Milton and Bourque's Tables 6.1 to 6.4) on which the map is based. First, the Milton and Bourque report does not provide information on the accuracy of the precipitation measurements made twice daily at the climate stations in the difficult conditions during the ice storm. Second, in assigning a fraction of the total precipitation to freezing rain at each climate station, the authors used an unrealistically low water equiva-

lent for ice pellets. They assumed that one centimeter of ice pellets was equivalent to one millimeter of water. This 1-to-10 ratio is much too low (see Appendix E) and results in too little of the total precipitation assigned to ice pellets and, therefore, too much to freezing rain. Finally, the Milton and Bourque assumption of spatial homogeneity of precipitation allows both measurement errors and errors in the assignment of the total precipitation to rain, freezing rain, and ice pellets to propagate from one climate station to nearby stations.

Using the hourly weather observations, a qualitative description of the distribution of ice thicknesses in the greater Montreal area can be attempted. The ice thicknesses from the Simple model for this storm cover a small range, from 48 mm for Dorval to 54 mm for Mirabel and 55 mm for St. Hubert. Comparing the number of hours in which a mixture of freezing rain and ice pellets was observed to the total number of hours with at least freezing rain provides some information for determining a gradient in the ice thickness on wires in this area. Fifty-one percent of the Dorval observations and 48% of the Mirabel observations of hours with freezing rain also included ice pellets, but only 29% of the observations at St. Hubert included ice pellets. Some of this difference may be because St. Hubert was running as an automatic station for part of the storm. Automatic stations report only one precipitation type for each hour. In hours when both ice pellets and freezing rain occurred, only freezing rain would be reported at an automatic station. The automatic hours at St. Hubert during the early morning of 5 January, and the nights of 5–6 January include 10 hours with freezing rain alone. For the same hours at Dorval observers reported one hour with ice pellets alone, and nine hours with freezing rain. During the night of 6–7 January no precipitation was recorded at St. Hubert, while there were three hours with freezing drizzle at Dorval. Based on this comparison, it is unlikely that the much more frequent observations of freezing rain alone at St. Hubert compared to the other Montreal stations is an artifact of the automatic observations. Thus, it is likely that the largest ice thicknesses in the Montreal area during this storm were nearer to St. Hubert than to Dorval or Mirabel. However, overlaid on this trend, there may also have been significant variations in ice thicknesses over short distances associated with local variations in wind speed, precipitation amount and type, and temperature.

6.4 Pre-1998 extreme value analysis

The variability of the calculated extreme ice thicknesses with period of record for the Upper Valley superstations, as well as for Dorval and St. Hubert alone, are shown in Figure 23. Extreme ice thicknesses for 50- and 200-year return periods are plotted for 5-year increments in the period of record, beginning with the period of record through 1963 and ending with the period of record

through 1998. In 1963 there was a 10-year period of record for weather data at Quebec, Ottawa, Dorval, and St. Hubert and 15 years at Massena, but the weather station at Mirabel had not yet been established. Mirabel is included in the superstations from 1988 on. In 1963 the Montreal region had experienced week-long outages in an ice storm just two years earlier (Fig. 7a and Table 3 #7), with much higher modeled ice thicknesses at Dorval than at St. Hubert. Immediately obvious in this figure is the much larger variation in ice thickness at the two single stations, which have much smaller samples of extremes than the superstations. The smaller ice thicknesses throughout most of this period at St. Hubert compared to Dorval, only 25 km away, also stand out. These differences are much less pronounced in the two Upper Valley superstations. The extreme ice thicknesses for the superstation including Dorval are consistently higher than those for the superstation including St. Hubert; however, they converge as the period of record increases. The superstation extremes are relatively low from the mid-1970s to the mid-1990s during a 20-year period of few severe ice storms. The extremes increase again to the level of the early 1970s after the 1998 ice storm.

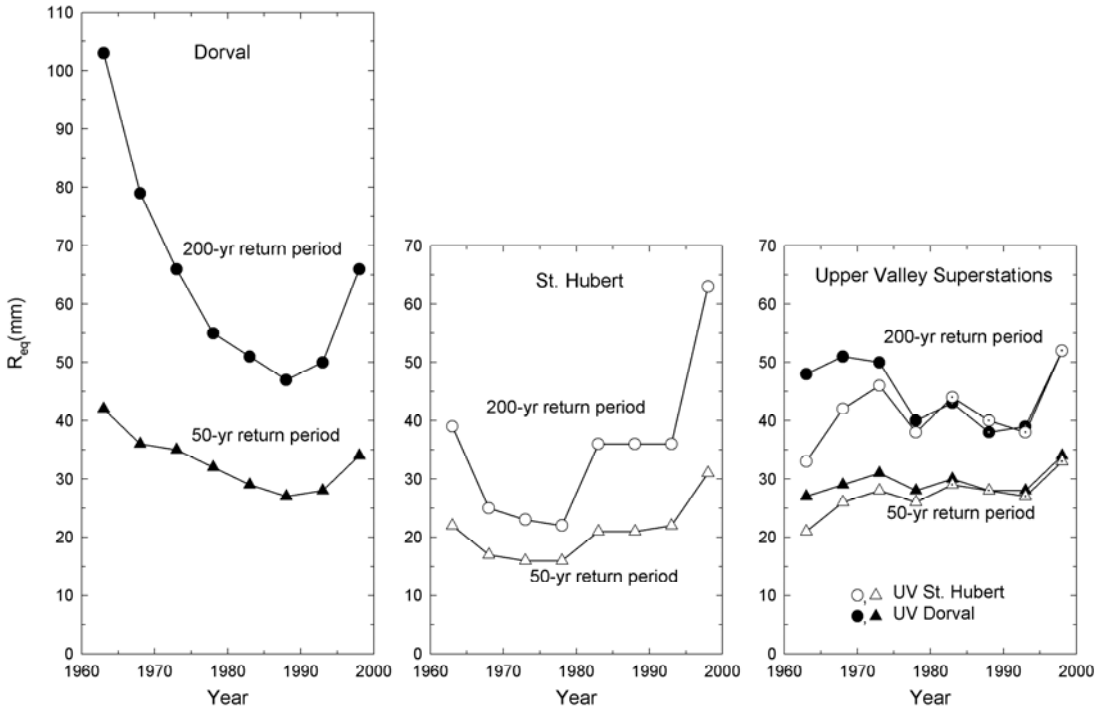

Figure 23. Variability of calculated extreme ice thicknesses with period of record for the Upper Valley superstations and Dorval and St. Hubert alone.

7. SUMMARY AND RECOMMENDATIONS FOR FURTHER WORK

Historical weather data beginning in the late 1940s and early 1950s and the Simple and CRREL ice accretion models were used to estimate ice thicknesses in freezing-rain storms that have occurred in the St. Lawrence Valley region. Storms with significant ice thicknesses were investigated in *Storm Data* and newspapers from cities in the region to obtain information on the storm's severity and extent.

Severe ice storms are not uncommon in the Upper St. Lawrence Valley. The January 1998 ice storm followed particularly damaging storms in March 1913, December 1942, February 1961, March 1972, December 1973, December 1983, and December 1996. There are, undoubtedly, additional severe ice storms that occurred prior to the beginning of the period of record of the electronically archived weather data that were not identified in this study. Tree damage to distribution lines is the primary cause of outages in many ice storms. In addition to tree damage and heavy ice loads on conductors and wires of both transmission and distribution lines, outages in these storms were attributed to pole fires, transformers exploding, galloping, sleet jumping, flashovers, frozen switches, insulator problems, shield wires breaking, frozen condensation inside transformers, wet snow, cars hitting poles, and technical problems. The duration of outages often depended on the extent of the storm and the population density in the storm footprint.

The thickness of the ice on wires of overhead lines depends on the orientation of the wire to the wind accompanying the freezing rain. In this analysis ice was accreted on wires that remained perpendicular to the wind. Wires that are parallel to the wind accrete less ice. The difference is more significant when it is windy and the wind direction is constant. In the St. Lawrence Valley winds accompanying freezing rain tend to be from the northeast sector, aligning with the edge of the higher terrain along the northern boundary of the valley.

An extreme value analysis of the ice thicknesses and wind-on-ice loads from the Simple model, using a peaks-over-threshold approach and grouping the stations into superstations to reduce sampling error, results in a 50-yr return period point ice thickness for this region of about 33 mm with a 19 m/s concurrent gust speed. A spatial extreme value analysis, using the maximum ice thickness in each storm at any weather station in the Upper Valley, results in a 50-yr ice thickness of 42 mm, about 25% more than the point value.

The analysis also showed that calculated extremes based on single stations can vary significantly as the period of record increases and the sample of extremes changes. This variation is considerably reduced when the stations are grouped into superstations to provide a larger sample of extremes. Since 1963 the calculated 50-yr ice thickness for the Upper St. Lawrence Valley has varied between 26 and 34 mm.

The maximum modeled 55-mm ice thickness for the January 1998 storm corresponds to a return period of about 250 years in the Upper Valley. However, ice on wires oriented parallel to the wind reached a thickness equivalent to less than a 50-yr return period by the end of the storm. An analysis based on fitting the two-parameter Gumbel distribution to the sample of annual extremes provides a poor fit to the data and results in a return-period estimate of 2200 years for this storm.

The calculation of extreme ice thicknesses from weather data could be improved in a number of ways. The qualitative information that was obtained for the PDSs indicated that a significant number of the storms were snowstorms rather than severe ice storms. This implies that at least in some conditions the precipitation weighting factors are assigning too much of the accumulated precipitation to hours with freezing rain when it should be assigned to hours with snow. Thus, the factors in Table 1 for prorating precipitation amounts to each hour should be reviewed and revised. The data for such a revision could be obtained from hourly and daily precipitation amounts during the winter months at weather stations where both measurements are archived. This analysis should be carried out for stations across the country to obtain factors that are appropriate for a variety of winter climates. In addition to the storms that were really snowstorms, some of the PDSs were described as cold rain without any significant ice accumulation on wires. Therefore, the more conservative assumptions, allowing for the accretion of ice when the precipitation is described as rain or a mixture of rain and snow with an air temperature at 0^{o}C or lower, should be reexamined.

The investigation of storms with significant modeled ice thicknesses is useful for determining whether the modeled values are too high, but tells us little about modeled loads that are too low. This would be best achieved by obtaining independent information on damaging ice storms and checking modeled ice thicknesses for weather stations in the area for those storms. Outage information, for both transmission and distribution lines, from the electric utility companies in the region would be ideal for this purpose. This complementary approach would also identify any local ice storms that fall between the relatively widely spaced weather stations.

This study focused on the Upper St. Lawrence Valley, so no extra effort was made to obtain additional data for Mont Joli and Baie Comeau from Environment Canada. Furthermore, the lack of daily newspaper at towns in that region made it difficult to obtain reliable newspaper coverage for the investigation of PDSs. That region should be reexamined, together with data from stations in the Gaspé Peninsula, the Maritime provinces, and Maine to provide more reliable estimates of extreme ice thicknesses in these border states and provinces.

The controversy over the magnitude of ice thicknesses over the St. Lawrence Valley region reemphasizes the need for high-quality field measurements for determining the equivalent uniform radial thickness of ice on wires in damaging ice storms. Such data are useful both for comparison with modeled ice thicknesses at weather stations and for mapping the geographical and topographical distribution of ice thicknesses across the storm.

LITERATURE CITED

Abild, J., E.Y. Andersen, and L. Rosbjerg (1992) The climate of extreme winds at the Great Belt, Denmark. *Journal of Wind Engineering and Industrial Aerodynamics*, **41–44**: 521–532.

Abramowitz, M., and I.A. Stegun (1970) *Handbook of mathematical functions*, Dover Publications, New York, 1046 pages.

ASCE (1991) *Guidelines for Electrical Transmission Line Structural Loading*, ASCE Manual 74. New York, 139 p.

ASCE (1993) *Minimum Design Loads for Buildings and Other Structures*, ASCE Standard 7-93. New York, 134 p.

ASCE (2000) *Minimum Design Loads for Buildings and Other Structures*, ASCE Standard 7-98. New York.

Atlas, D., and C.W. Ulbrich (1977) Path- and area-integrated rainfall measurement by microwave attenuation in the 1–3 cm band. *Journal of Applied Meteorology*, **16**: 1322–1331.

Best, A.C. (1950a) The size distribution of raindrops. *Quarterly Journal of the Royal Meteorological Society*, **76**: 16–36.

Best, A.C. (1950b) Empirical formulae for the terminal velocity of water drops falling through the atmosphere. *Quarterly Journal of the Royal Meteorological Society*, **76**: 302–311.

Bocchieri, J.R. (1980) The objective use of upper air soundings to specify precipitation type. *Monthly Weather Review*, **108**: 596–603.

Chaîné, P.M. (1973) Glaze and its misery: The ice storm of 22–23 March 1972 north of Montreal. *Weatherwise*, June 1973: 124–127.

Chaîné, P.M., and G. Castonguay (1974) New approach to radial ice thickness concept applied to bundle-like conductors, Industrial Meteorology-Study IV. Environment Canada, Toronto.

Cunanne, C. (1978) Unbiased plotting positions: A review. *Journal of Hydrology*, **37**: 205–222.

ElFashny, K.N.G., V.T.V. Nguyen, L.E. Chouinard, and J.N. Laflamme (1998) Statistical analysis of ice observations in Quebec, Canada. In *Proceedings of the Eighth International Workshop on Atmospheric Icing of Structures*, p. 273–278.

Felin, B. (1988) Freezing rain in Quebec: Field observations compared to model estimations. In *Proceedings of the Fourth International Workshop on Atmospheric Icing of Structures*, p. 119–123.

Finstad, K.F., E.P. Lozowski, and E.M. Gates (1988) A computational investigation of water droplet trajectories. *Journal of Atmospheric and Oceanic Technology*, **5**: 160–170.

Golikova, T.N., B.F. Golikov, and D.S. Savvaitov (1983) Methods of calculating ice loads on overhead lines as spatial constructions. In *Proceedings of the First International Workshop on Atmospheric Icing of Structures*. U.S. Army Cold Regions Research and Engineering Laboratory, Hanover, New Hampshire, Special Report 83-17, p. 341–346.

Goodwin, E.J., J.D. Mozer, A.M. DiGiola, and B.A. Power (1983) Predicting ice and snow loads for transmission line design. In *Proceedings of the First International Workshop on Atmospheric Icing of Structures*. U.S. Army Cold Regions Research and Engineering Laboratory, Hanover, New Hampshire, Special Report 83-17, Special Report 83-17.

Gringorten, I.I. (1963a) A plotting rule for extreme probability paper. *Journal of Geophysical Research*, **68**: 813–814.

Gringorten, I.I. (1963b) Envelopes for ordered observations. *Journal of Geophysical Research*, **68**: 815–826.

Gringorten, I.I. (1973) Stochastic modeling of the areal extent of weather conditions. Air Force Cambridge Research Laboratories, Bedford, Massachusetts, AD-775-986, 50 pages.

Gross, J., A. Heckert, J. Lechner, and E. Simiu (1994) Novel extreme value estimation procedures: Application to extreme wind data. In *Extreme Value Theory and Applications* (J. Galambos et al., Ed.). The Netherlands: Kluwer Academic Publishers, p. 139–158.

Hosking, J.R.M., and J.R Wallis (1987) Parameter and quantile estimation for the generalized Pareto distribution. *Technometrics*, **29**(3): p. 339–349.

Hosking, J.R.M., and J.R Wallis (1997) *Regional Frequency Analysis*. Cambridge: Cambridge University Press, 224 p.

Jones, K.F. (1990) The density of natural ice accretions related to nondimensional icing parameters. *Quarterly Journal of the Royal Meteorological Society*, **116**: 477–496.

Jones, K.F. (1996a) A simple model for freezing rain ice loads. In *Proceedings of the 7th International Workshop on Atmospheric Icing of Structures*, Chicoutimi, Canada, p. 412–416.

Jones, K.F. (1996b) Ice accretion in freezing rain. U.S. Army Cold Regions Research and Engineering Laboratory, Hanover, New Hampshire, CRREL Report 96-2.

Jones, K.F. (1997) EPRI freezing rain ice mapping project: Region 2, CR-00020, Project 3748-09. Final report for EPRI Power Delivery Center, June 1997.

Jones, K.F. (1999) Ice storms, trees and power lines. In *Proceedings of the 10th International Conference on Cold Regions Engineering*, American Society of Civil Engineers, Reston, Virginia, p. 757–767.

Jones, K.F., and Y.G. Koh (1995) The rotating multicylinder. In *Proceedings of the Fourth Annual Mt. Washington Observatory Symposium*, p. 35–43.

Jones, K.F., and N.D. Mulherin (1998) An evaluation of the severity of the January 1998 ice storm in Northern New England. Report for FEMA Region 1, published on the CRREL Web site at www.crrel.usace.army.mil, 67 pages.

Kumai, M. (1973) Arctic fog droplet size distribution and its effect on light attenuation. *Journal of the Atmospheric Sciences*, **30**: 635–643.

Laflamme, J. (1993) Spatial variation of extreme values in the case of freezing rain icing. In *Proceedings of the Sixth International Workshop on Atmospheric Icing of Structures*, Budapest. Hungarian Electrotechnical Association, p. 19–24.

Lanctot, E.K., E.L. Peterson, H.E. House, and E.S. Zobel (1960) Ice build-up on conductors of different diameters. *AIEE Proceedings*, p. 1610–1615.

Mahaffy, F.J. (1961) The ice storm of 25–26 February 1961 at Montreal. *Weatherwise*, p. 241–244.

Makkonen, L. (1985) Heat transfer and icing of a rough cylinder. *Cold Regions Science and Technology*, **10**: 105–116.

Makkonen, L. (1996) Modeling power line icing in freezing precipitation. In *Proceedings of the 7th International Workshop on Atmospheric Icing of Structures*, Chicoutimi, Canada, p. 195–200.

Milton, J., and A. Bourque (1999) A climatological account of the January 1998 ice storm in Quebec, Atmospheric Sciences and Environmental Issues Division, Environment Canada, Quebec Region, CES-Q99-01, 87 p.

MRI (1977) Ontario Hydro wind and ice loading model, MRI 77 FR-1496. Ontario Hydro, Toronto.

Nash, J.E. (1966) Applied flood hydrology. In *River Engineering and Water Conservation Works* (R.B. Thorn, Ed.). Washington, D.C.: Butterworth, Inc., p. 63–110.

Newfoundland and Labrador Hydro, Ontario Hydro Technologies and École de Technologie Supérieure (1998) Validation of ice accretion models for freezing precipitation using field data, Canadian Electrical Association, 331 T 992 (A–D).

NOAA (1959–1998) *Storm Data*. Asheville, North Carolina: National Climate Data Center.

NOAA (1942) *Local Climatological Data, Annual Summaries*. Asheville, North Carolina: National Climate Data Center.

NOAA (1950–1959) *Climatological Data, National Summary.* Asheville, North Carolina: National Climate Data Center.

Okert, R. (2000) Depending on electricity. *The Courier*, Russellville, Arkansas, 29 December 2000, p 4A.

Oliver, H.R. (1971) Wind profiles in and above a forest canopy. *Quarterly Journal of the Royal Meteorological Society*, **97**: 548–553.

Peterka, J.A. (1992) Improved extreme wind prediction for the United States. *Journal of Wind Engineering and Industrial Aerodynamics*, **41–44**: 533–541.

Press, W.H., B.P. Flannery, S.A. Teukolsky, and W.T. Vetterling (1987) *Numerical Recipes*. Cambridge: Cambridge University Press.

Richards, T.L. (1954) An approach to forecasting snowfall amounts. Department of Transport, Meteorological Division, CIR-2421, TEC-177, 19 January 1954.

Simiu, E., and N.A. Heckert (1995) *Extreme wind distribution tails: A "Peaks over Threshold" Approach*. National Institute of Standards and Technology Building Science Series 174,. Washington, D.C.: U.S. Government Printing Office, 72 pages.

Simiu, E., and R.H. Scanlan (1996) *Wind effects on structures, Third Edition*. New York: John Wiley and Sons.

Stallabrass, J.R. (1983) Aspects of freezing rain simulation and testing. In *Proceedings of the First International Workshop on Atmospheric Icing of Structures*. U.S. Army Cold Regions Research and Engineering Laboratory, Hanover, New Hampshire, CRREL Report 83-17, p. 67–74.

Stallabrass, J.R., and P.F. Hearty (1967) The icing of cylinders in conditions of simulated sea spray. Mechanical Engineering Report MD-50, National Research Council of Canada, Ottawa.

Stewart, R.E. (1992) Precipitation types in the transition region of winter storms. *Bulletin of the American Meteorological Society*, **73**(3): 287–296.

Torres, D.S., J.M Porra, and J-D Creutin (1994) A general formulation for raindrop size distribution. *Journal of Applied Meteorology*, **33**: 1494–1502.

Twisdale, L.A. (1982) Wind-loading underestimate in transmission line design. *Transmission and Distribution*, December 1982, p. 40–45.

Vickery, P.J., and L.A. Twisdale (1995) Prediction of hurricane wind speeds in the United States. *ASCE Journal of Structural Engineering*, November 1995.

Walshaw, D. (1994) Getting the most from your extreme wind data: A step by step guide. *Journal of Research of the National Institute of Standards and Technology*, **99**: 399–411.

Wang, Q.J. (1991) The POT model described by the generalized Pareto distribution with Poisson arrival rate. *Journal of Hydrology*, **129**: 263–280.

Wang, P.K., and H.R. Pruppacher (1977) Acceleration to terminal velocity of cloud and raindrops. *Journal of Applied Meteorology*, **16**: 275–280.

Yip, T.C. (1993) Estimating icing amounts caused by freezing precipitation. In *Proceedings of the 6th International Workshop on Atmospheric Icing of Structures*, p. 73–78.

Yip, T.C., and P. Mitten (1991) Comparisons between different ice accretion models. Canadian Electrical Association, Transmission Line Design Section, Engineering and Operating Division, May 1991.

Newspapers (various dates)

Burlington Daily News, Burlington, Vermont

Burlington Free Press, Burlington, Vermont

Hebdomadaire Regional Information, Mont Joli, Quebec

La Presse, Montreal, Quebec

La Tribune, Sherbrooke, Quebec

La Voix Gaspésienne, Matane, Quebec

Le Droit, Ottawa–Hull, Ontario

Le Journal de Montreal, Montreal, Quebec

Le Journal de Quebec, Quebec City, Quebec

Le Rimouskois, Rimouski, Quebec

Le Soleil, Quebec City, Quebec

Massena Observer, Massena, New York

The Gazette, Montreal, Quebec

The Ottawa Citizen, Ottawa, Ontario

The Record, Sherbrooke, Quebec

Times Argus, Barre, Vermont

Watertown Daily Times, St. Lawrence Edition, Watertown, New York

Watertown Daily Times, Watertown, New York

APPENDIX A. MISCELLANEOUS INFORMATION

A.1 Acronyms

AES	Atmospheric Environment Service, part of Environment Canada
AFCCC	Air Force Combat Climatology Center
CEA	Canadian Electricity Association
CRREL	Cold Regions Research and Engineering Laboratory
EC	Environment Canada
FAA	Federal Aviation Administration
GPD	Generalized Pareto distribution
MANOBS	Manual of Surface Weather Observations
MEP	Meteorological and Environmental Planning Ltd.
NCDC	National Climate Data Center
NOAA	National Oceanic and Atmospheric Administration
NWS	National Weather Service
PIM	Passive Ice Meter
UTC	Universal Coordinate Time

A.2 Symbols

A_a	Area of ice cross section in SH runs
A_i	Area of ice cross section in Chaîné model
C_D	Drag coefficient of ice-covered wire
D	Diameter of wire
D_i	Diameter of icicles
d_s	Sauter mean diameter
F	Wind-on-ice load from hourly wind data
$F(x)$	Cumulative distribution of x
F_{50}	50-yr return period wind-on-ice load

f_{gust}	G_{50}/U_{50}
G_c	Gust speed equivalent to U_c
h_A	Height of anemometer above ground
h_W	Height of wire above ground
k	Shape parameter for GPD; correction factor in Chaîné model
L	Length of ice sample
L_i	Length of icicles
m	Mass of ice sample
N	Number of hours in storm
n	Number of years of record
P	Water equivalent of precipitation
p_i	Plotting probability for the ith extreme
p_N	Probability of exceeding a point load in N years
R_{eq}	Equivalent uniform radial ice thickness
R_{eq50}	50-yr return period uniform radial ice thickness
r	Radius of cylinder in Chaîné model
T	Return period
t	Thickness of ice on wire in CRREL model
t_h	Thickness of ice on horizontal surface in Chaîné model
t_v	Thickness of ice on vertical surface in Chaîné model
U	Wind speed
U_A	Wind speed at height of anemometer
U_c	1- or 2-min wind speed associated with R_{eq50} and F_{50}
U_T	Terminal velocity of raindrops
U_W	Wind speed at height of wire
u	Threshold for GPD; location parameter for Gumbel
V	Visibility
W	Liquid water content
$x_{(i)}$	ith extreme load

x_T	T-year return-period load
α	Scale parameter for generalized Pareto and Gumbel distributions
λ	Occurrence rate of extreme loads
π	3.14159
ρ_a	Density of air
ρ_i	Density of glaze ice
ρ_o	Density of water
θ	Wire direction
φ	Wind direction

A.3 Glossary

Potentially Damaging Storms (PDSs) are ice storms chosen for further investigation because the CRREL and Simple model ice thickness at one or more stations satisfied at least one of three criteria.

Damaging storms are PDSs for which newspaper accounts and other reports indicate that trees and power lines were damaged by the accreted ice.

Extreme storms are storms for which the ice thickness at a station at the end of the storm exceeds the threshold ice thickness for the superstation that includes the station.

APPENDIX B. CHAÎNÉ MODEL

In this appendix the derivation of the Chaîné model is described and critiqued. The experimental results on which Chaîné and Castonguay (1974) base their model are in a paper by Stallabrass and Hearty (1967). These references will be referred to as CC and SH, respectively, in this appendix.

The experiments in SH were done to simulate sea-spray icing on the superstructure and rigging of vessels. These components are simulated by cylinders with diameters of 1.5, 3, 6, and 18 in., mounted either vertically or horizontally in the wind tunnel test section, fixed against rotation. Each of the 21 simulations was run for one hour, with a wind speed of 50 mph and a spray liquid water content of 3.2 g/m^3. The temperature in the wind tunnel was held at about –14°C for half the tests and at about –7°C for the other half. The same mixture of English and metric units will be used in this appendix as was used in SH.

B.1. Simulation conditions compared to typical freezing rain conditions

Severe freezing-rain storms typically occur in a relatively narrow band of weather conditions characterized by temperatures just below freezing, light to moderate wind speeds, and low precipitation rates:

- Temperature: –5 to 0°C
- Wind speed: 2 to 7 m/s
- Precipitation rate: <1 to 5 mm/hr, corresponding to liquid water contents of 0.05 to 0.3 g/m^3.

The conditions in the wind tunnel experiments to simulate sea-spray icing were significantly colder, windier, and wetter:

- Temperature: –16 to –6°C
- Wind speed: 22 m/s
- Liquid water content: 3.2 g/m^3.

Thus the ice that accreted on the cylinders in the hour-long simulations formed in very different conditions from the ice that accretes on conductors and wires in freezing-rain storms.

These very different conditions are sufficient to preclude the use of the SH data for a freezing rain model. However, CC used this data to calibrate a model based on the "elliptical concept."

B.2. Elliptical concept

In CC's elliptical concept, the ice accretion on half a wire is assumed to have the shape of a half-ellipse. The maximum ice thickness is assumed to be equal to $\left(t_h^2 + t_v^2\right)^{1/2}$, where t_h is the amount of ice accumulated on a horizontal surface and t_v is the amount accumulated on a vertical surface. This results in a cross-sectional area of the ice

$$A_i = \frac{\pi r}{2}\left(t_h^2 + t_v^2\right)^{1/2} \tag{B1}$$

where r is the cylinder diameter. However, the actual ice accretion area A_a may be different from A_i by a factor K. Thus, the uniform radial ice thickness R_{eq} that corresponds to this corrected ice area is calculated from

$$A_a = \pi\left[\left(r + R_{eq}\right)^2 - r^2\right] = K\ \frac{\pi r}{2}\left(t_h^2 + t_v^2\right)^{1/2} \tag{B2}$$

to give

$$R_{eq} = -r + \left[r^2 + \frac{Kr}{2}\left(t_h^2 + t_v^2\right)^{1/2}\right]^{1/2}. \tag{B3}$$

Thus CC are basing the shape of the ice accretion on the amount of ice accreted on horizontal and vertical surfaces, correcting the area of that shape by a yet unspecified factor K, and then determining the equivalent uniform radial ice thickness for that corrected area.

B.3 Determination of *K*

CC used the SH data to determine K. The elliptical concept requires the ice thickness on horizontal and vertical surfaces, neither of which was measured in the SH experiments. In fact, there was no rain falling on a horizontal surface in those experiments. There was only wind-blown rain. Thus $t_h = 0$ and $t_v \approx 100$ mm for each hour-long simulation. But CC chose to use the ice thickness maxima, dimensions C and D in Figure B1, measured to the nearest 1/4", as t_h and t_v.

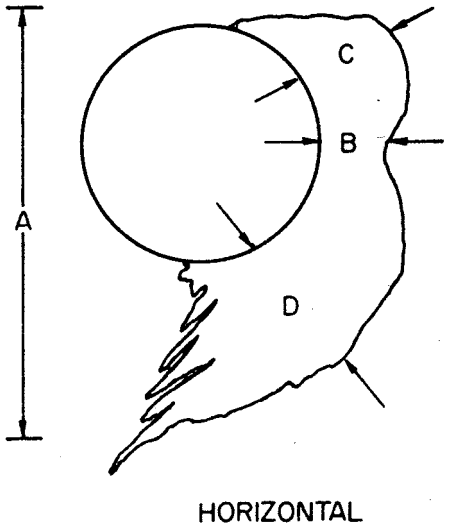

Figure B1. Dimensions A, B, C, and D reported in SH. (From Stallabrass and Hearty 1967.)

The cross-sectional area of each accretion is calculated using SH's ice mass for a 3-ft cylinder length for each run, assuming an ice density of 56 lb/ft:

$$A_a = \frac{M(144)}{(3)(56)} \text{ in}^2. \tag{B4}$$

K is then the ratio of A_a and A_i. For example, for Run #2, the ice weight is 18 lb, so the actual ice cross-sectional area A_a is 15.4 in^2. With CC's assumptions, the area based on the elliptical concept is given by equation B1 with t_h = C = 3", t_v = D = 4", and r = 0.75". This gives A_i = 5.9 in^2, so K = 15.4/5.9 = 2.62. The SH data for simulating sea-spray icing and the CC determination of K for freezing rain from these data are shown in Table B1. CC used only the results from the horizontal cylinders, and only for cylinder diameters of 1.5", 3", and 6", SH's runs 1 through 6, in determining K. These values of K are shown as squares in Figure B2. CC drew curves near these points and then extrapolated them to smaller diameter cylinders and warmer air temperatures.

The use of two measurements of ice thickness on a cylinder exposed only to wind-carried water drops as substitutes for the amount of ice accreted on horizontal and vertical surfaces in wind-blown freezing rain is sufficient to rule out the use of this model. But CC continued, extrapolating their values of K to other diameters and temperatures.

Table B1. Chaîné and Castonguay analysis of Stallabrass and Hearty data.								
Stallabrass and Hearty data						Chaîné and Castonguay		
Run	Cylinder diameter (*in.*)	T (°*C*)	Ice weight (*lb*)	Dimensions (in.)		A_a ($in.^2$)	A_i ($in.^2$)	*K*
				C	D			
1	1.5	–15	33.75	4.25	5.0	28.92	7.73	3.74
2	1.5	–8	18.0	3.0	4.0	15.4	5.9	2.62
3	3.0	–14	37.0	3.75	5.5	31.71	15.7	2.02
4	3.0	–7	23.0	3.25	3.25	19.71	10.9	1.81
5	6.0	–16	53.5	5.0	6.0	45.8	36.8	1.24
6	6.0	–7.5	31.0	3.75	4.0	26.57	25.9	1.03

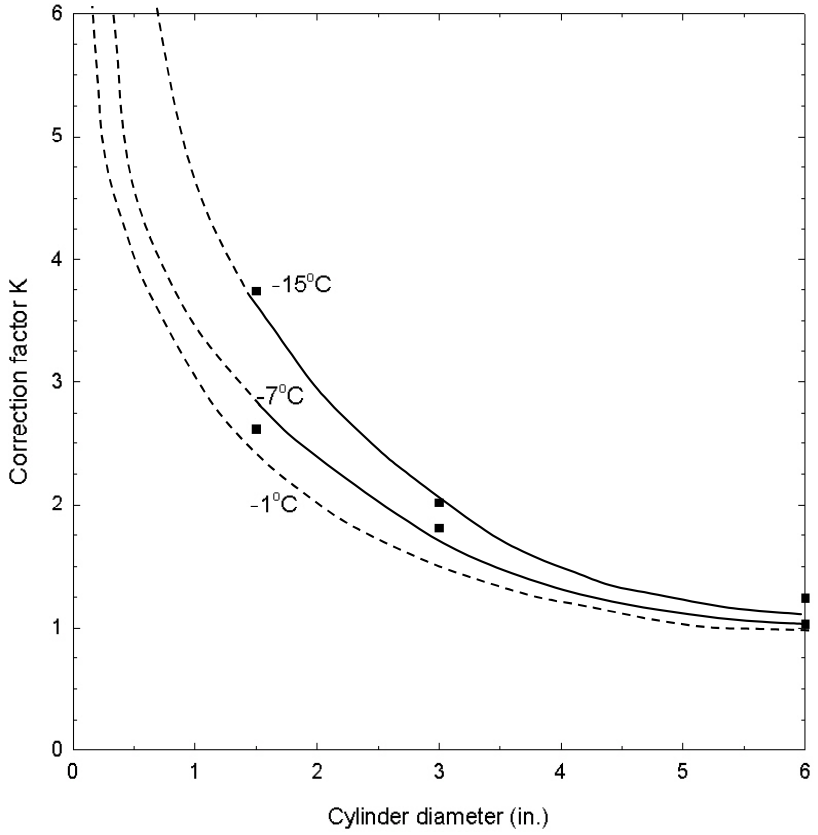

Figure B2. Correction factor *K* for the Chaîné model.

B.4. Extrapolation to smaller cylinder diameters and warmer air temperatures

Most conductors and ground wires have diameters smaller than 1.5". Thus Chaîné model results showing a strong dependence of equivalent radial ice thickness on wire diameter are based on CC's extrapolation of their six *K* values. They continued their curves for small diameters up to *K* values of 6, with apparently no limit on *K* for very small wire diameters (Fig. B.2).

They also extrapolated their two curves at –7°C and –15°C to get a third curve at –1°C. They seem to have used the separation of the –15°C and –7°C curves to determine the location of the –1°C curve.

B.5. Internal consistency

The values of *K* calculated by CC and tabulated in Table B.1 can be used to compare the CC modeled equivalent radial ice thicknesses using equation B3 with those determined from the cross-sectional areas of the six ice samples in Table B.1. In equation B3 $t_h = 0$, because there is only wind-blown water, and t_v is calculated from the wind speed and the liquid water content in the wind tunnel:

$$t_v = \frac{(3.2\ \text{g/m}^3)(22.4\ \text{m/s})(3600s)}{(0.9\ \text{g/cm}^3)(10^4\,\text{cm}^2/\text{m}^2)(2.54\,\text{cm/in.})} = 11.3\ \text{in.} \tag{B5}$$

The equivalent radial ice thickness of each sample is

$$R_{eq} = -\frac{r}{2} + \sqrt{\frac{r^2}{4} + \frac{A_a}{\pi}}\ . \tag{B6}$$

The CC modeled equivalent radial ice thicknesses from equation B3 using equation B5 are compared to SH's measured equivalent radial ice thicknesses from equation B6 in Figure B3. The modeled values are significantly greater than the measured values. This discrepancy stems from CC using the dimensions C and D of the ice samples to represent the ice thickness on vertical and horizontal surfaces.

B.6 Summary

As detailed above, there are many reasons to not use, and not believe the results of, the Chaîné model to determine the amount of ice accreted on conductors and wires in freezing rain:

- The SH simulations on which the Chaîné model is based were intended to simulate sea-spray icing rather than freezing rain. The conditions in the wind tunnel test were perfect for sea-spray icing, but too cold, much too wet, and too windy for freezing rain.
- There were no measurements of the ice thickness on vertical and horizontal surfaces in the SH simulations that CC needed to get the maximum ice thickness for their elliptical concept. Thus their determination of *K* based on the ice thicknesses that were measured on the cylinders is inconsistent with their own conceptual model.
- Most conductors and wires have diameters less than 1.5". Thus they are in the range where *K* was extrapolated from the six "measured" *K*s.
- The CC model is internally inconsistent, resulting in modeled equivalent radial ice thicknesses that are greater than the thicknesses based on the measured ice mass in the six SH runs that were used to calculate values for *K*.

The Chaîné model is not credible.

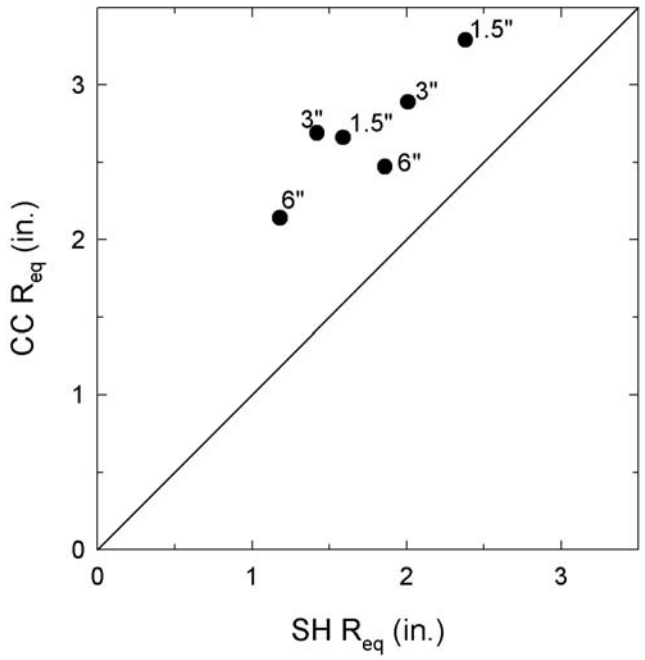

Figure B3. Comparison of CC and SH equivalent radial ice thicknesses.

APPENDIX C. TERMINAL VELOCITY OF RAINDROPS

This appendix provides a derivation of the terminal velocity as a function of precipitation rate. The derivation in Section C1 is based on Best's liquid water content (1950a). In section C2 the liquid water content weighted terminal velocity is determined from Best's drop size distribution and the terminal velocity as a function of the drop diameter. In the following, drop diameters d are in mm, precipitation rates P are in mm/h, liquid water contents W are in g/m^3, and terminal velocities U_T are in m/s.

C1. Terminal velocity from liquid water content

The fall speed U_T of the rain drops is related to the liquid water content W of the precipitation by

$$WU_T = \rho_o P \,. \tag{C1}$$

For W in g/m^3, U_T in m/s, ρ_o in g/cm^3, and P in mm/hr, this results in

$$WU_T = \frac{\rho_o P}{3.6} \,. \tag{C2}$$

ρ_o = 1 g/cm^3 and the Best relationship for liquid water content as a function of precipitation rate, which is used for the Simple and CRREL models, is $W = 0.067P^{0.846}$. Thus

$$U_T = 4.15P^{0.154} \tag{C3}$$

as given in Section 2.2.1.

C2. Liquid water content weighted terminal velocity

A number of authors have reported the terminal velocities for raindrops as a function of the drop diameter. According to Best (1950b), for drop diameters between 0.5 and 6 mm the terminal velocity (m/s) at the earth's surface in a standard atmosphere is

$$U_T(d) = 9.32\left(1 - e^{-[d/1.77]^{1.147}}\right). \tag{C4}$$

Beard (1976) provides a set of formulas for computing terminal velocities in three size ranges. These complicated formulas are not reproduced here. However, Wang and Pruppacher (1977) extend Beard's theory to also compute the time and distance to reach terminal velocity and plot 99% of the terminal velocity as a function of drop diameter for drop diameters up to 7 mm. Atlas and Ulbrich (1977) use

$$U_{\mathrm{T}}(d) = 9.65\left(1 - 1.067e^{-0.6d}\right) \tag{C5}$$

to which they fit a power law for $0.5 < d < 5$ mm:

$$U_{\mathrm{T}}(d) = 3.778d^{0.67}\,. \tag{C6}$$

The formula from Best (Equation C1), the curve in Wang and Pruppacher, and the Atlas and Ulbrich formula (Equation C5) are plotted in Figure C1.

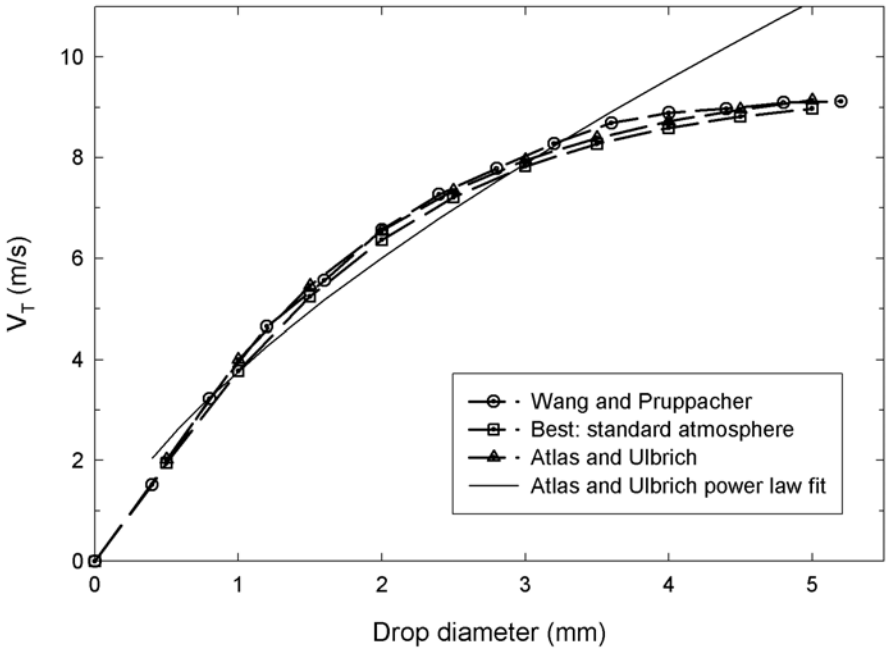

Figure C1. Variation of terminal velocity with drop diameter.

Torres et al. (1994) provide a general formulation for drop size distributions. The many drop size distributions that have been proposed by researchers over the

years all fit this formulation. They show that if this general formulation is appropriate, self-consistency requires that drop velocity be expressed as a power law in drop diameter. The Atlas and Ulbrich power law fit (equation C6) is plotted as a solid line in Figure C.1 for comparison to the theoretical and measured terminal velocity curves. Using the power law formula for terminal velocity with the probability density function for Best's drop size distribution (1950a),

$$f(d) = \frac{n}{a^{\mathrm{n}}} d^{\mathrm{n-1}} e^{-(\mathrm{d/a})^{\mathrm{n}}} \tag{C7}$$

where

d = drop diameter (mm)

$n = 2.25$

$a = AP^{\mathrm{p}}$

$A = 1.30$

$p = 0.232$

results in a liquid water content weighted terminal drop velocity in terms of the precipitation rate:

$$U_T(P) = \frac{n}{a^{\mathrm{n}}} U_{\mathrm{o}} \int_0^{\infty} x^{\mathrm{u}} x^{\mathrm{n-1}} e^{-(\mathrm{x/a})^{\mathrm{n}}} dx \tag{C8}$$

where $U_{\mathrm{o}} = 3.778$ and $u = 0.67$ from equation C6. Integrating gives

$$U_{\mathrm{T}}(P) = U_{\mathrm{o}} \left(AP^{\mathrm{p}} \right)^{\mathrm{u}} \Gamma\left(\frac{u}{n} + 1 \right) \tag{C9}$$

where $\Gamma(x)$ is the gamma function (Abramowitz and Stegun 1970, p. 253–270). Substituting the values of the parameters results in

$$U_{\mathrm{T}}(P) = 4.05 P^{0.155} . \tag{C10}$$

For precipitation rates between 0.5 and 4 mm/hr these terminal velocities are between 1 and 3% smaller than the terminal velocities in equation C3 derived from the liquid water content.

APPENDIX D. FOOTPRINTS OF THE PDSs

Maps of the 61 PDSs are included in this appendix. The maps are labeled with the start and end date of the storm (UTC) and include the modeled maximum ice thickness (mm) at each weather station from freezing rain and from freezing rain and ice pellets. The format is

R_{eq} (Z only) CRREL/Simple

R_{eq} (Z+IP) CRREL/Simple.

For clarity, on the often crowded PDS maps, when the CRREL and Simple model ice thicknesses differed by 1 mm or less, either for freezing rain only or freezing rain with ice pellets, they were reported as a single number on that line. When all four results were essentially the same they were reported as a single number.

The footprint of each storm, delineating the region where there was tree and power line damage as determined from the qualitative storm descriptions, is shown with a dashed line boundary. Summary information for the PDSs is in Table 3 and the footprints of the damaging storms are compiled in Figure 8. Reports and newspapers from which information on these storms was obtained are listed in "Literature Cited."

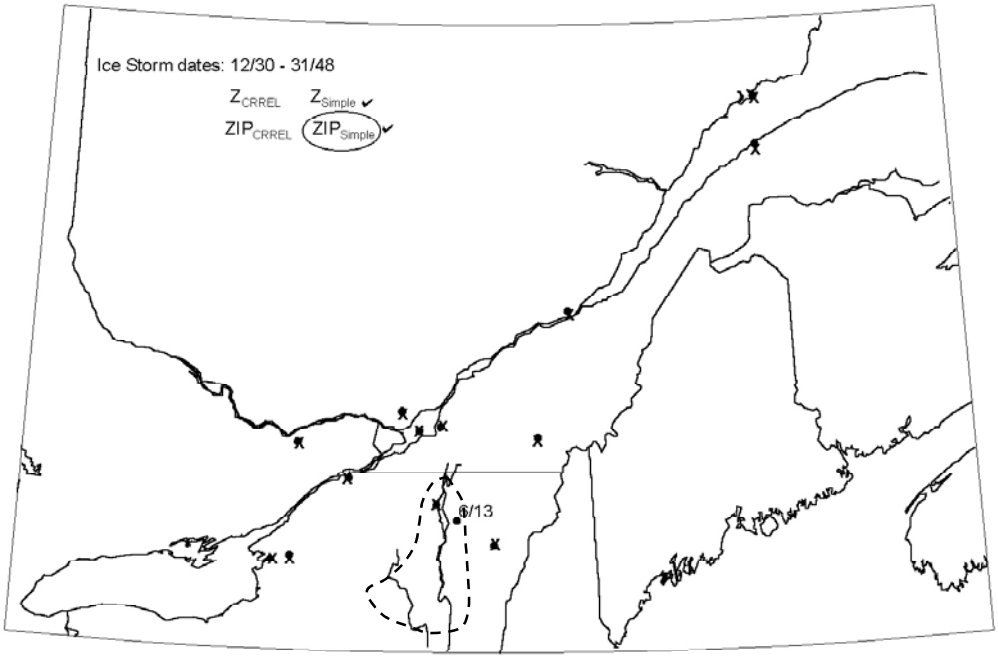
Ice Storm dates: 12/30 - 31/48
Z_{CRREL} Z_{Simple} ✔
ZIP_{CRREL} ZIP_{Simple} ✔
6/13

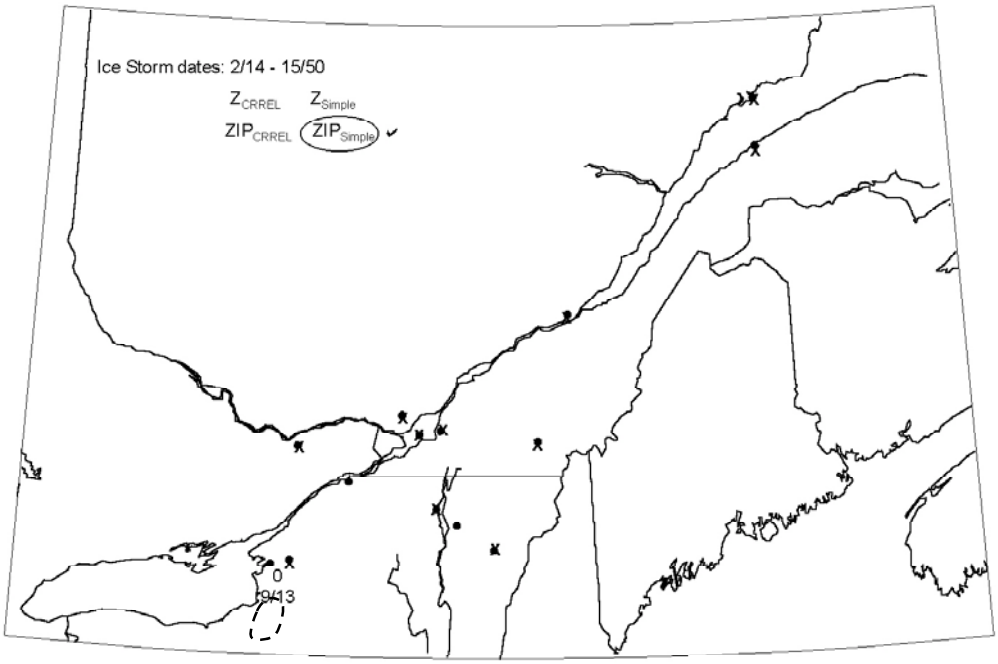
Ice Storm dates: 2/14 - 15/50
Z_{CRREL} Z_{Simple}
ZIP_{CRREL} ZIP_{Simple} ✔
0
9/13

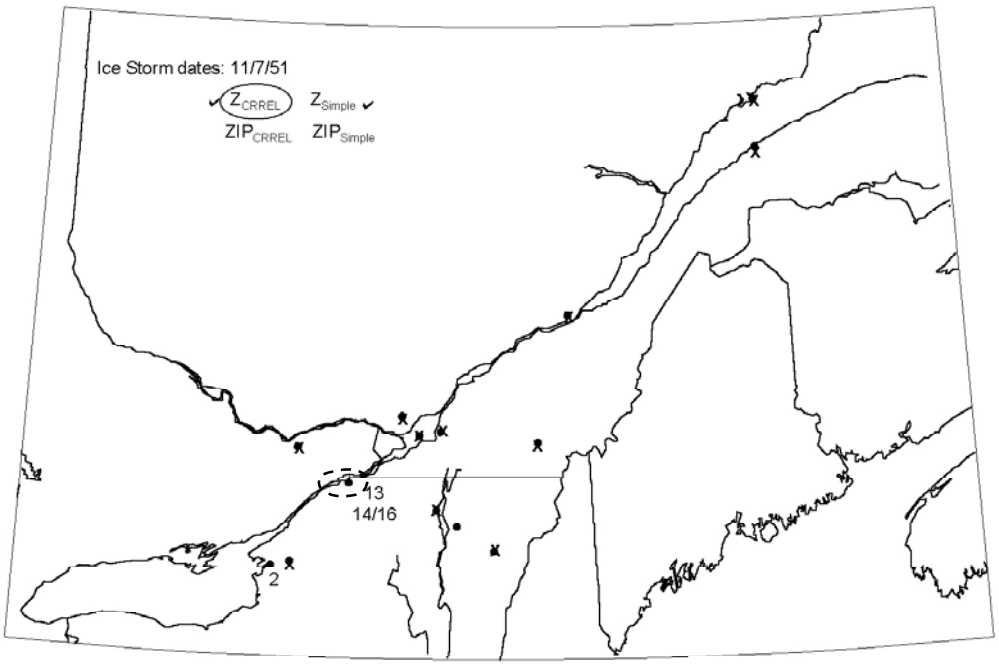
Ice Storm dates: 11/7/51
Z_{CRREL}
Z_{Simple} ✔
ZIP_{CRREL}
ZIP_{Simple}
13
14/16
2

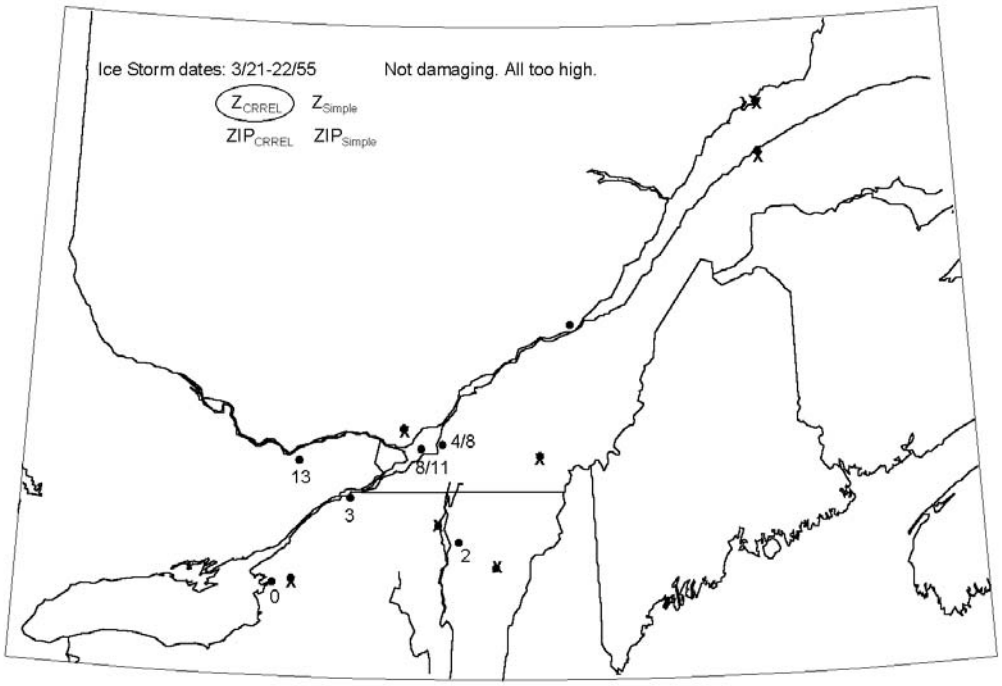
Ice Storm dates: 3/21-22/55
Not damaging. All too high.
Z_{CRREL}
Z_{Simple}
ZIP_{CRREL}
ZIP_{Simple}
13
4/8
8/11
3
2
0

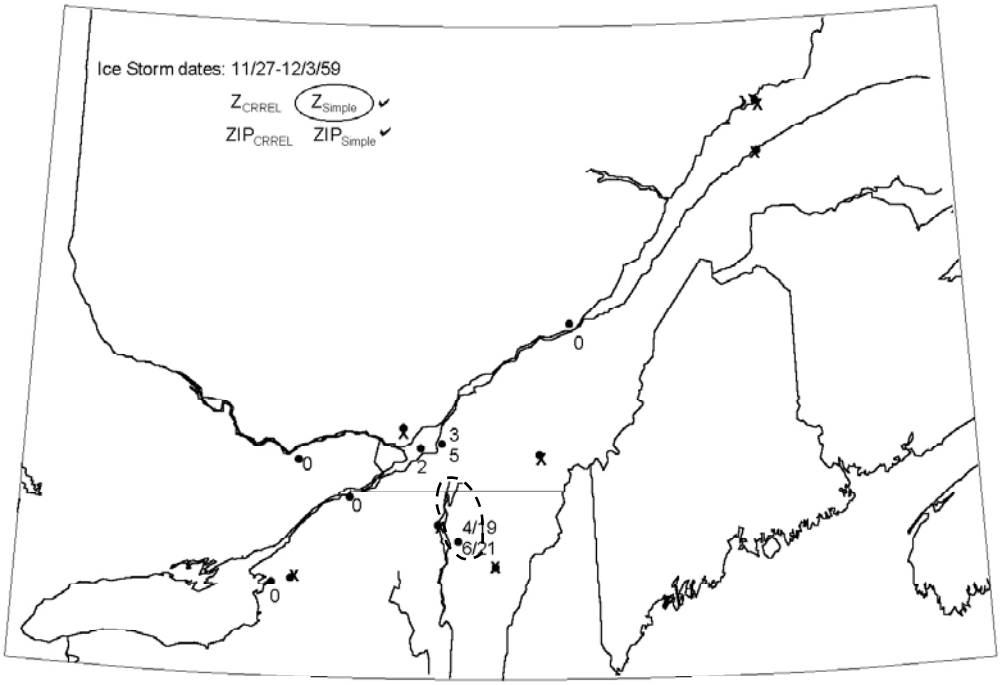
Ice Storm dates: 11/27-12/3/59
Z_{CRREL} Z_{Simple} ✓
ZIP_{CRREL} ZIP_{Simple} ✓
0
0
3
5
2
0
4/19
6/21
0

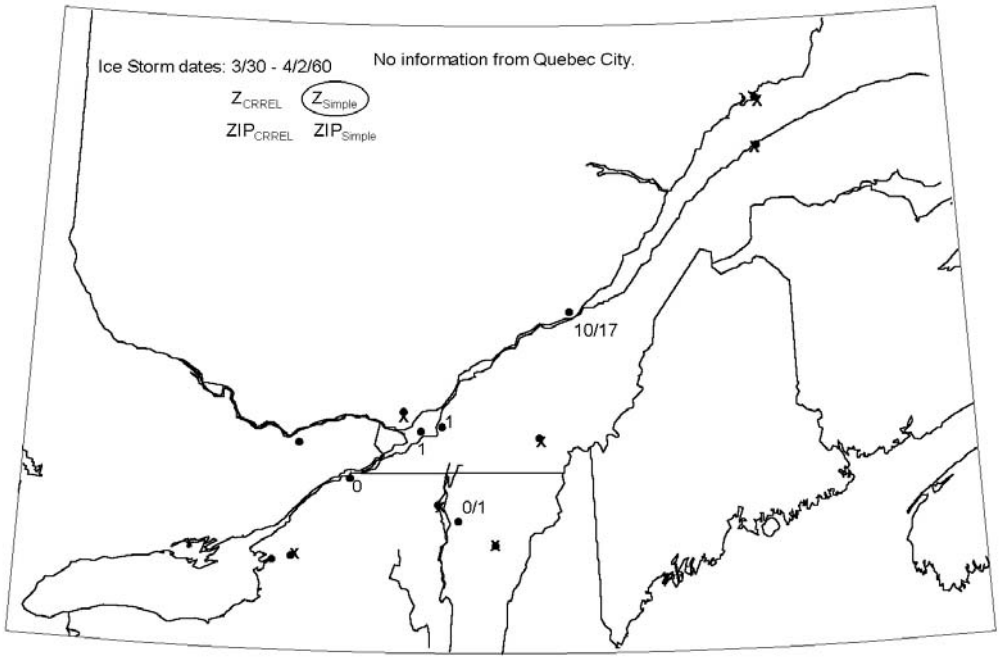
Ice Storm dates: 3/30 - 4/2/60
No information from Quebec City.
Z_{CRREL} Z_{Simple}
ZIP_{CRREL} ZIP_{Simple}
10/17
1
1
0
0/1

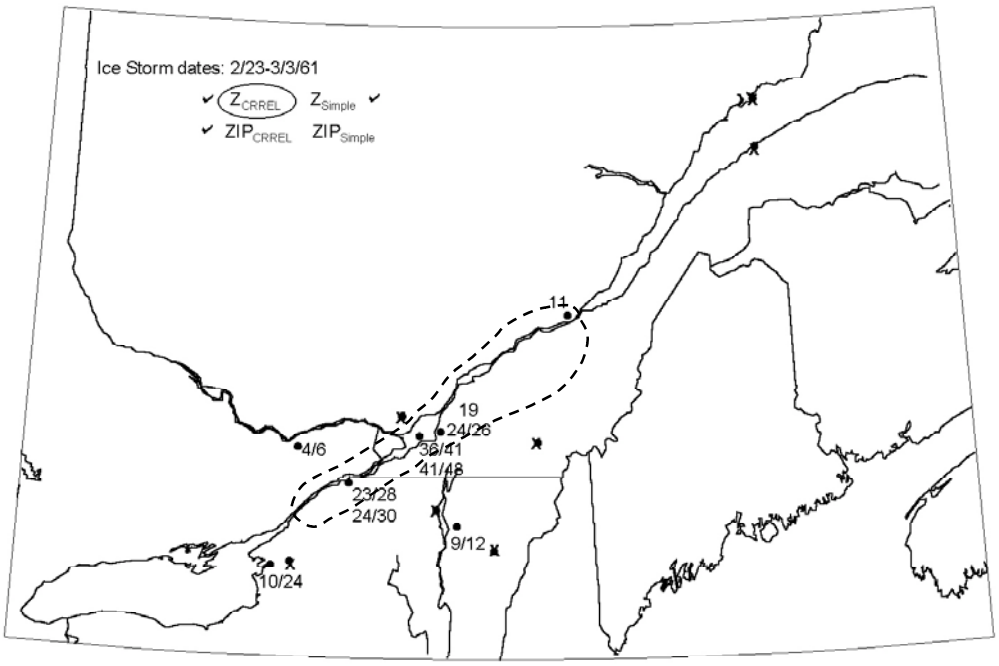
Ice Storm dates: 2/23-3/3/61
✔ Z_{CRREL} Z_{Simple} ✔
✔ ZIP_{CRREL} ZIP_{Simple}
11
19
24/26
4/6
35/41
41/48
23/28
24/30
9/12
10/24

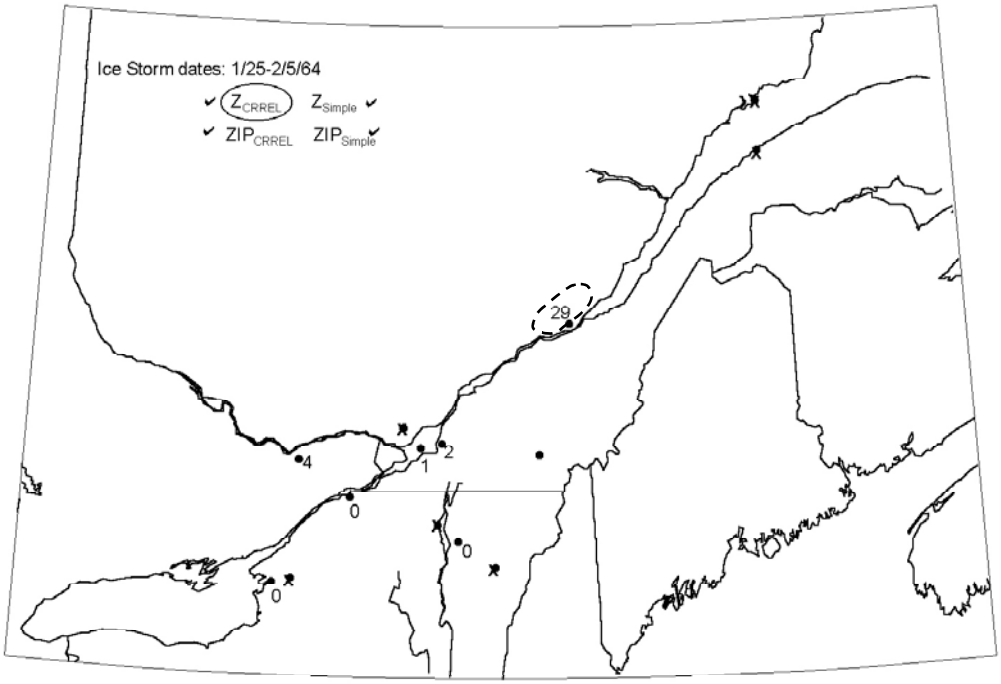
Ice Storm dates: 1/25-2/5/64
✔ Z_{CRREL} Z_{Simple} ✔
✔ ZIP_{CRREL} ZIP_{Simple} ✔
29
4
1
2
0
0
0

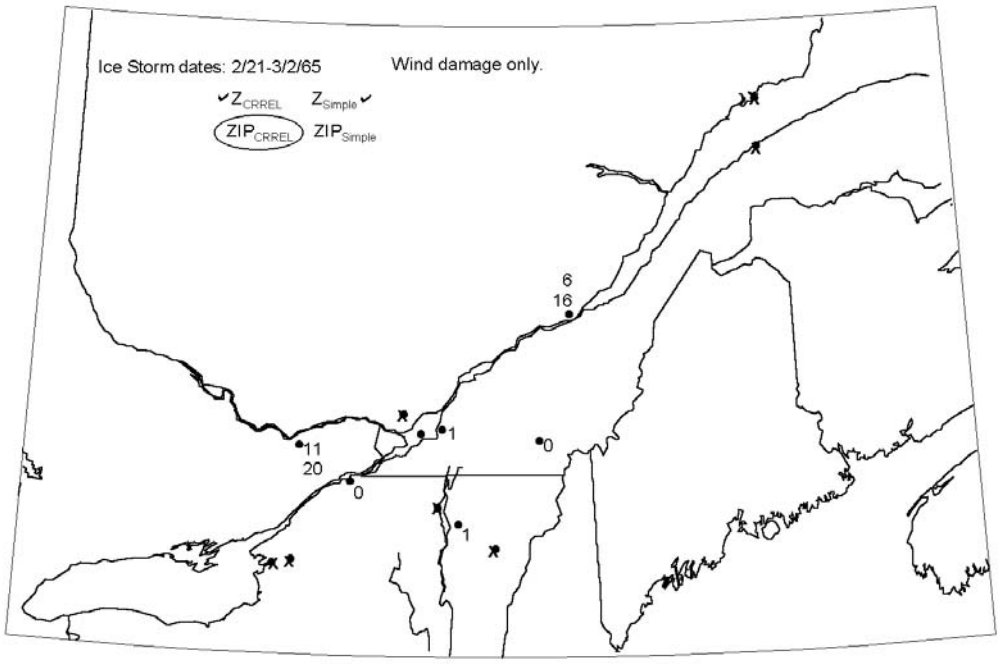
Ice Storm dates: 2/21-3/2/65
Wind damage only.
✔ZCRREL ZSimple ✔
ZIPCRREL ZIPSimple
6
16
11
20
0
1
0
1

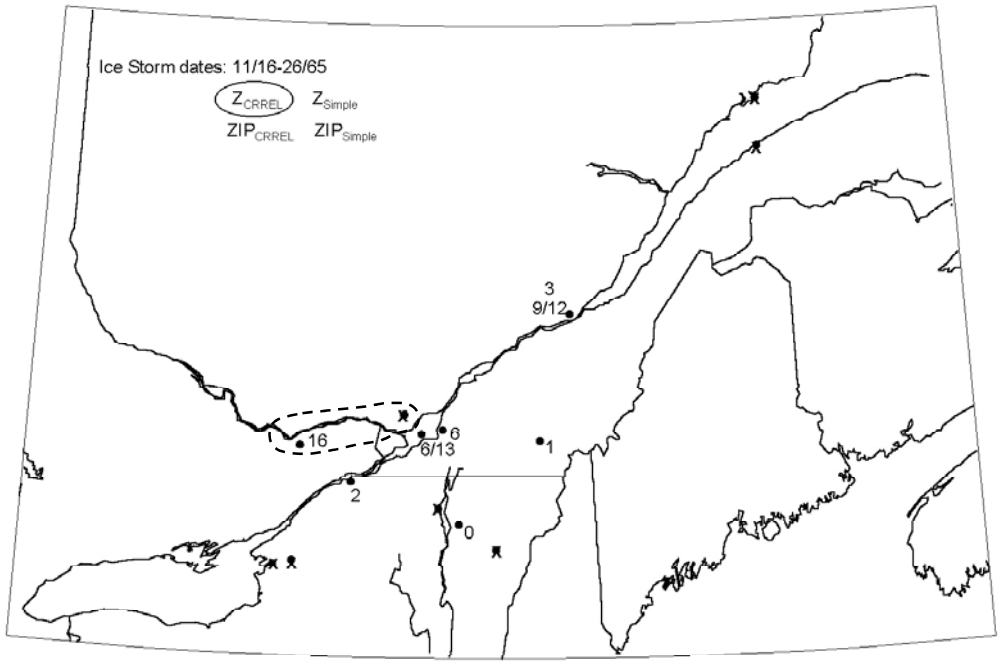
Ice Storm dates: 11/16-26/65
ZCRREL ZSimple
ZIPCRREL ZIPSimple
3
9/12
16
6
6/13
1
2
0

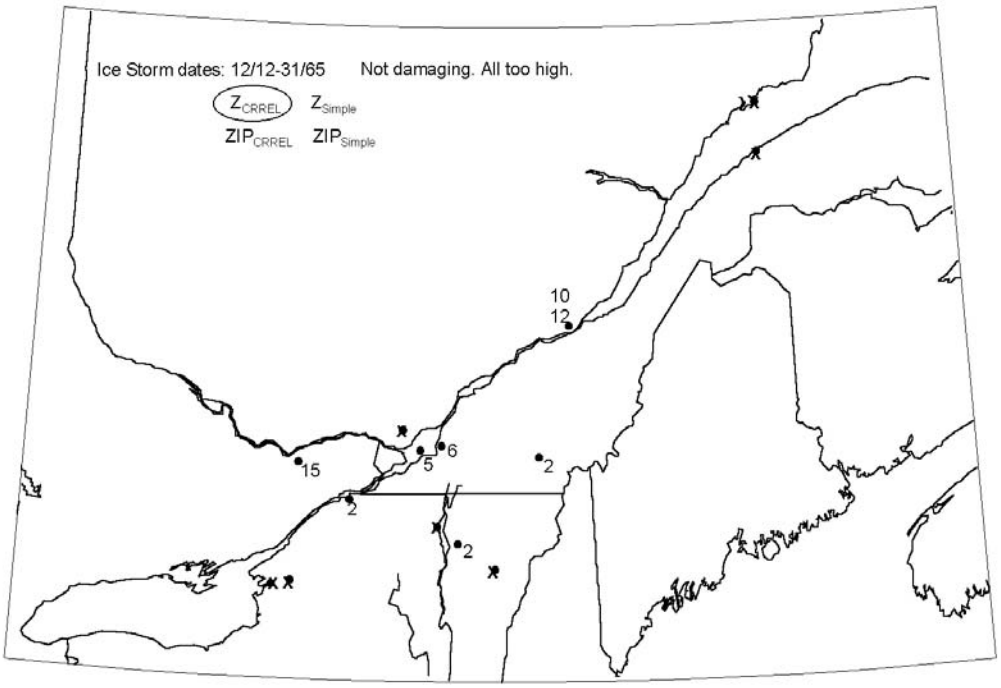
Ice Storm dates: 12/12-31/65
Not damaging. All too high.
Z_{CRREL}
Z_{Simple}
ZIP_{CRREL}
ZIP_{Simple}
10
12
15
5
6
2
2
2

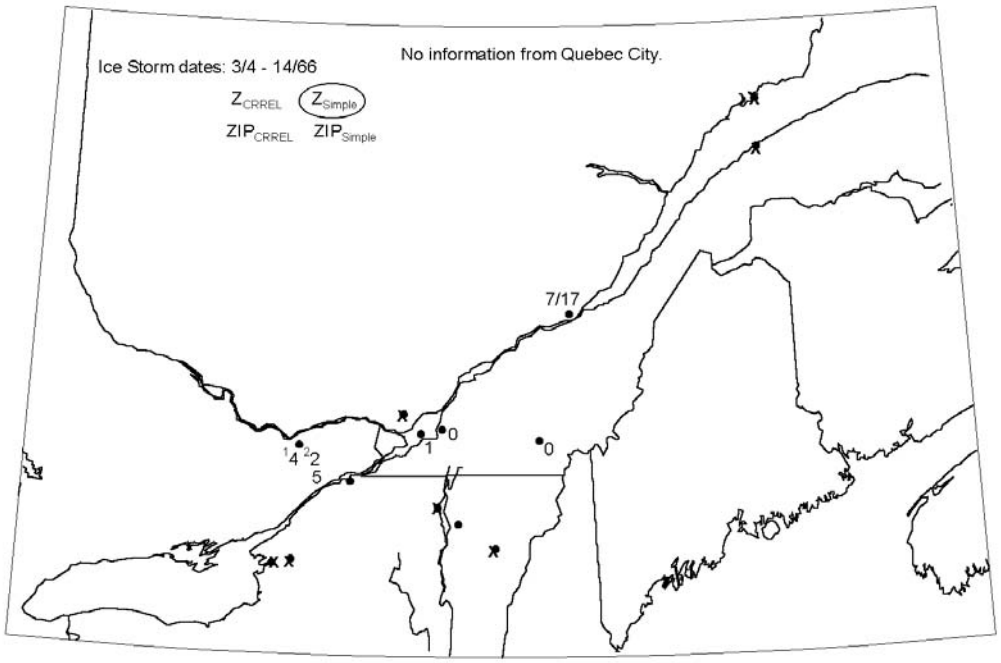
Ice Storm dates: 3/4 - 14/66
No information from Quebec City.
Z_{CRREL}
Z_{Simple}
ZIP_{CRREL}
ZIP_{Simple}
7/17
1
4
2
5
1
0
0

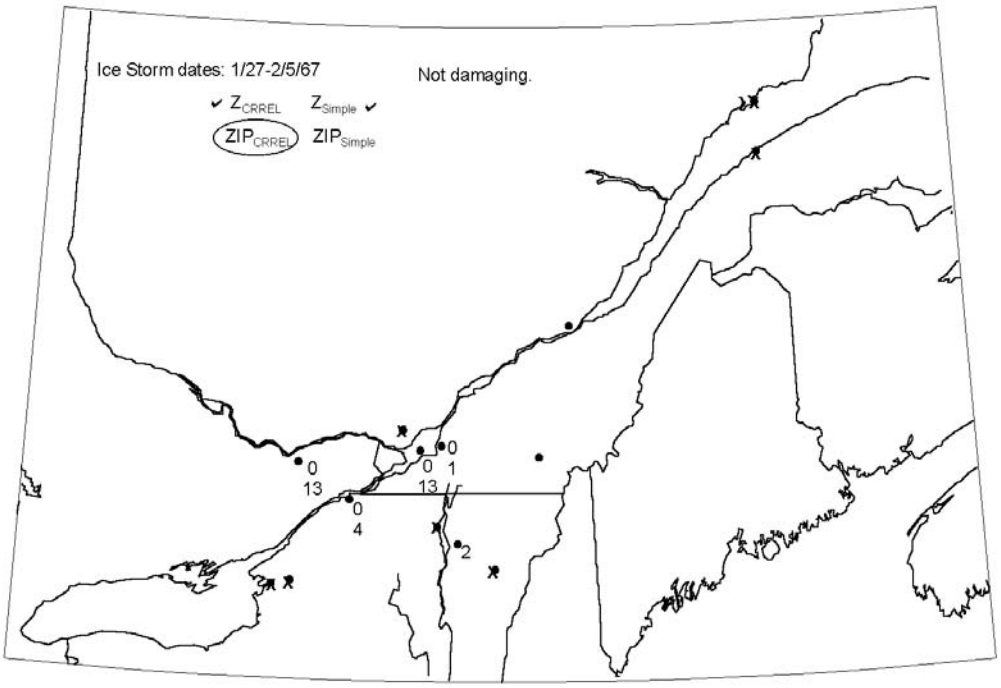
Ice Storm dates: 1/27-2/5/67
Not damaging.
✔ Z_{CRREL} Z_{Simple} ✔
ZIP_{CRREL} ZIP_{Simple}
0
13
0
4
0
0
1
13
2

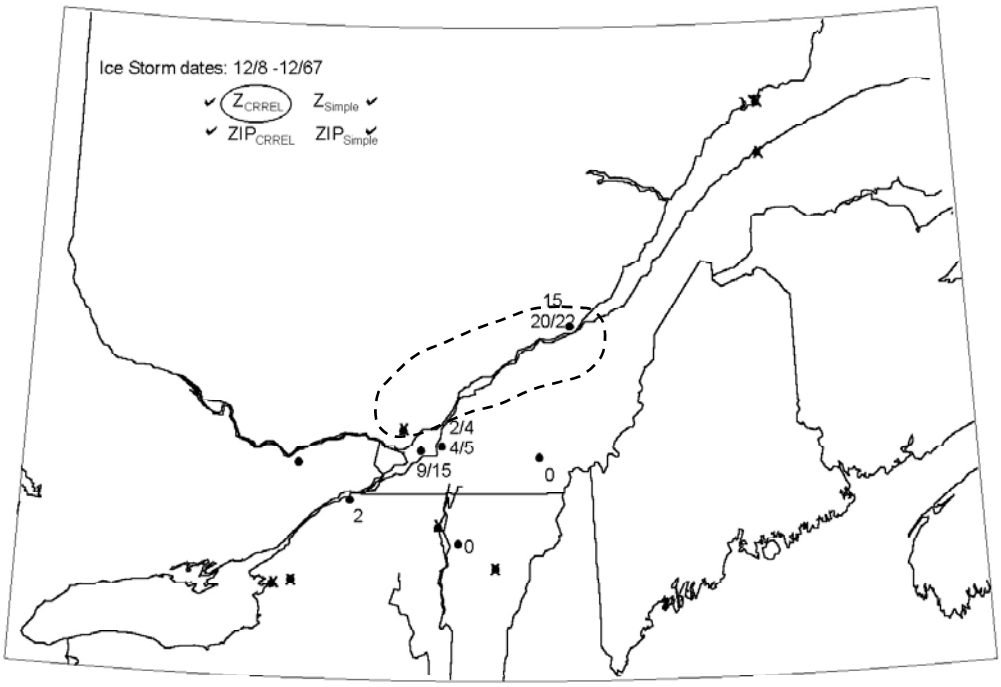
Ice Storm dates: 12/8 -12/67
✔ Z_{CRREL} Z_{Simple} ✔
✔ ZIP_{CRREL} ZIP_{Simple} ✔
15
20/22
2/4
4/5
9/15
2
0
0

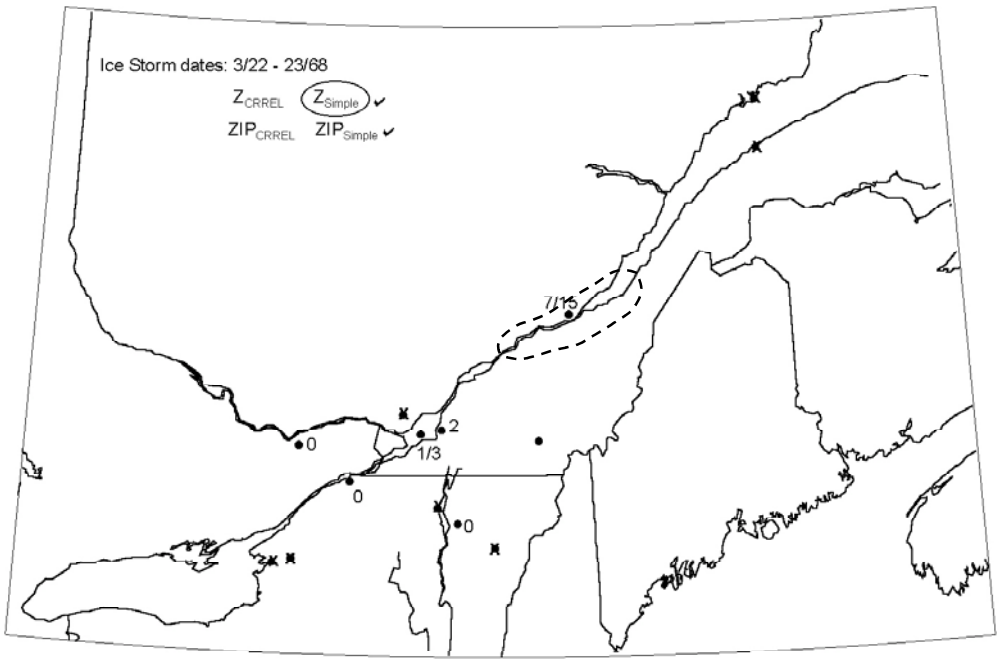
Ice Storm dates: 3/22 - 23/68
Z_{CRREL} Z_{Simple} ✔
ZIP_{CRREL} ZIP_{Simple} ✔
7/15
0
2
1/3
0
0

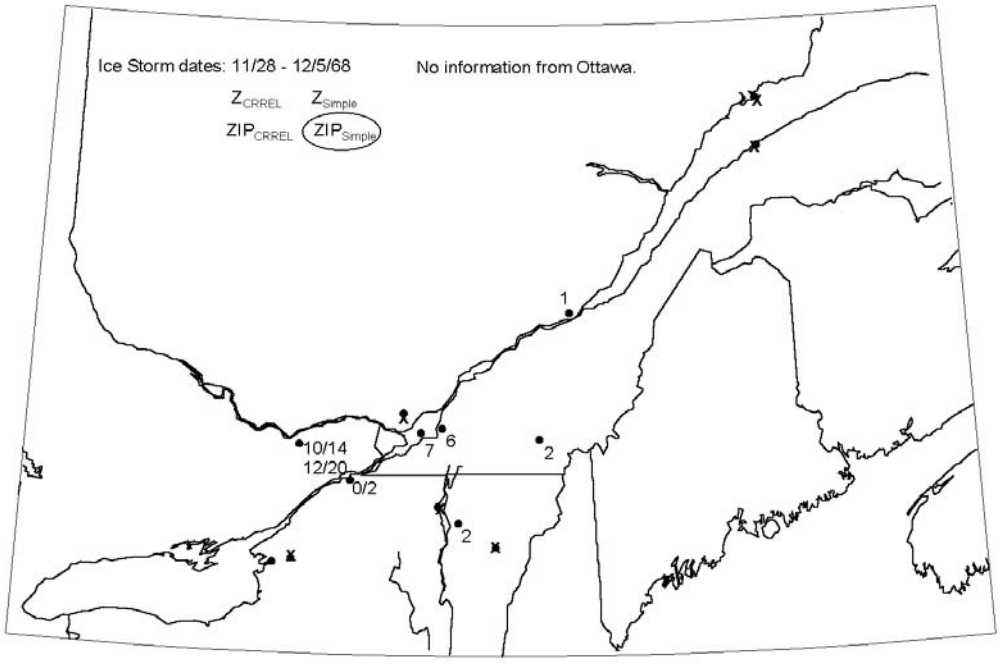
Ice Storm dates: 11/28 - 12/5/68
No information from Ottawa.
Z_{CRREL} Z_{Simple}
ZIP_{CRREL} ZIP_{Simple}
1
10/14
12/20
0/2
7
6
2
2

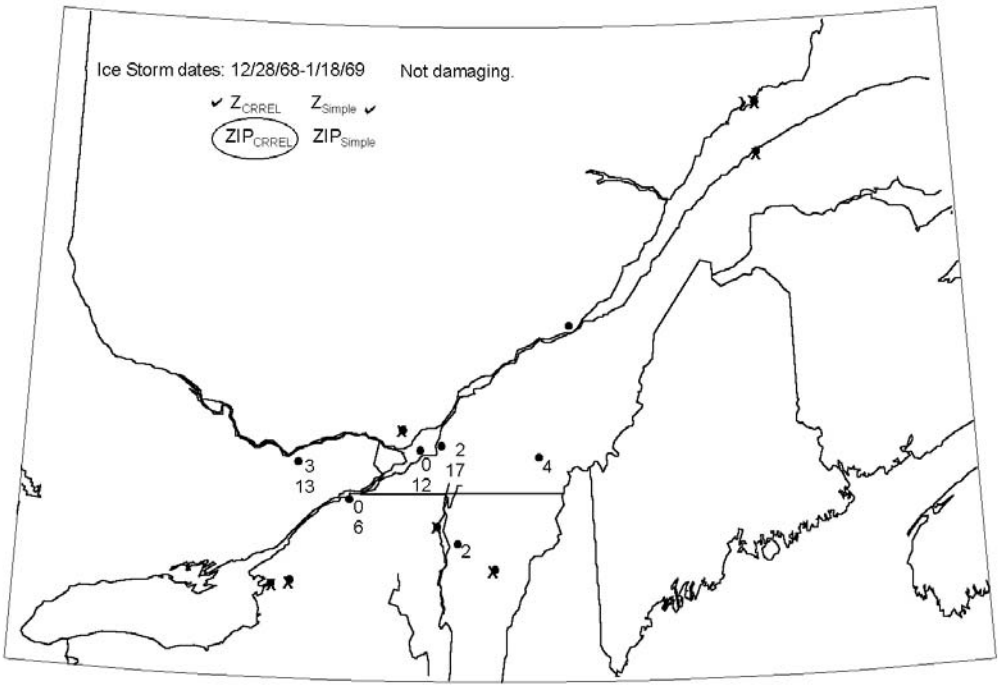
Ice Storm dates: 12/28/68-1/18/69
Not damaging.
✔ Z_{CRREL}
Z_{Simple} ✔
ZIP_{CRREL}
ZIP_{Simple}
3
13
0
6
0
12
2
17
4
2

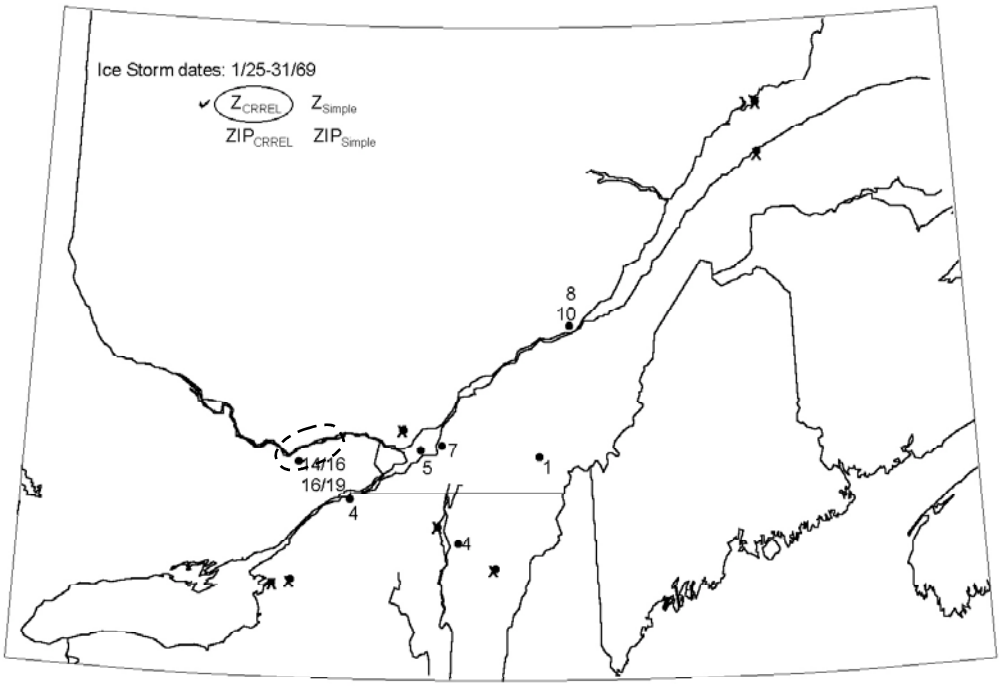
Ice Storm dates: 1/25-31/69
✔ Z_{CRREL}
Z_{Simple}
ZIP_{CRREL}
ZIP_{Simple}
8
10
14/16
16/19
4
5
7
1
4

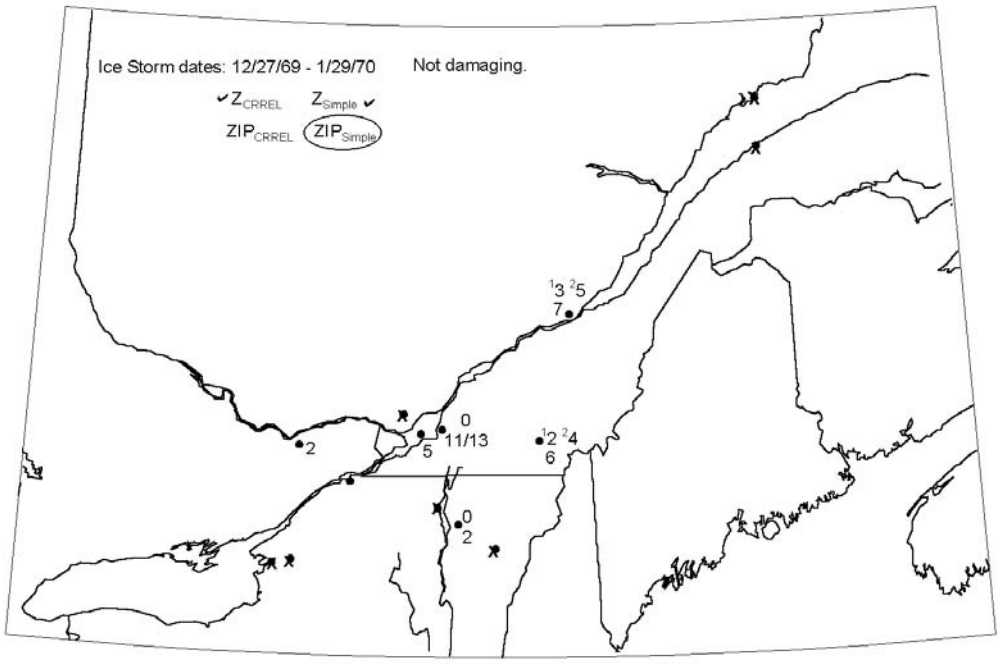
Ice Storm dates: 12/27/69 - 1/29/70
Not damaging.
✔ZCRREL ZSimple ✔
ZIPCRREL ZIPSimple
1 3 2 5
7
0
11/13
5
2
1 2 2 4
6
0
2

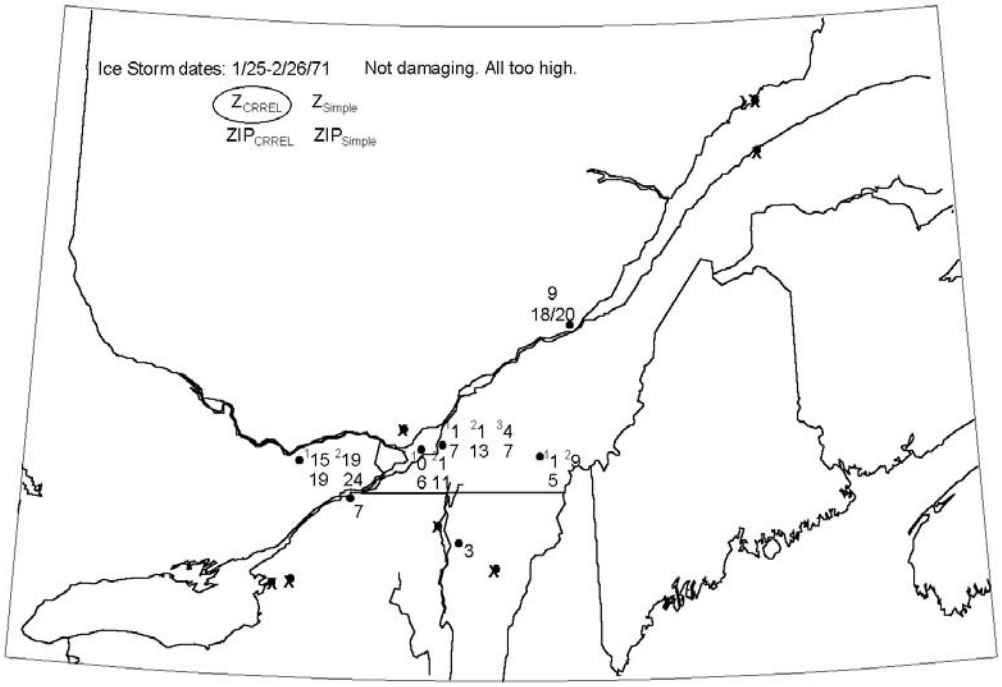
Ice Storm dates: 1/25-2/26/71
Not damaging. All too high.
ZCRREL ZSimple
ZIPCRREL ZIPSimple
9
18/20
1 2 1 3 4
7 13 7
0 1
6 11
1 2 9
5
1 15 2 19
19 24
7
3

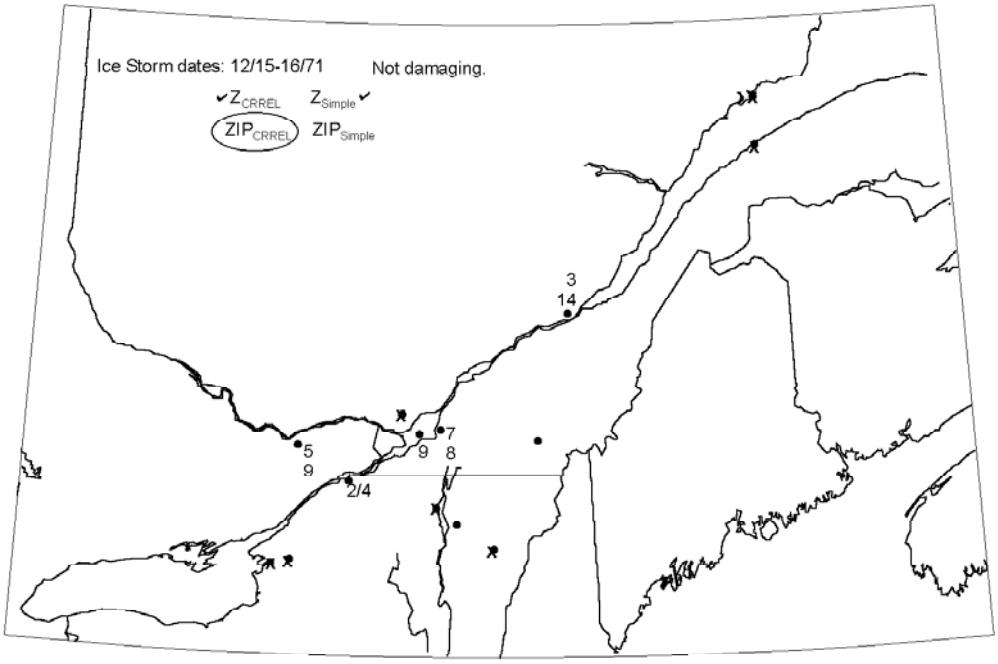
Ice Storm dates: 12/15-16/71
Not damaging.
✔ZCRREL
ZSimple ✔
ZIPCRREL
ZIPSimple
3
14
5
9
9
7
8
2/4

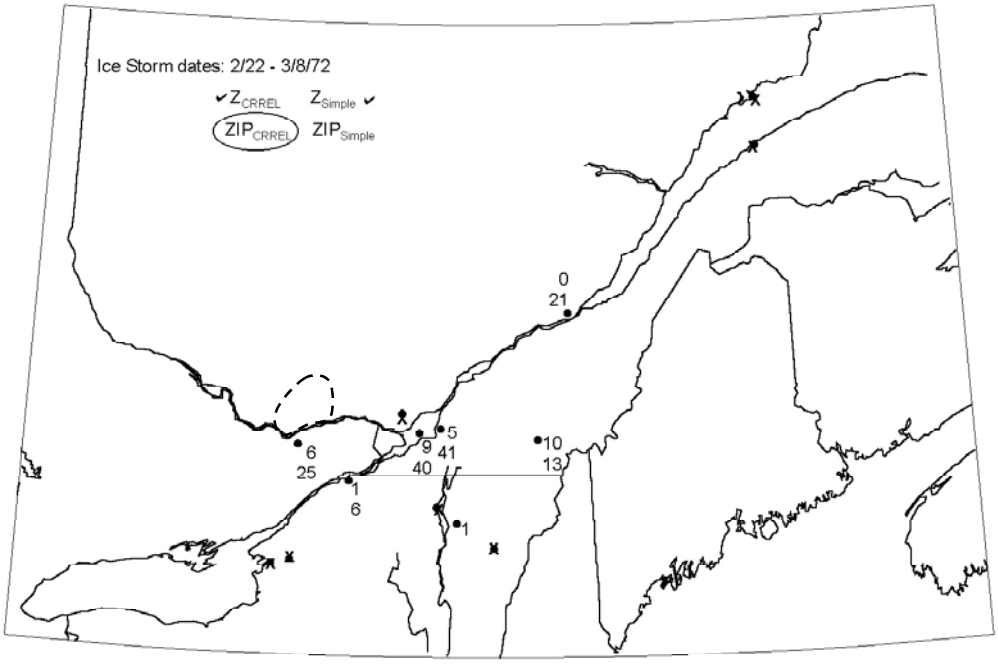
Ice Storm dates: 2/22 - 3/8/72
✔ZCRREL
ZSimple ✔
ZIPCRREL
ZIPSimple
0
21
6
25
1
6
9
5
41
40
10
13
1

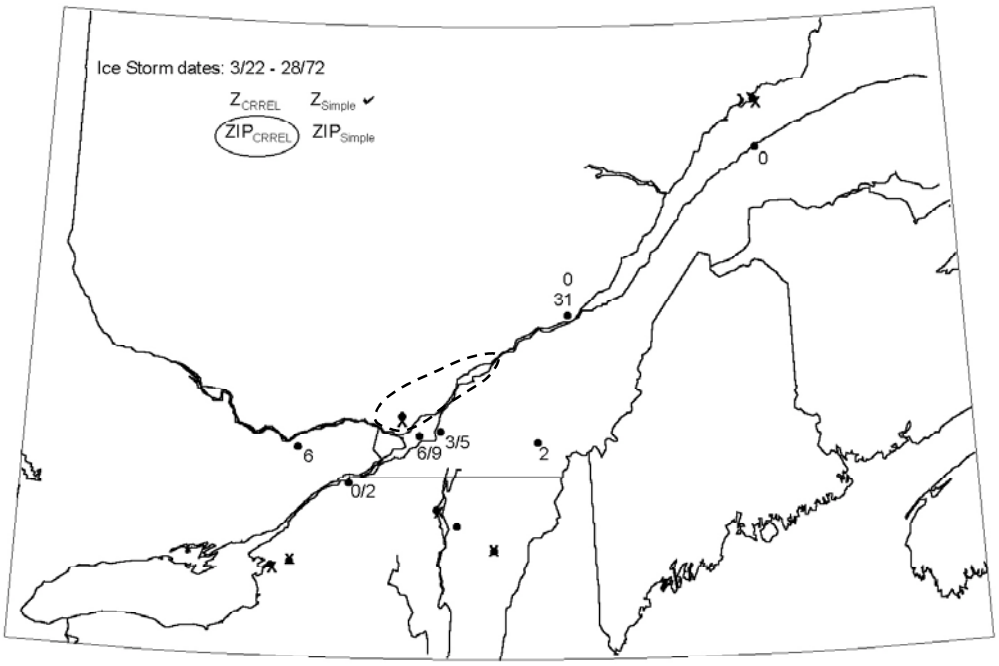
Ice Storm dates: 3/22 - 28/72
Z_{CRREL} Z_{Simple} ✔
ZIP_{CRREL} ZIP_{Simple}
0
0
31
6
6/9
3/5
2
0/2

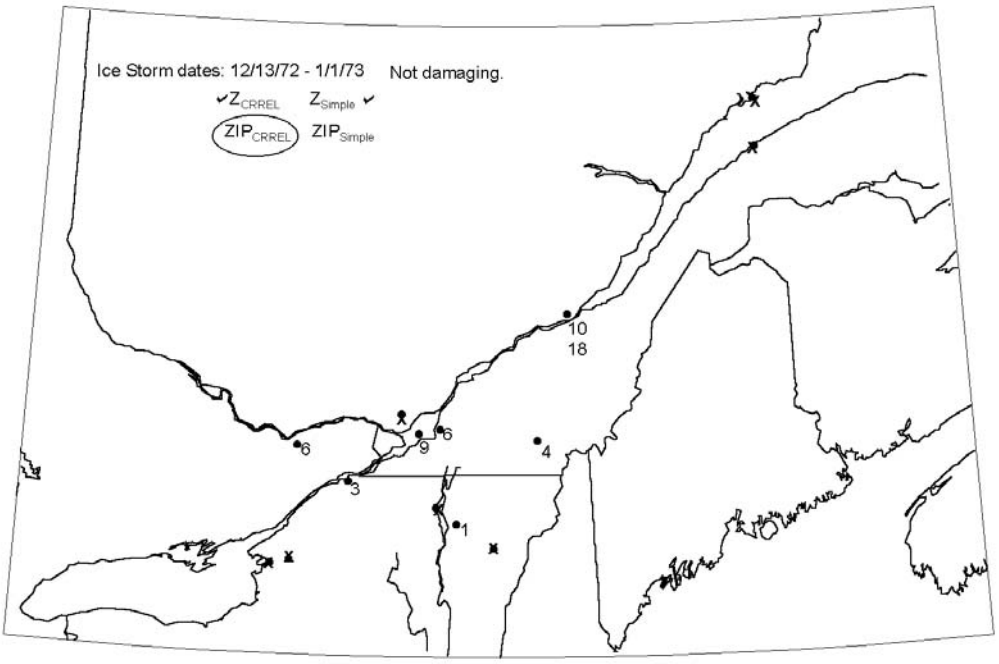
Ice Storm dates: 12/13/72 - 1/1/73 Not damaging.
✔Z_{CRREL} Z_{Simple} ✔
ZIP_{CRREL} ZIP_{Simple}
10
18
6
9
6
4
3
1

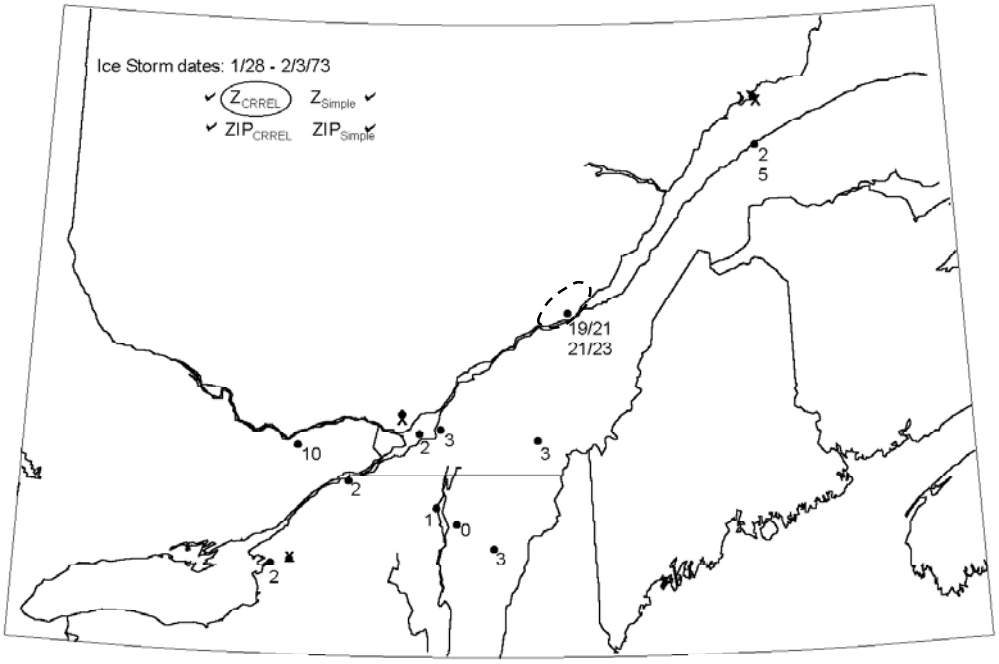
Ice Storm dates: 1/28 - 2/3/73
Z_CRREL
Z_Simple
ZIP_CRREL
ZIP_Simple
2
5
19/21
21/23
10
2
3
2
3
1
0
3
2

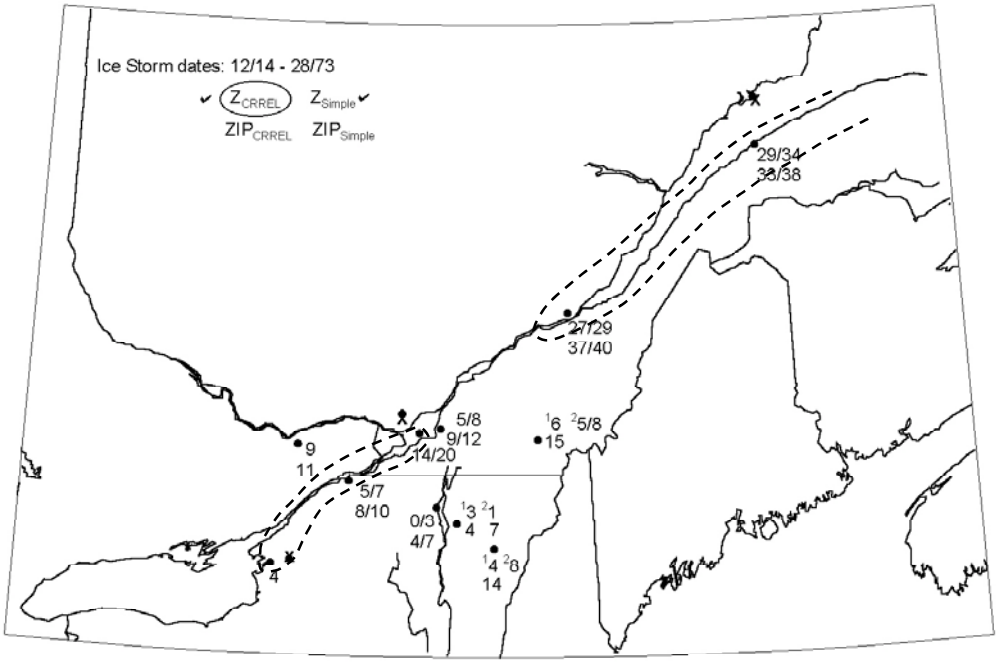
Ice Storm dates: 12/14 - 28/73
Z_CRREL
Z_Simple
ZIP_CRREL
ZIP_Simple
29/34
33/38
27/29
37/40
5/8
9/12
14/20
9
11
5/7
8/10
0/3
4/7
4
1 6 2 5/8
15
1 3 2 1
4 7
1 4 2 8
14

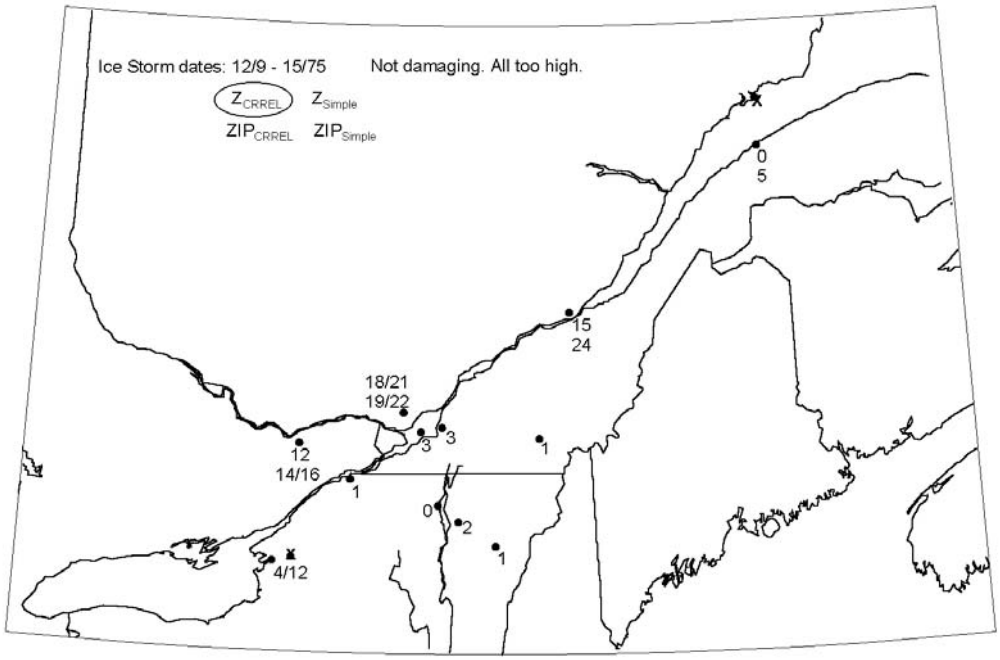
Ice Storm dates: 12/9 - 15/75
Not damaging. All too high.
Z_{CRREL}
Z_{Simple}
ZIP_{CRREL}
ZIP_{Simple}
0
5
15
24
18/21
19/22
3
3
1
12
14/16
1
0
2
1
4/12

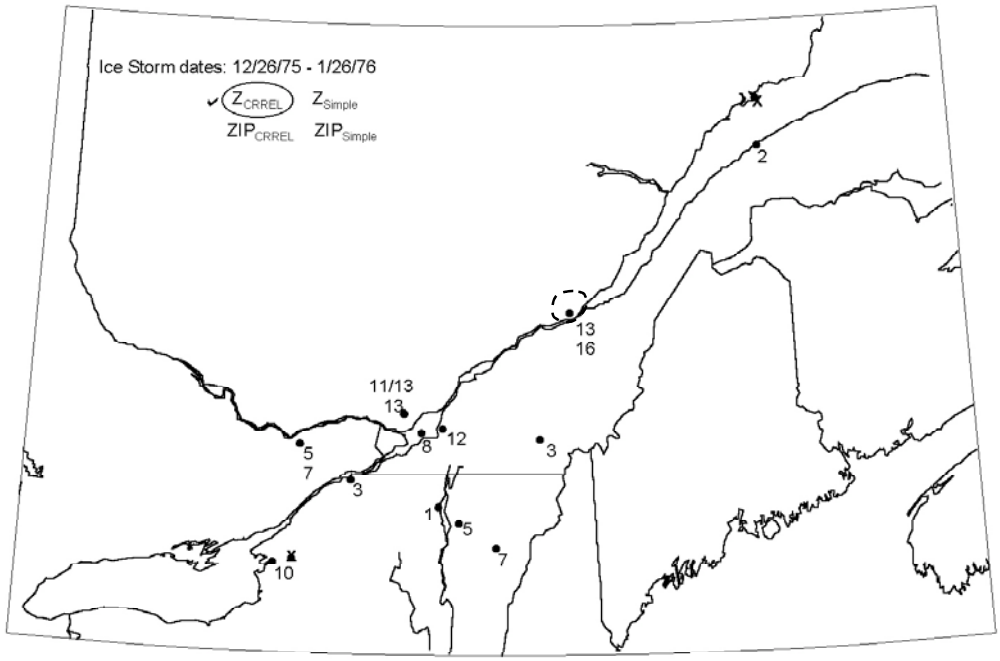
Ice Storm dates: 12/26/75 - 1/26/76
Z_{CRREL}
Z_{Simple}
ZIP_{CRREL}
ZIP_{Simple}
2
13
16
11/13
13
5
7
8
12
3
3
1
5
7
10

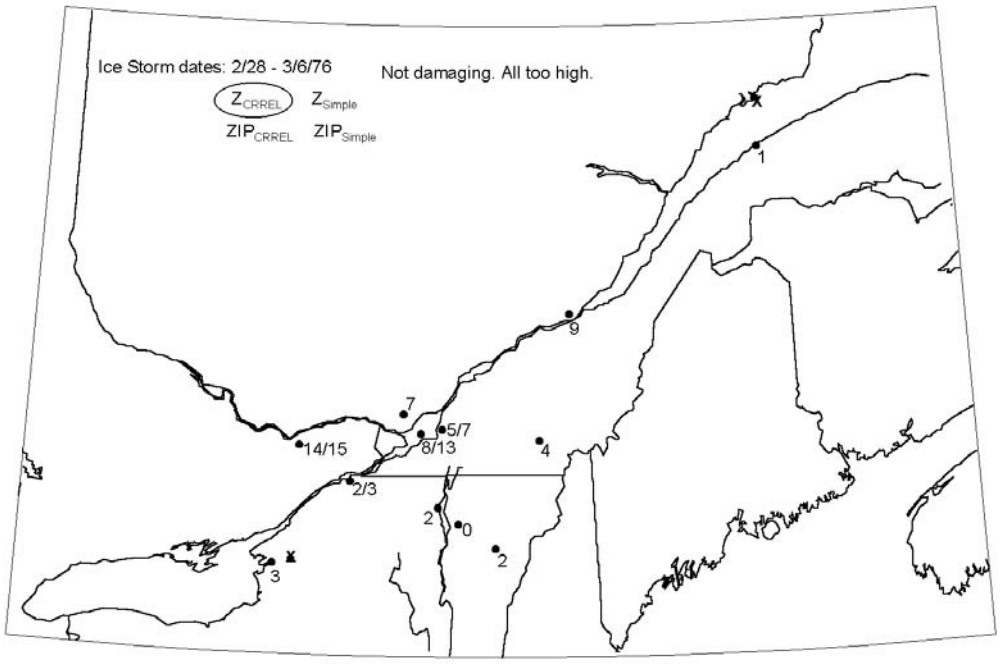
Ice Storm dates: 2/28 - 3/6/76
Not damaging. All too high.
Z_{CRREL}
Z_{Simple}
ZIP_{CRREL}
ZIP_{Simple}
1
9
7
5/7
8/13
14/15
4
2/3
2
0
2
3

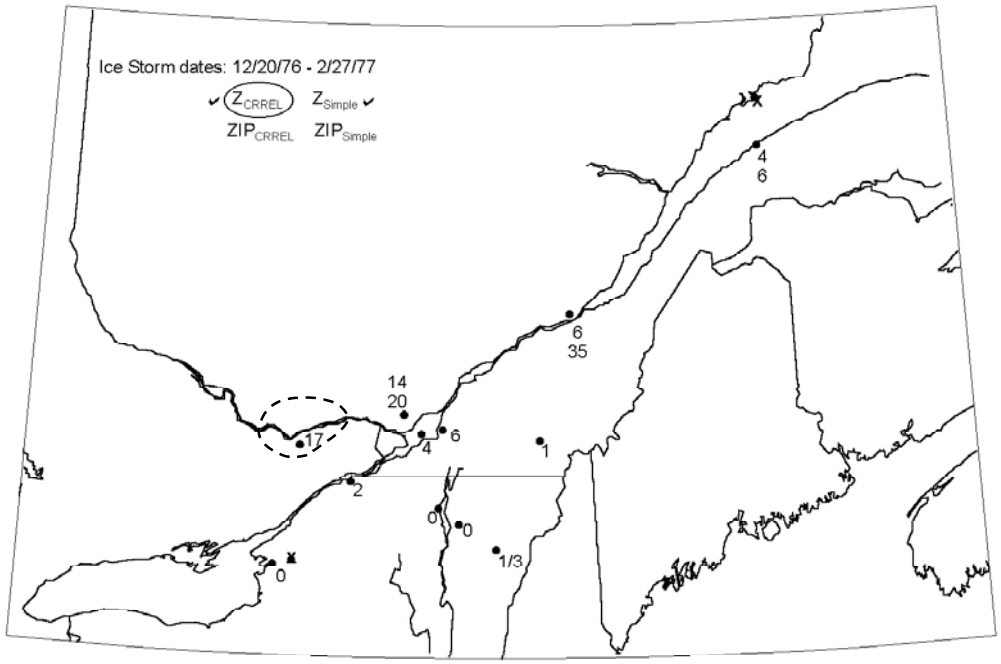
Ice Storm dates: 12/20/76 - 2/27/77
Z_{CRREL}
Z_{Simple}
ZIP_{CRREL}
ZIP_{Simple}
4
6
6
35
14
20
17
4
6
1
2
0
0
1/3
0

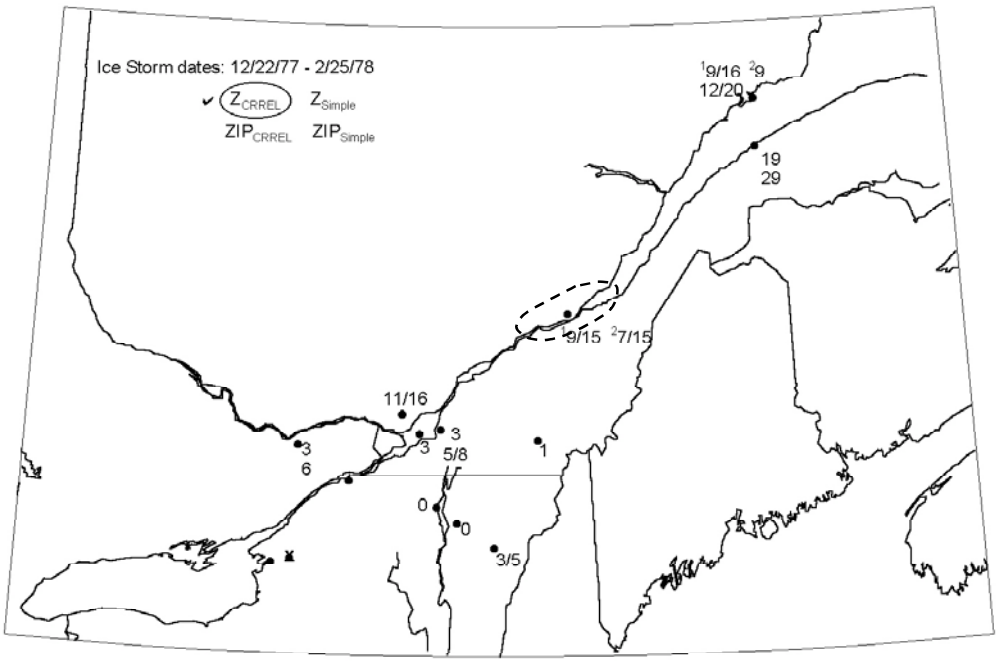
Ice Storm dates: 12/22/77 - 2/25/78
✔ Z_CRREL Z_Simple
ZIP_CRREL ZIP_Simple
[1]9/16 [2]9
12/20
19
29
[1]9/15 [2]7/15
11/16
3
6
3
3
5/8
1
0
0
3/5

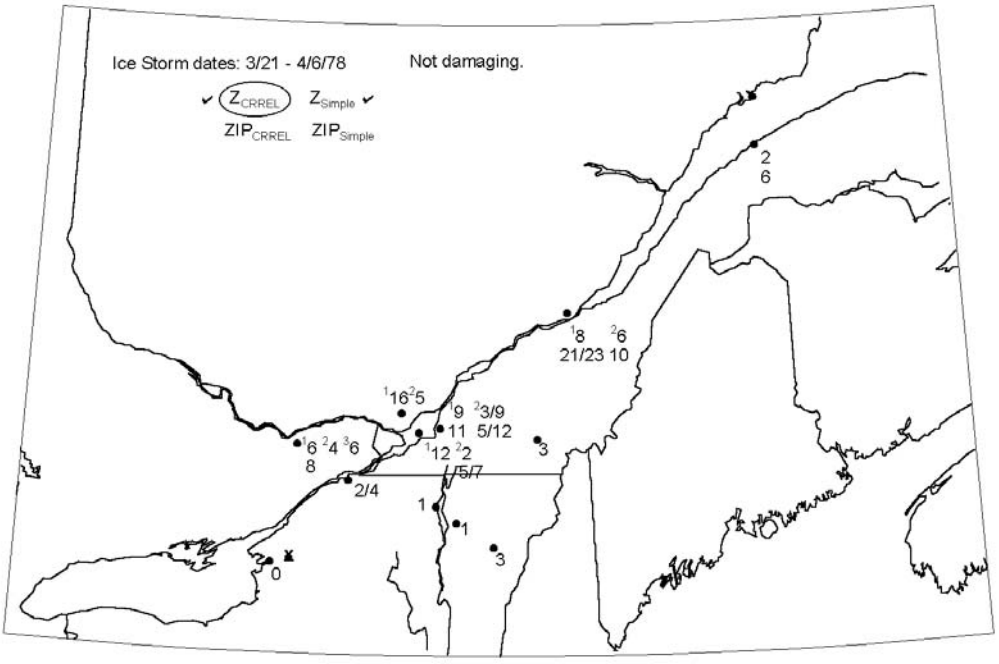
Ice Storm dates: 3/21 - 4/6/78
Not damaging.
✔ Z_CRREL Z_Simple ✔
ZIP_CRREL ZIP_Simple
2
6
[1]8 [2]6
21/23 10
[1]16 [2]5
[1]9 [2]3/9
11 5/12
[1]6 [2]4 [3]6
8
[1]12 [2]2
3
5/7
2/4
1
1
0
3

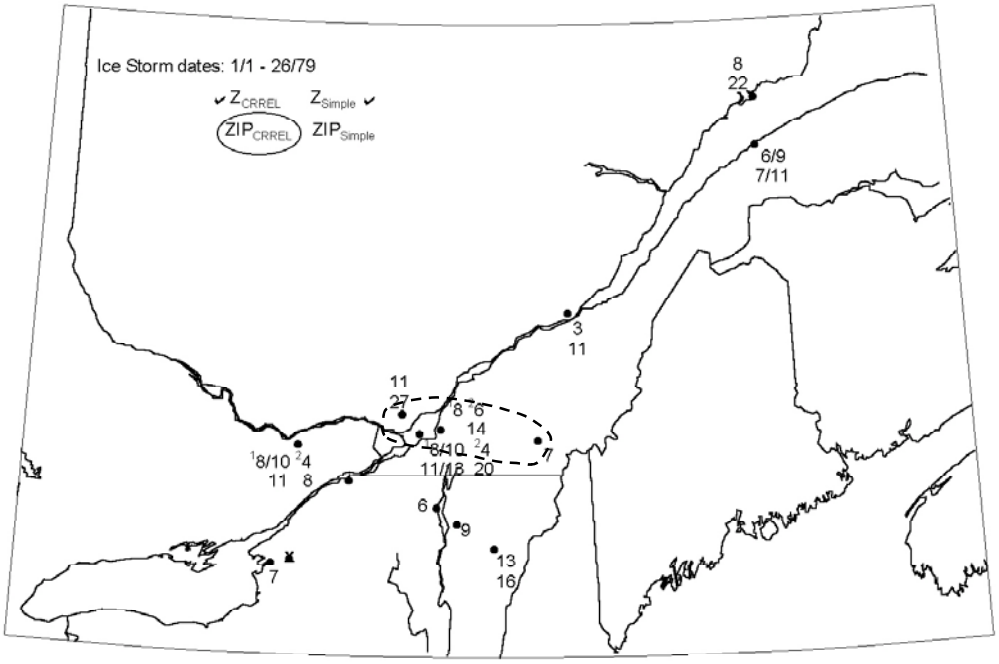
Ice Storm dates: 1/1 - 26/79
Z CRREL
Z Simple
ZIP CRREL
ZIP Simple
8
22
6/9
7/11
3
11
11
27
8
6
14
8/10
2
4
11/18
20
7
1
8/10
2
4
11
8
6
9
13
16
7

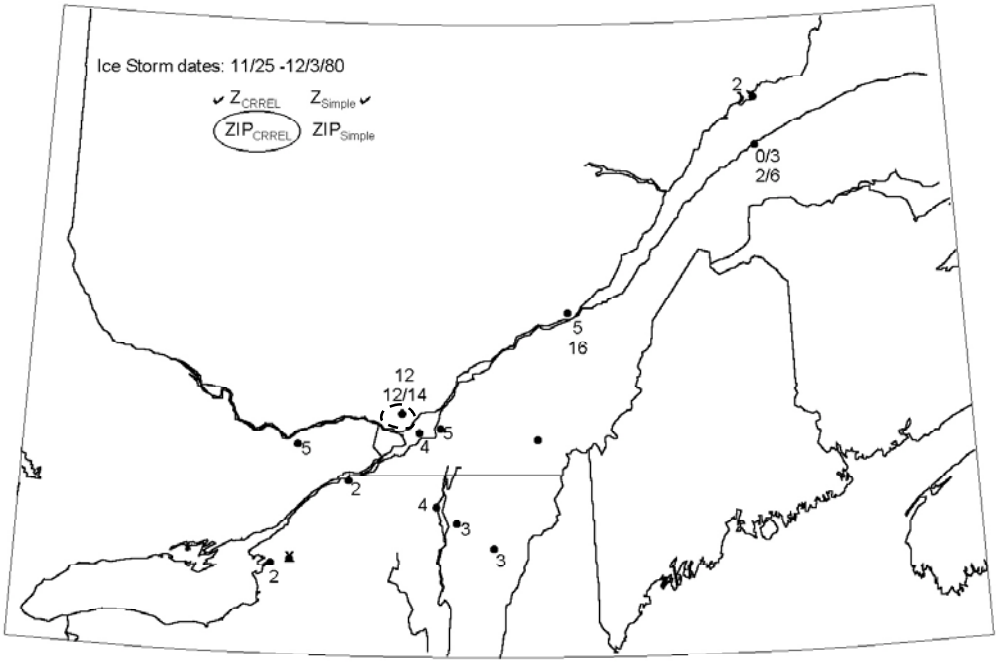
Ice Storm dates: 11/25 -12/3/80
Z CRREL
Z Simple
ZIP CRREL
ZIP Simple
2
0/3
2/6
5
16
12
12/14
5
4
5
2
4
3
3
2

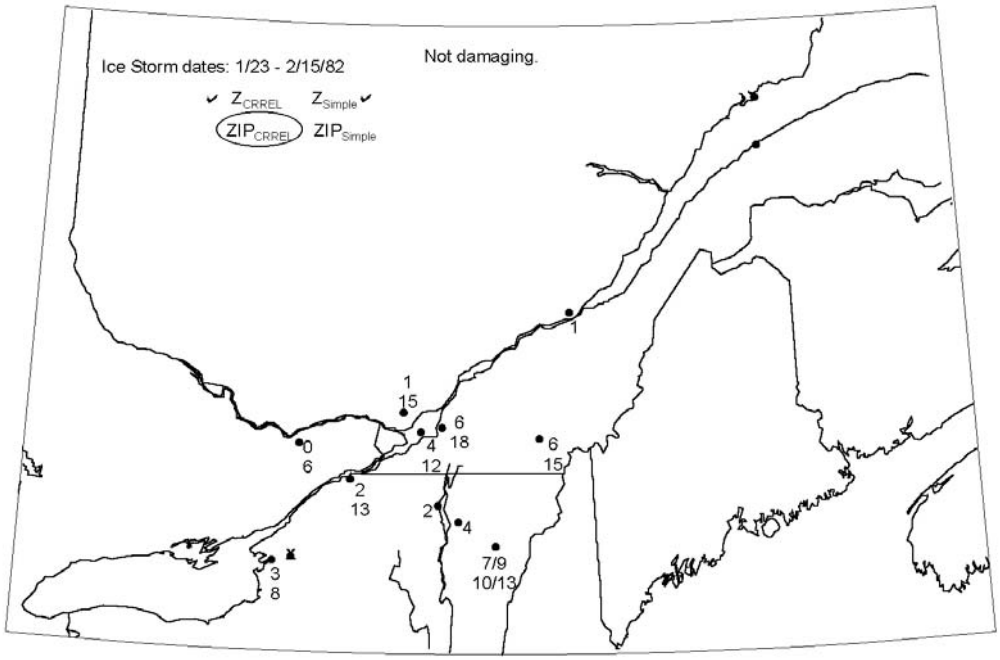
Ice Storm dates: 1/23 - 2/15/82
Not damaging.
✔ Z_{CRREL} Z_{Simple} ✔
ZIP_{CRREL} ZIP_{Simple}
1
1
15
6
18
4
12
0
6
2
13
6
15
2
4
7/9
10/13
3
8

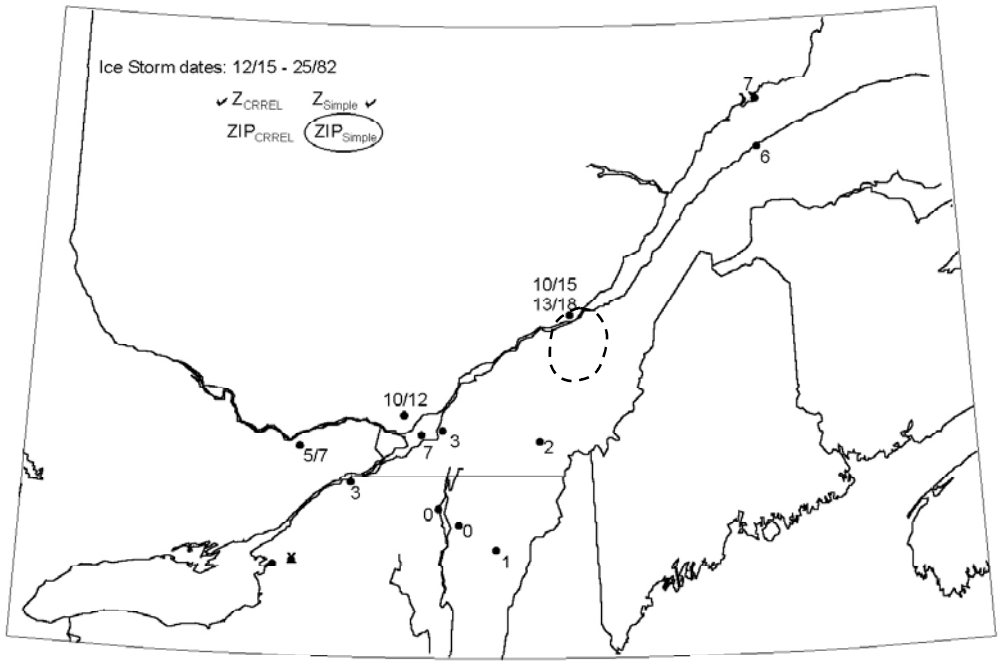
Ice Storm dates: 12/15 - 25/82
✔ Z_{CRREL} Z_{Simple} ✔
ZIP_{CRREL} ZIP_{Simple}
7
6
10/15
13/18
10/12
5/7
7
3
3
2
0
0
1

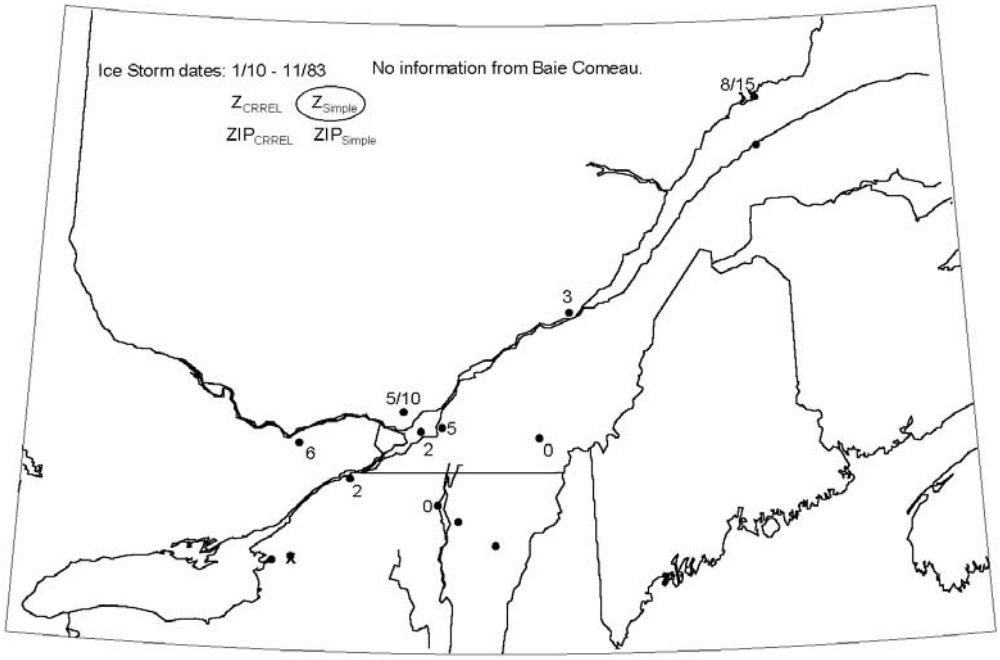
Ice Storm dates: 1/10 - 11/83
No information from Baie Comeau.
Z_{CRREL} Z_{Simple}
ZIP_{CRREL} ZIP_{Simple}
8/15
3
5/10
6
2
5
2
0
0

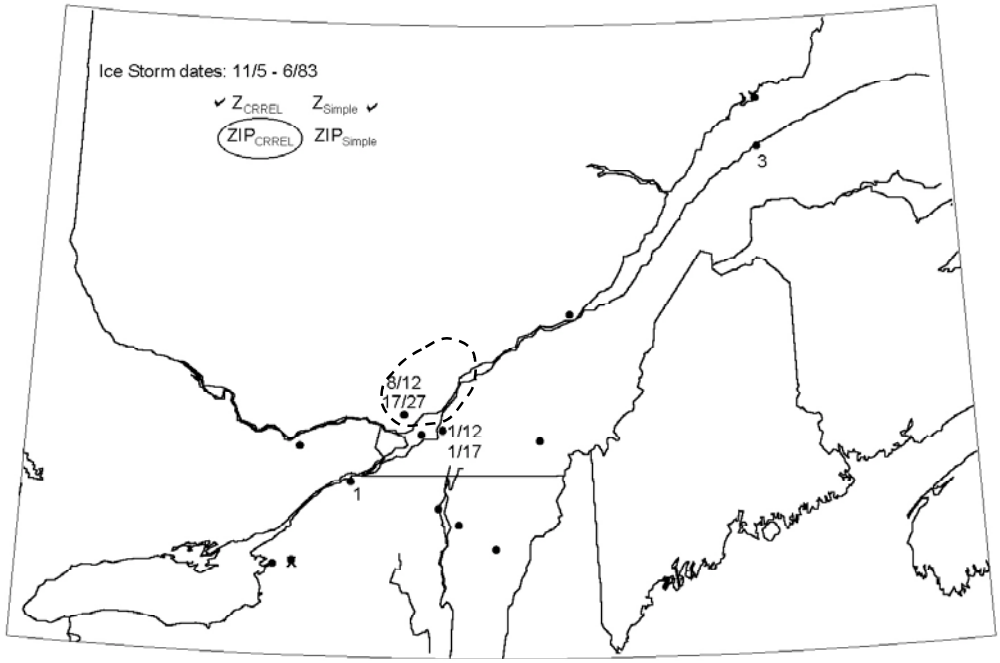
Ice Storm dates: 11/5 - 6/83
✔ Z_{CRREL} Z_{Simple} ✔
ZIP_{CRREL} ZIP_{Simple}
3
8/12
17/27
1/12
1/17
1

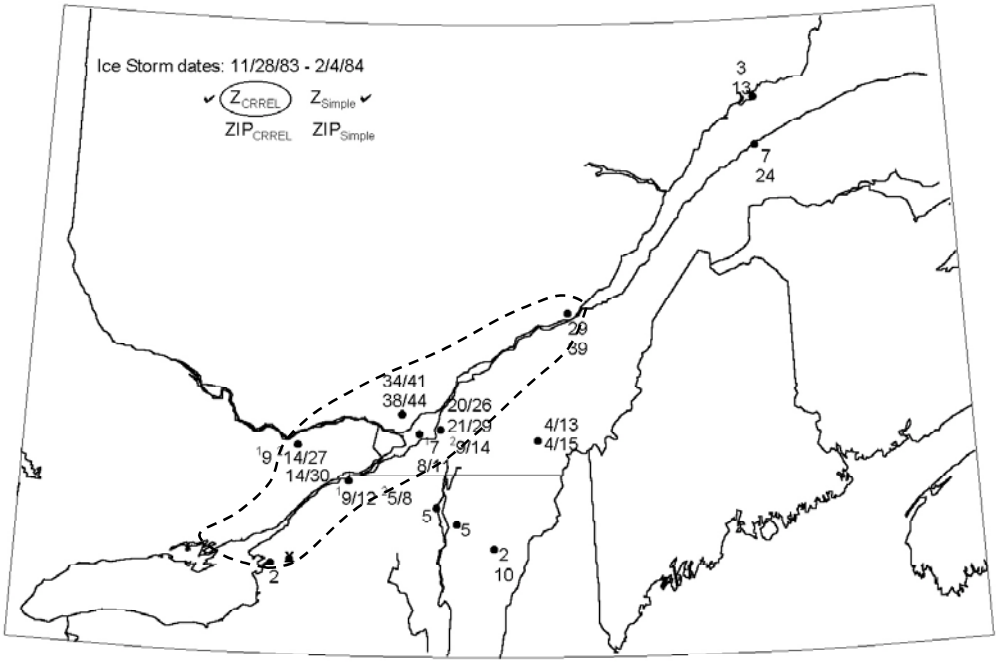
Ice Storm dates: 11/28/83 - 2/4/84
✔ Z_CRREL Z_Simple ✔
ZIP_CRREL ZIP_Simple
3
13
7
24
29
39
34/41
38/44
20/26
21/29
4/13
4/15
14/27
14/30
9/12
5/8
9/14
8/11
5
5
2
10
2

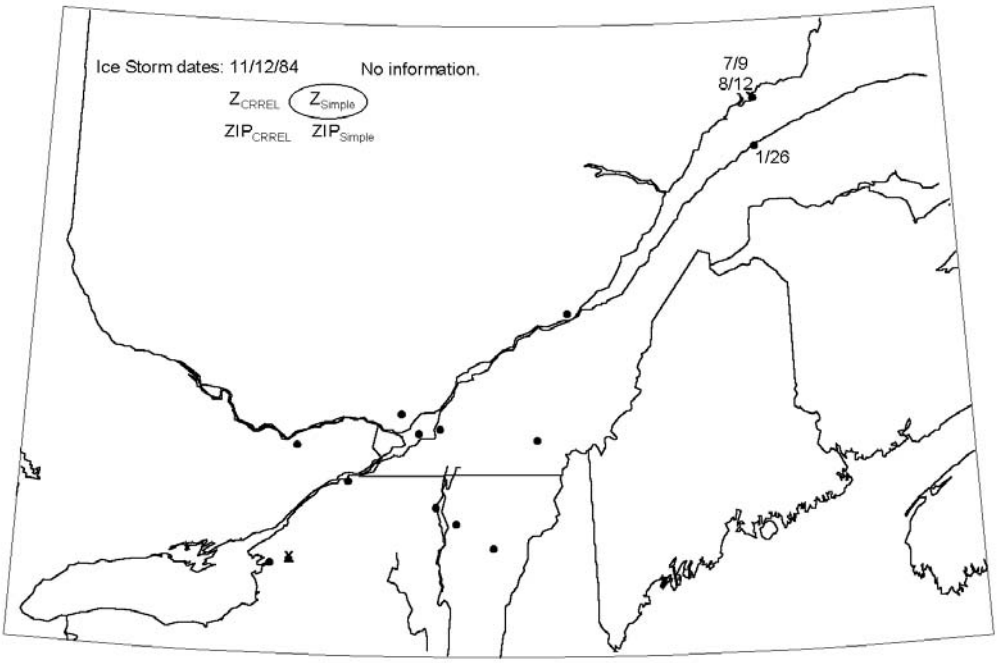
Ice Storm dates: 11/12/84
No information.
Z_CRREL Z_Simple
ZIP_CRREL ZIP_Simple
7/9
8/12
1/26

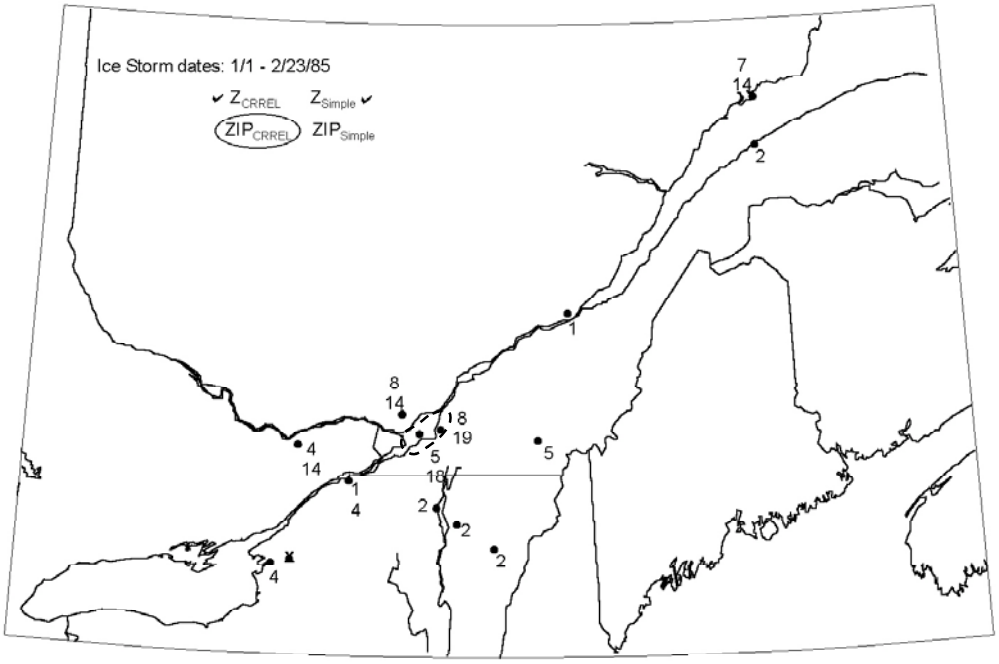
Ice Storm dates: 1/1 - 2/23/85
✔ Z_CRREL Z_Simple ✔
ZIP_CRREL ZIP_Simple
7
14
2
1
8
14
8
19
5
4
14
5
1
4
18
2
2
2
4

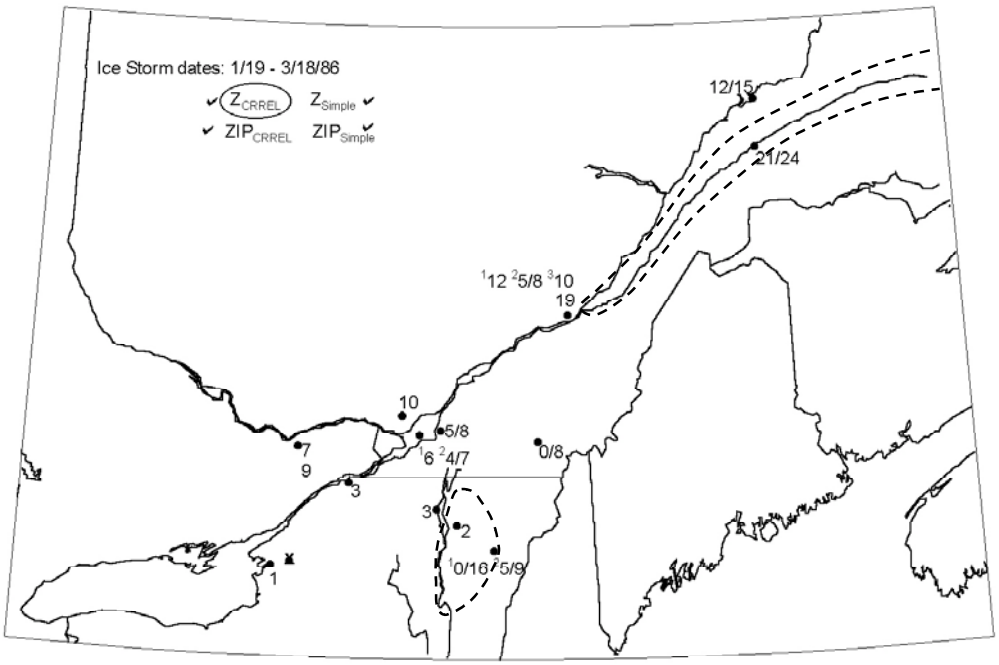
Ice Storm dates: 1/19 - 3/18/86
✔ Z_CRREL Z_Simple ✔
✔ ZIP_CRREL ZIP_Simple ✔
12/15
21/24
[1]12 [2]5/8 [3]10
19
10
5/8
7
9
3
[1]6 [2]4/7
0/8
3
2
1
[1]0/16 [2]5/9

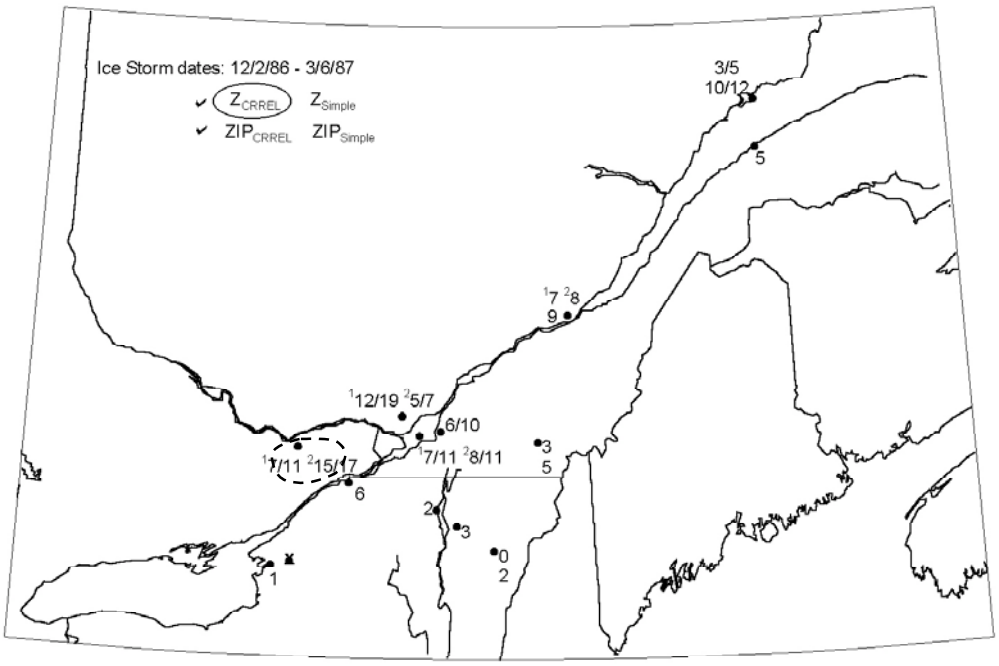
Ice Storm dates: 12/2/86 - 3/6/87
✔ Z_CRREL Z_Simple
✔ ZIP_CRREL ZIP_Simple
3/5
10/12
5
[1]7 [2]8
9
[1]12/19 [2]5/7
6/10
[1]7/11 [2]15/17
[1]7/11 [2]8/11
6
3
5
2
3
0
2
1

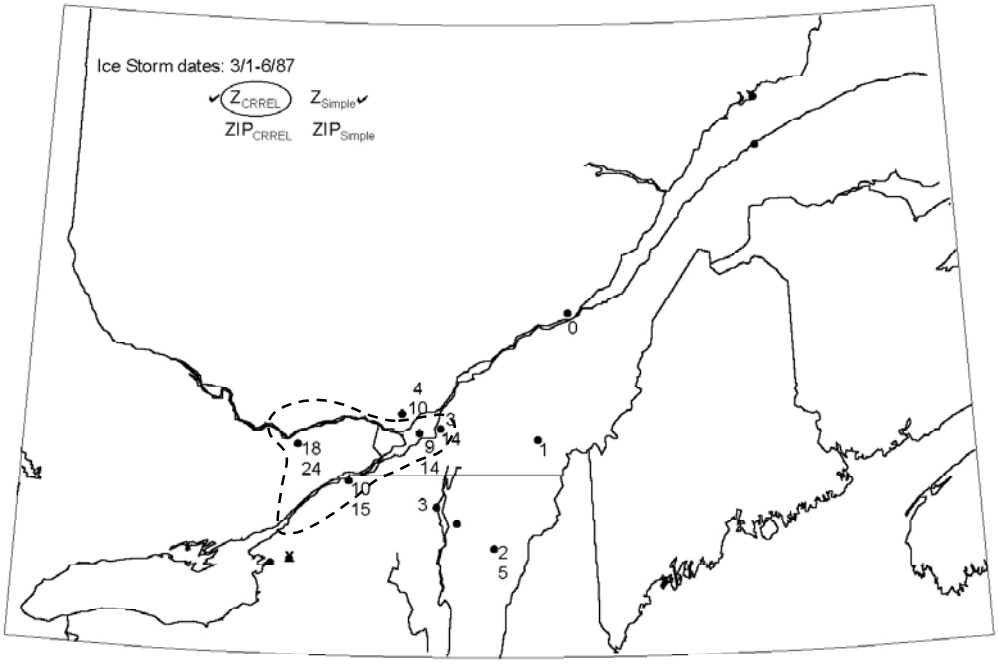
Ice Storm dates: 3/1-6/87
✔ Z_CRREL Z_Simple ✔
ZIP_CRREL ZIP_Simple
0
4
10
3
9
4
18
24
14
10
15
3
1
2
5

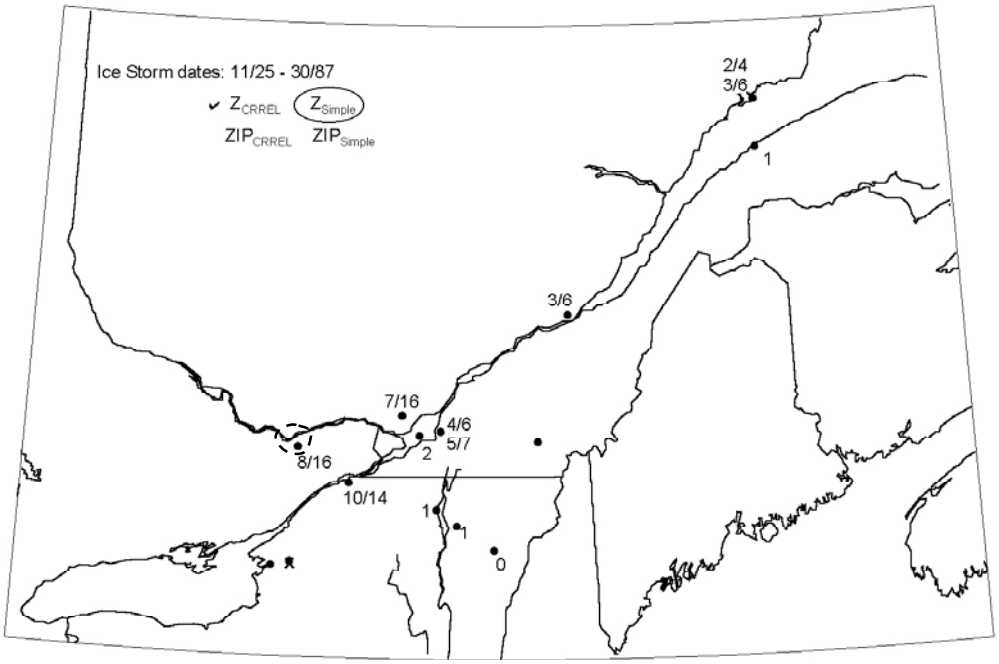
Ice Storm dates: 11/25 - 30/87
✔ Z_{CRREL} Z_{Simple}
ZIP_{CRREL} ZIP_{Simple}
2/4
3/6
1
3/6
7/16
4/6
5/7
2
8/16
10/14
1
1
0

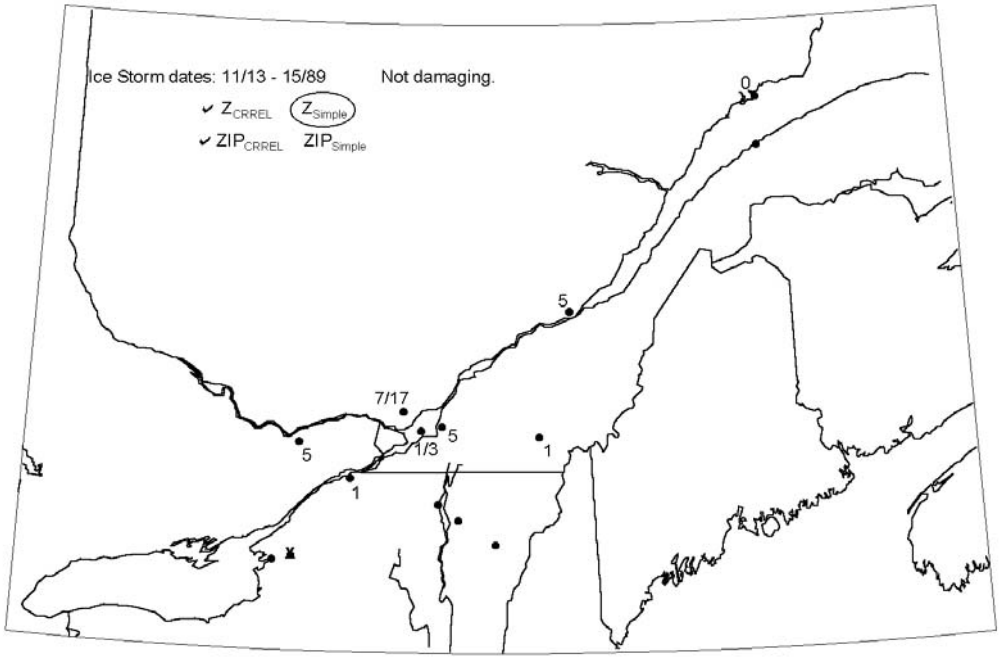
Ice Storm dates: 11/13 - 15/89
Not damaging.
✔ Z_{CRREL} Z_{Simple}
✔ ZIP_{CRREL} ZIP_{Simple}
0
5
7/17
5
1/3
5
1
1

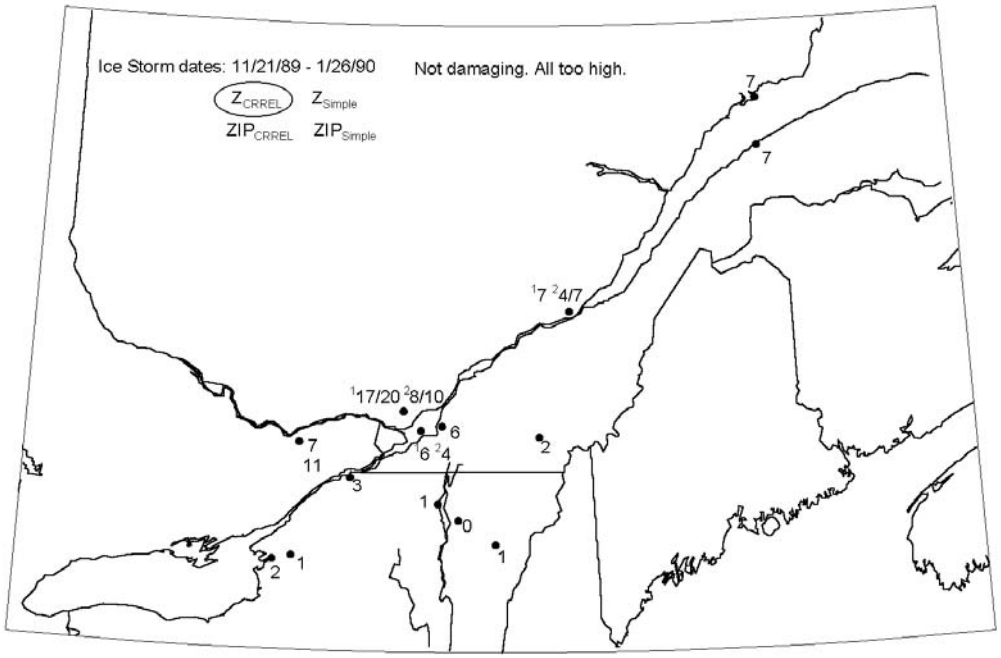
Ice Storm dates: 11/21/89 - 1/26/90
Not damaging. All too high.
Z_{CRREL} Z_{Simple}
ZIP_{CRREL} ZIP_{Simple}
7
7
[1]7 [2]4/7
[1]17/20 [2]8/10
6
[1]6 [2]4
7
11
3
2
1
1
2
0
1

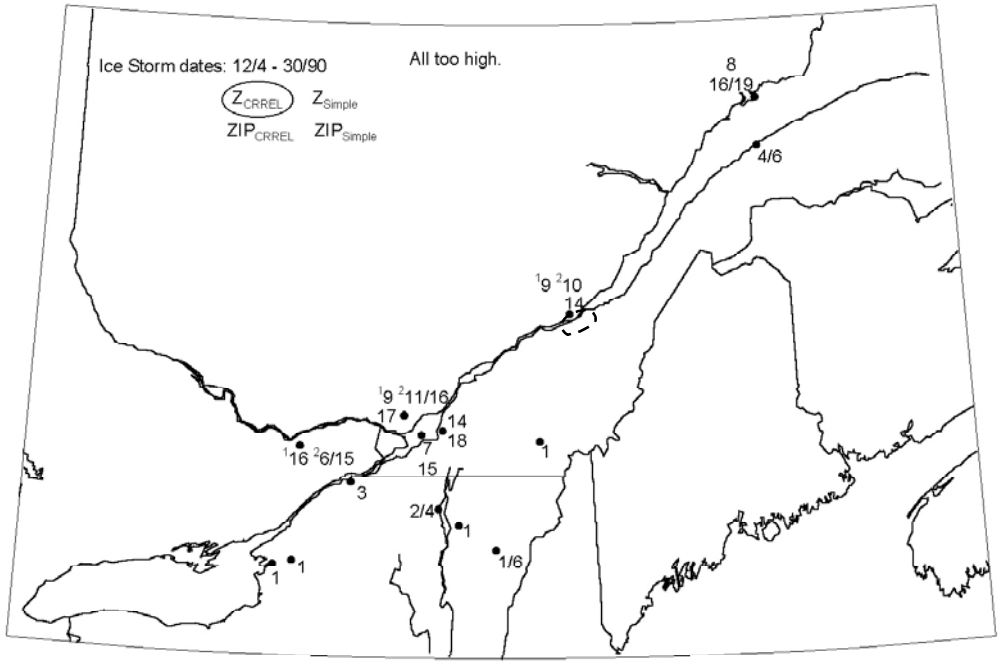
Ice Storm dates: 12/4 - 30/90
All too high.
Z_{CRREL} Z_{Simple}
ZIP_{CRREL} ZIP_{Simple}
8
16/19
4/6
[1]9 [2]10
14
[1]9 [2]11/16
17
14
18
7
[1]16 [2]6/15
3
15
1
2/4
1
1/6
1
1

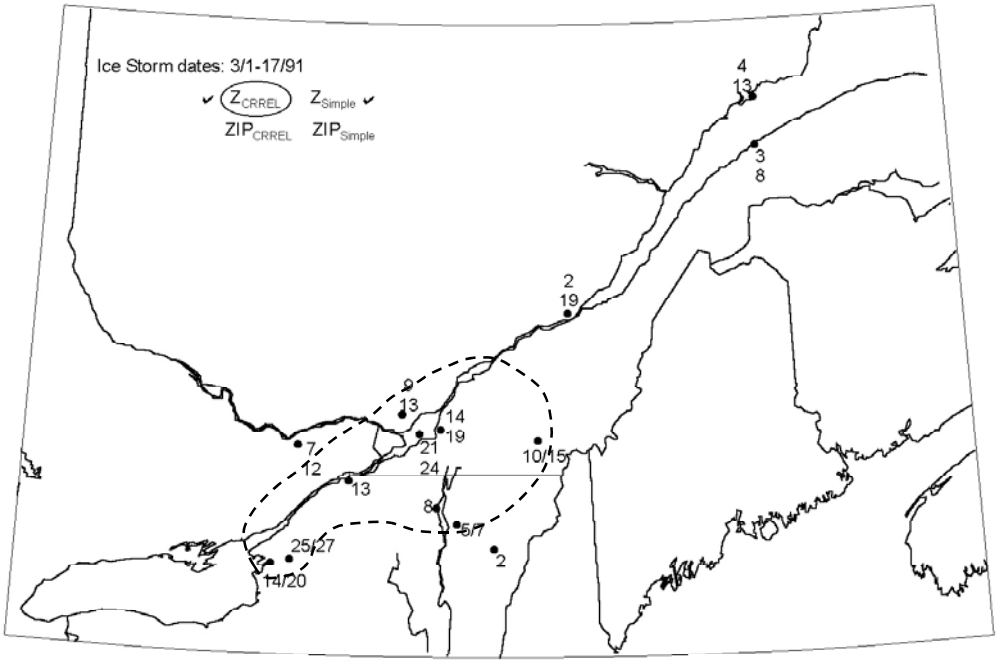
Ice Storm dates: 3/1-17/91
✔ Z_CRREL Z_Simple ✔
ZIP_CRREL ZIP_Simple
4
13
3
8
2
19
13
14
19
7
12
21
24
10/15
13
8
5/7
2
25/27
14/20

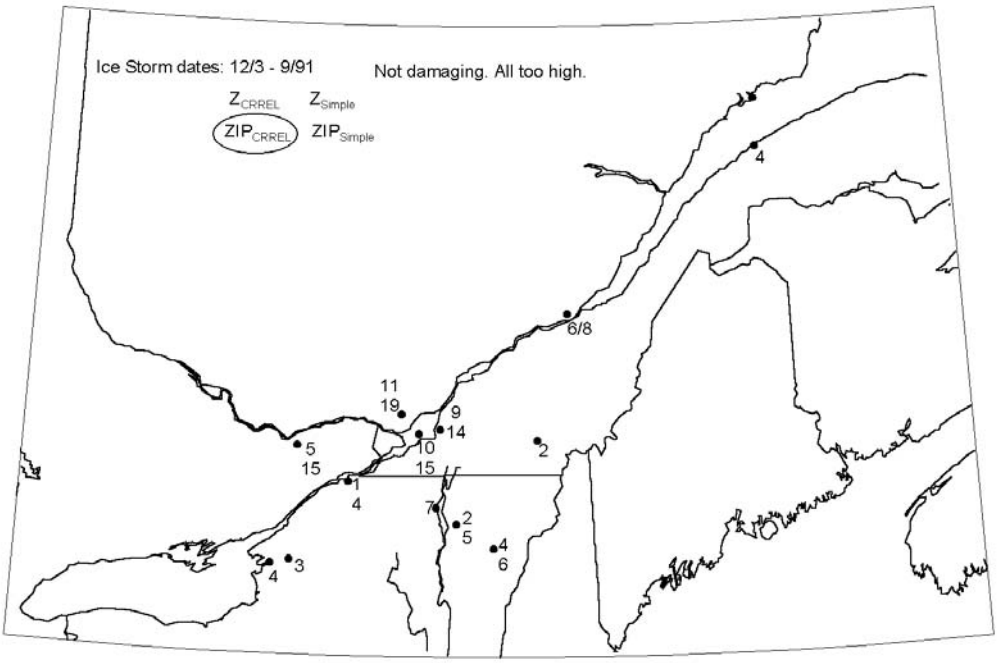
Ice Storm dates: 12/3 - 9/91
Not damaging. All too high.
Z_CRREL Z_Simple
ZIP_CRREL ZIP_Simple
4
6/8
11
19
9
14
5
15
10
15
2
1
4
7
2
5
4
6
4
3

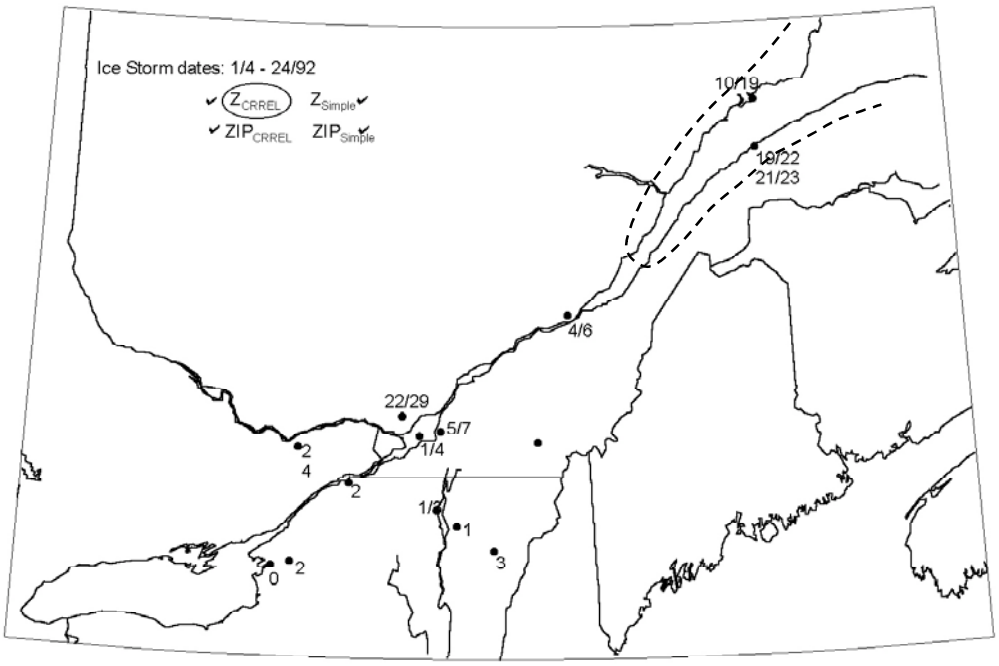
Ice Storm dates: 1/4 - 24/92
✔ Z CRREL
Z Simple ✔
✔ ZIP CRREL
ZIP Simple
10/19
19/22
21/23
4/6
22/29
5/7
1/4
2
4
2
1/
1
3
0
2

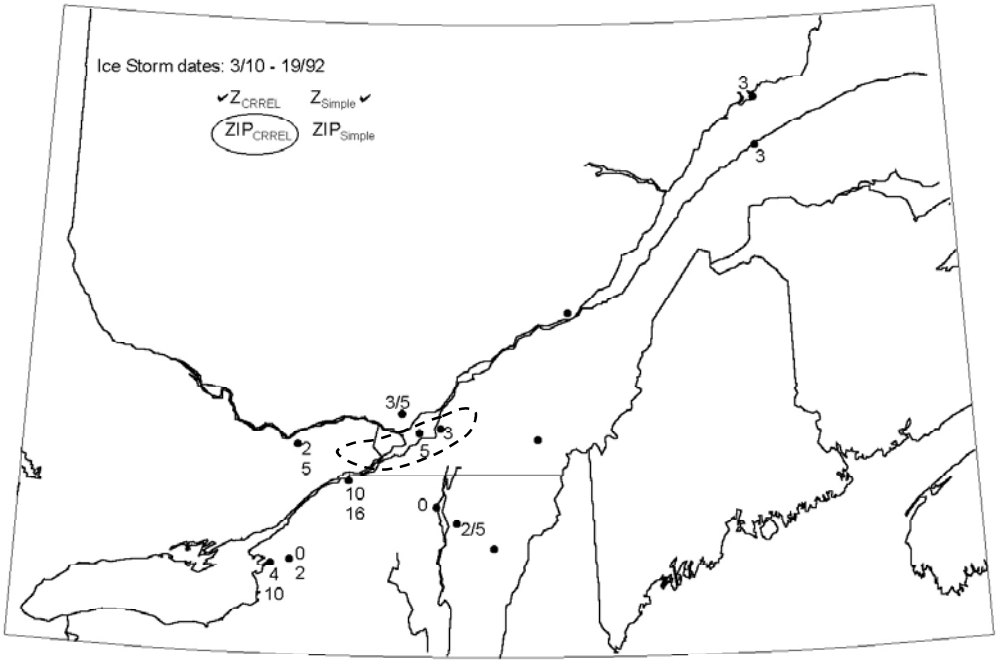
Ice Storm dates: 3/10 - 19/92
✔ Z CRREL
Z Simple ✔
ZIP CRREL
ZIP Simple
3
3
3/5
3
5
2
5
10
16
0
2/5
0
2
4
10

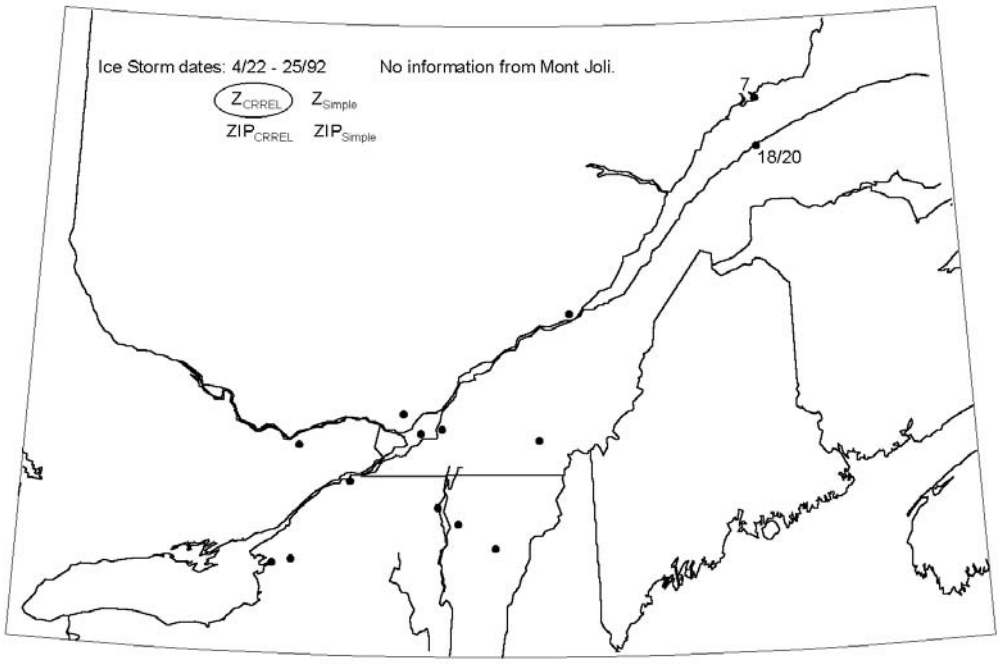
Ice Storm dates: 4/22 - 25/92
No information from Mont Joli.
Z CRREL
Z Simple
ZIP CRREL
ZIP Simple
7
18/20

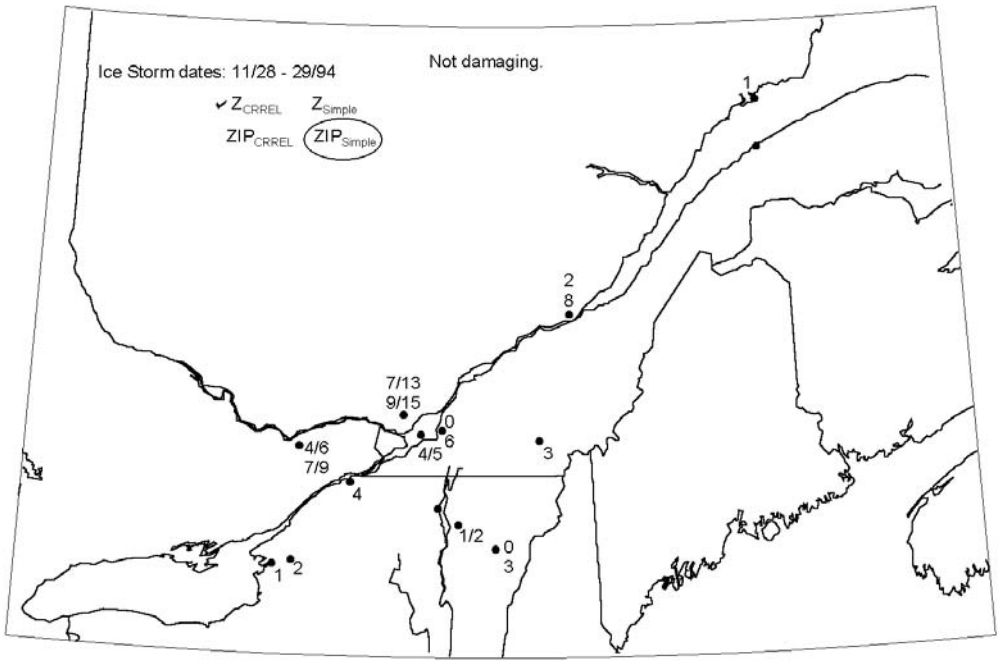
Ice Storm dates: 11/28 - 29/94
Not damaging.
Z CRREL
Z Simple
ZIP CRREL
ZIP Simple
1
2
8
7/13
9/15
0
6
4/6
7/9
4/5
3
4
1/2
0
3
1
2

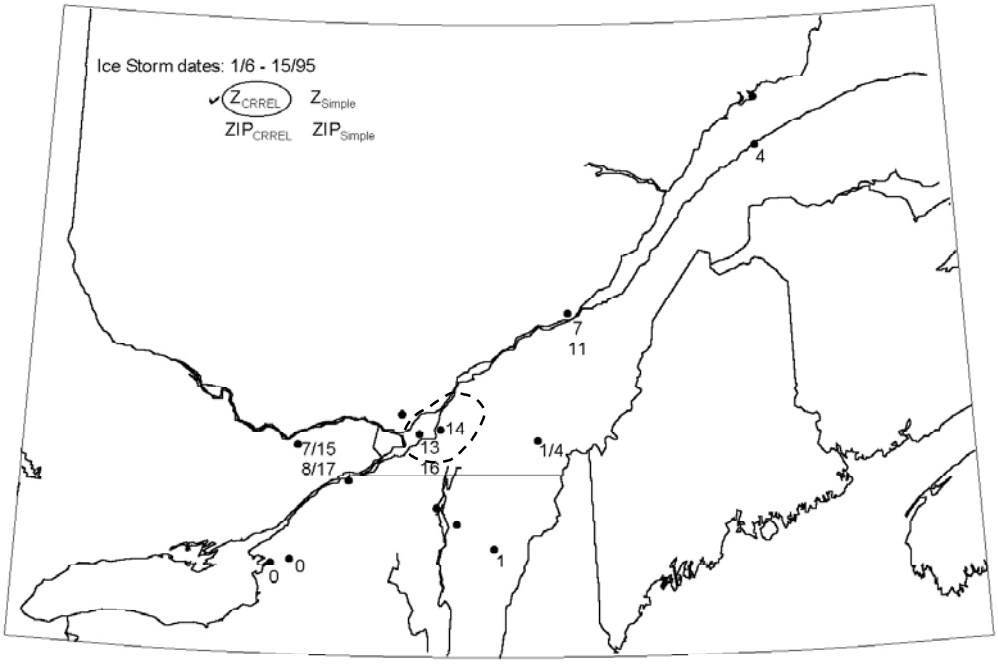
Ice Storm dates: 1/6 - 15/95
Z_{CRREL} Z_{Simple}
ZIP_{CRREL} ZIP_{Simple}
4
7
11
14
13
16
7/15
8/17
1/4
0
0
1

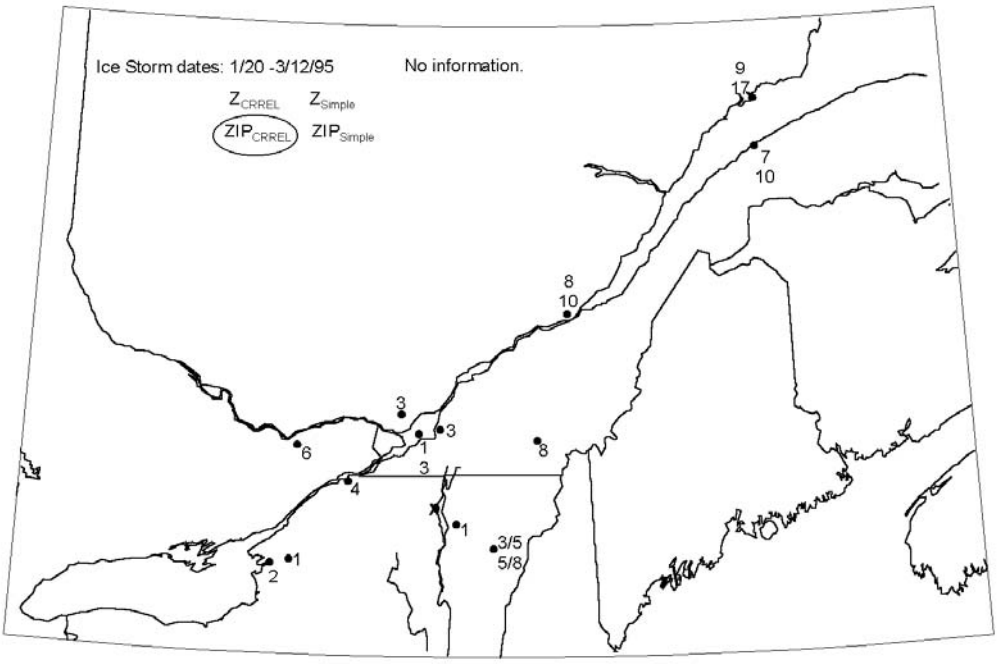
Ice Storm dates: 1/20 -3/12/95
No information.
Z_{CRREL} Z_{Simple}
ZIP_{CRREL} ZIP_{Simple}
9
17
7
10
8
10
3
3
1
6
3
8
4
1
3/5
5/8
2
1

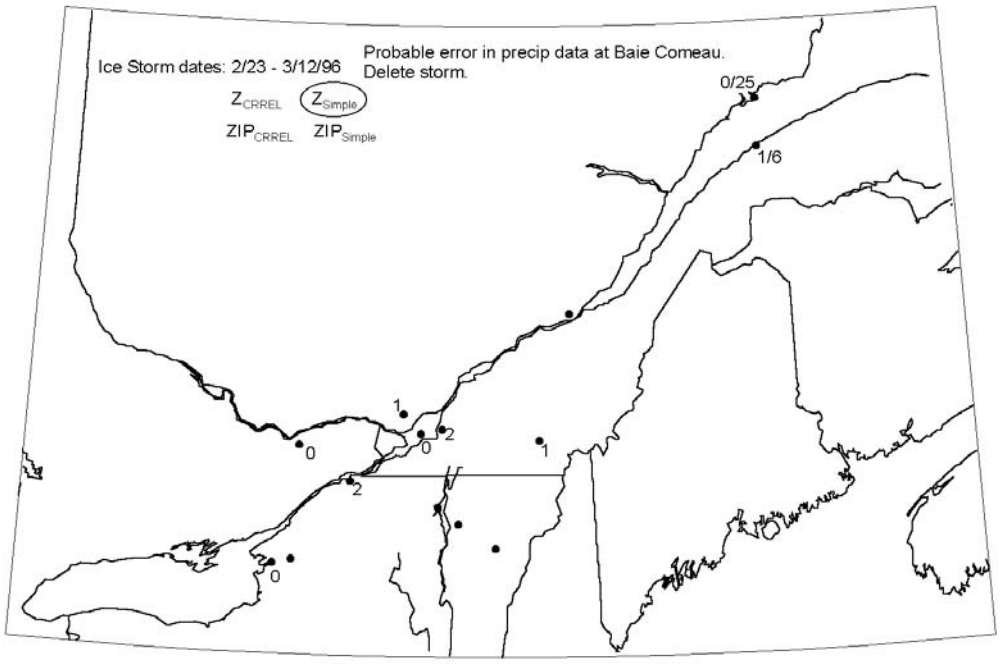
Ice Storm dates: 2/23 - 3/12/96
Probable error in precip data at Baie Comeau.
Delete storm.
Z_CRREL
Z_Simple
ZIP_CRREL
ZIP_Simple
0/25
1/6
1
0
0
2
1
2
0

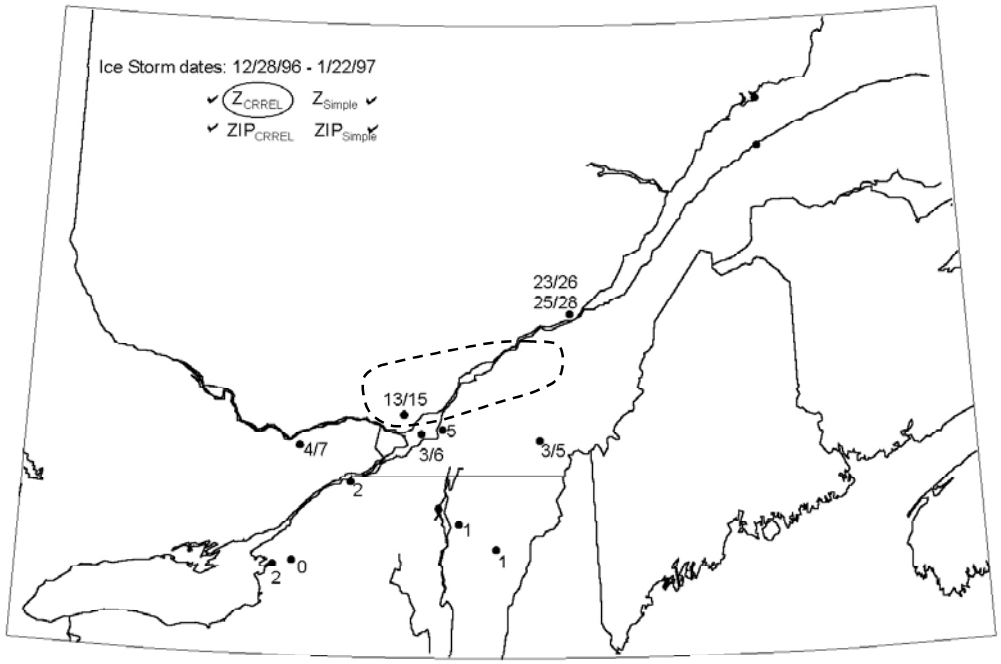
Ice Storm dates: 12/28/96 - 1/22/97
Z_CRREL
Z_Simple
ZIP_CRREL
ZIP_Simple
23/26
25/26
13/15
5
4/7
3/6
3/5
2
1
1
2
0

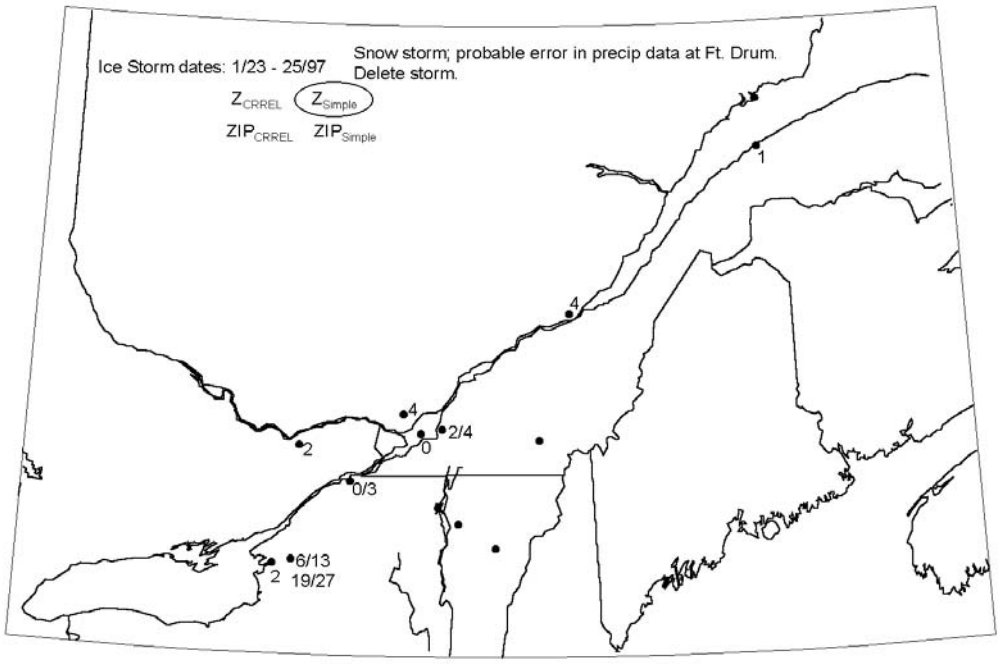
Ice Storm dates: 1/23 - 25/97
Snow storm; probable error in precip data at Ft. Drum.
Delete storm.
Z_{CRREL} Z_{Simple}
ZIP_{CRREL} ZIP_{Simple}
1
4
4
2/4
0
2
0/3
6/13
2 19/27

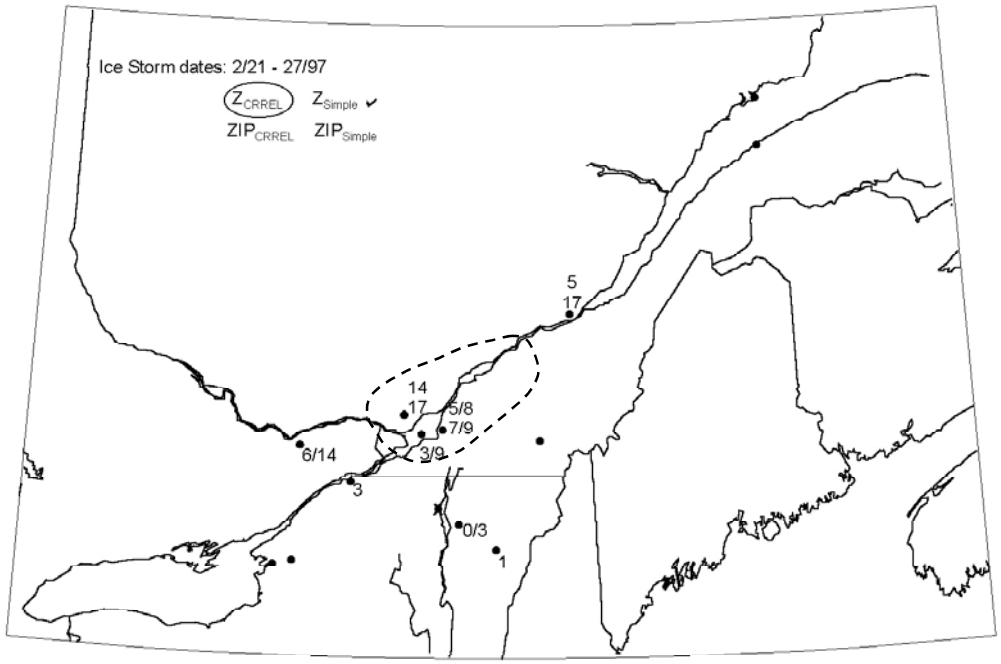
Ice Storm dates: 2/21 - 27/97
Z_{CRREL} Z_{Simple} ✔
ZIP_{CRREL} ZIP_{Simple}
5
17
14
17
5/8
7/9
6/14
3/9
3
0/3
1

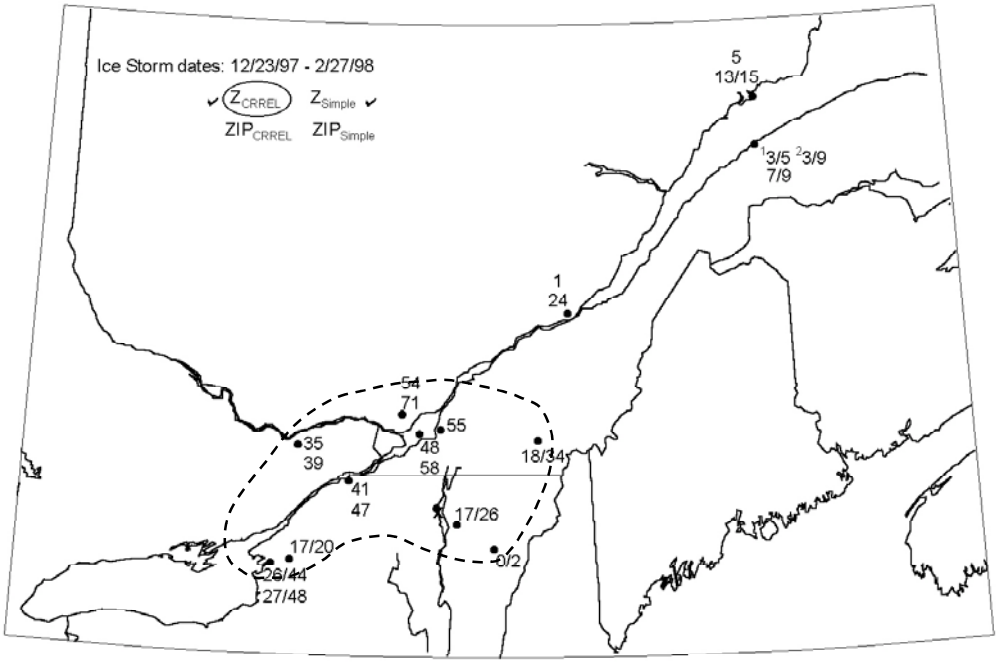
Ice Storm dates: 12/23/97 - 2/27/98
✔ Z_CRREL Z_Simple ✔
ZIP_CRREL ZIP_Simple
5
13/15
1 3/5 2 3/9
7/9
1
24
54
71
55
48
58
35
39
18/34
41
47
17/26
17/20
26/44
27/48
0/2

APPENDIX E. WATER EQUIVALENT OF ICE PELLETS

There is little information available on the bulk density of ice pellets. The information that was found is primarily from locations where winter precipitation is significant agriculturally. An article in *The Daily Oklahoman* on 11 January 1949 reported that the Weather Bureau used a value of about 0.33 in. of moisture for 1 in. of sleet. Three years later, on 3 January 1952, an article in *The Elk City Daily News* quoted a weather observer in Oklahoma City saying that 2 in. of well-packed sleet was equivalent to 1 in. of rainfall. Moving north, *The Windsor Star* in Ontario, Canada, on 27 January 1967, stated that although 1 in. of snow was equivalent to about 0.1 in. of precipitation, the addition of ice pellets increased that ratio to 0.64 in. of precipitation. Most recently, on 31 October 1991, an article in *The Elk City Daily News* quoted an official weather observer in saying that 1.5 inches of sleet was equivalent to 0.75 inches of moisture. In all of these reports it was clear from the context that the term "sleet" was referring to ice pellets, rather than to freezing rain.

These water equivalent ratios for ice pellets range from 0.33 to 0.64, with a median of 0.5. All these values are significantly higher than the 0.1 ratio that is often used in estimating the water equivalent of a snowfall.

REPORT DOCUMENTATION PAGE

Form Approved
OMB No. 0704-0188

1. REPORT DATE *(DD-MM-YY)*	2. REPORT TYPE	3. DATES COVERED *(From - To)*
January 2003	Technical Report	

4. TITLE AND SUBTITLE

Ice Storms in the St. Lawrence Valley Region

5a. CONTRACT NUMBER

5b. GRANT NUMBER

5c. PROGRAM ELEMENT NUMBER

6. AUTHOR(S)

Kathleen F. Jones

5d. PROJECT NUMBER

5e. TASK NUMBER

5f. WORK UNIT NUMBER

7. PERFORMING ORGANIZATION NAME(S) AND ADDRESS(ES)

U.S. Army Engineer Research and Development Center
Cold Regions Research and Engineering Laboratory
72 Lyme Road
Hanover, NH 03755-1290

8. PERFORMING ORGANIZATION REPORT NUMBER

ERDC/CRREL TR-03-1

9. SPONSORING/MONITORING AGENCY NAME(S) AND ADDRESS(ES)

Office of the Chief of Engineers
Washington, DC

10. SPONSOR / MONITOR'S ACRONYM(S)

11. SPONSOR / MONITOR'S REPORT NUMBER(S)

12. DISTRIBUTION / AVAILABILITY STATEMENT

Approved for public release; distribution is unlimited.

Available from NTIS, Springfield, Virginia 22161.

13. SUPPLEMENTARY NOTES

14. ABSTRACT

The severe ice storm in January 1998 in Quebec, eastern Ontario, northern New York, and New England disrupted the lives of millions of people. The ice that accreted on trees and wires damaged electrical transmission and distribution lines, causing power outages that lasted many weeks in some areas. In this report, ice storms in the St. Lawrence Valley region of Quebec, eastern Ontario, and northern New York and Vermont are analyzed, focusing on the amount of ice on power lines. Although there are many photographs of ice-covered wires from this storm, only rough estimates of the equivalent radial thickness of ice on the wires can be obtained from these photos. The analysis in this report relies on historical weather data and ice accretion models to estimate the equivalent ice thickness on wires both in this storm and in past freezing-rain storms. The CRREL and Simple ice accretion models incorporate a physical model of the process of ice accretion with empirically determined parameters. Qualitative information from newspapers, *Storm Data,* and other reports on damaging storms supplement the model results to provide a better understanding of the climatology of ice storms in the region. Ultimately, all this information is used to calculate equivalent ice thicknesses from freezing rain for long return periods. For the St. Lawrence Valley region in the vicinity of Montreal, ice thicknesses on wires 10 m above ground and perpendicular to the wind for 50- and 200-year return periods are estimated to be 33 mm and 52 mm, respectively. Gust speeds concurrent with these ice thicknesses are about 20 m/s. Ice thickness estimates for the 1998 storm at the three weather stations in the Montreal area range from 48 to 55 mm.

15. SUBJECT TERMS

Extreme value analysis
Freezing rain
Ice storm
Models
Weather data

16. SECURITY CLASSIFICATION OF:			17. LIMITATION OF ABSTRACT	18. NUMBER OF PAGES	19a. NAME OF RESPONSIBLE PERSON
a. REPORT	b. ABSTRACT	c. THIS PAGE			19b. TELEPHONE NUMBER *(include area code)*
U	U	U	U	130	

DEPARTMENT OF THE ARMY
ENGINEER RESEARCH AND DEVELOPMENT CENTER, CORPS OF ENGINEERS
COLD REGIONS RESEARCH AND ENGINEERING LABORATORY, 72 LYME ROAD
HANOVER, NEW HAMPSHIRE 03755-1290

Official Business